Title	DEVELOPMENT OF AN ECO-FRIENDLY APPROACH FOR COASTAL EROSION PROTECTION USING BIO-MEDIATED TECHNOLOGY
Author(s)	Imran, Md Al
Citation	. ( ) 14682
Issue Date	2021-09-24
DOI	10.14943/doctoral.k14682
Doc URL	http://hdl.handle.net/2115/86929
Type	theses (doctoral)
File Information	Imran_Md_Al.pdf

Instructions for use

DEVELOPMENT OF AN ECO-FRIENDLY APPROACH FOR COASTAL EROSION PROTECTION USING BIO-MEDIATED TECHNOLOGY

by

MD AL IMRAN

DISSERTATION

Presented in Partial Fulfilment of the Requirements for the Degree of

DOCTOR OF PHILOSOPHY

in

Graduate School of Engineering

of the

Japan

<table>
<tr><td>Examination committee:</td><td>Laboratory of Biotechnology for Resources Engineering,</td></tr>
<tr><td>Prof. Satoru KAWASAKI, Chair</td><td></td></tr>
<tr><td>Prof. Tsutomu SATO</td><td>Division of Sustainable Resources Engineering,</td></tr>
<tr><td>Prof. Toshifumi IGARASHI</td><td>Graduate School of Engineering,</td></tr>
<tr><td>A/Prof. Kazunori NAKASHIMA</td><td>Hokkaido University, Japan</td></tr>
</table>

September, 2021

DECLARATION

I hereby declare that this thesis is original work of mine and I am submitting it for the partial fulfilment of the requirements for the degree of "DOCTOR OF PHILOSOPHY" from Graduate School of Engineering, Hokkaido University, Japan. Additionally, I am ensuring that it contains no material previously published or written by another person nor material which to a substantial extent that has been accepted for the award of any other degree of the university or another institute, except where due acknowledgement has been made in the text.

Name: MD AL IMRAN

ACKNOWLEDGEMENTS

ABSTRACT

At present, coastal erosion is a major problem all over the world. Limitations of traditional countermeasures put an importance to develop an alternative sustainable and eco-friendly methods for coastal erosion protection. As an alternative countermeasure, bio-stabilization approaches drawn substantial attention for the researcher around the world which included MICP (Microbial Induced Carbonate Precipitation) and EICP (Enzyme Induced Carbonate Precipitation) method. In the bio-stabilization technique as a consequence of bio-chemical reactions of urease enzyme calcium carbonate precipitated which act as a major cementing material in between the sand-soil particles and improve the physical properties of targeted materials (strength and stiffness). The objective of the research presented in this dissertation was to assess the viability of MICP and EICP technique as a novel alternative and effective countermeasures for the coastal erosion protection by distinguishing their mode of actions. Moreover, this study aimed to find out an appropriate or feasible conditions and methods that would be useful in making artificial beachrocks for coastal erosion protection in Greece and in Mediterranean countries, in an inexpensive, eco-friendly, and sustainable way. Natural jute fiber and watermelon seeds were also used as advanced bio-mediated technology in this study to increase the sample's strength and durability. In future, the findings of this study could play an important source of information for commercial applications in protecting against coastal erosion and for other bio-engineering applications.

TABLE OF CONTENTS

LIST OF FIGURES

xvi

LIST OF TABLES

CHAPTER 1 : GENERAL INTRODUCTION

1.1 Background and motivation of the study

Coastal erosion has been a significant problem globally due to anthropogenic changes along the coastline. Due to climate change, some islands around the world are in danger of being flooded. Embankments, revetments, jetties, artificial reefs, offshore breakwaters, and sand bypassing are just some of the systems and processes that have been used in the past to avoid or at least mitigate erosion damage (Danjo et al., 2014). However, the installation and maintenance of these systems are costly. On the other hand, the environmental issues associated with conventional construction materials such as chemical grouts (e.g., cement, fly-ash, epoxy, acrylamide, phenoplasts, silicates, polyurethane, etc.) and geosynthetic products necessitate alternative approaches in geotechnical applications. For example, production of Ordinary Portland Cement (OPC), the effective and widely used soil stabilizer, causes the significant release of major greenhouse gas, carbon dioxide (CO_2). According to the reports of Intergovernmental Panel on Climate Change (IPCC), the production of OPC contributes around 5-6% of global CO_2 emission. As per the prediction, if the present rate continues in cement manufacture, the emission of carbon would reach to 260% in 2050 (Cuzman et al., 2015), which would significantly impact the earth's atmosphere and climate. It is also apparent that most of the chemical grouts are environmentally toxic and/or hazardous (Cheng et al., 2014a; Karol, 2003); thus, these materials are extensively under the scrutiny of public policy. For instance, leaching of acrylamide grout caused severe water poisoning in Japan in 1974, leading to the subsequent ban of nearly all the chemical grouts (Karol, 2003). Since that, the initiatives are being undertaken in several countries to ban synthetic grouting materials, and to the withdrawal of most of the products in market (DeJong et al., 2010). The use of inexpensive alternative materials should be considered, to cope with the increase in costs related to the maintenance and management of concrete structures. Previously, Danjo and Kawasaki 2013 focused on using alternative materials to replace beachrock to reduce lifecycle costs associated with the currently employed methods. Beachrock forms much more quickly than other sedimentary rocks within the intertidal zone and is composed of coastal sediments that have been cemented together mainly by $CaCO_3$

(Danjo and Kawasaki 2013). By using the processes that solidify beach sand, we hypothesized that could create a highly durable artificial beachrock that would be comparable in efficacy to the existing concrete structures. Artificial beachrocks (manufacture artificially in the natural condition) have the potential to inhibit coastal erosion (Danjo et al., 2013b). Beachrocks are coastal deposits cemented mainly by calcium carbonate cement; these deposits are found in the tidal and intertidal zone of sandy beaches in tropical and subtropical regions (Danjo and Kawasaki 2013). For the formation of beachrock various factors have been considered. Among them, Danjo and Kawasaki (2014), focused on the possibility of promoting solidification by microbial processes, specifically urea decomposition by microorganisms. In this study, the microbial induced calcium carbonate precipitation (MICP) and enzyme induced carbonate precipitation (EICP) method was utilized, which relies on the microbial metabolism of urea that generates carbon dioxide and precipitates $CaCO_3$ (Whiffin et al., 2007). This low environmental impact method was assessed to determine its efficiency as an alternative means to alleviate coastal erosion. Considering the use of artificial rock in order to preserve such submerged-looking islands above sea level, (Danjo and Kawasaki 2012) and (Danjo et al., 2012) conducted several studies in Okinawa and Ishikawa, Japan. They found sufficient information to build artificial beachrock. Traditional grouting methods for ground improvement employ particulate (cement/bentonite) or chemical grouts that can be rather expensive and environmentally unfriendly (Ivanov and Chu 2008). Recently, novel grouting techniques have been developed to treat unsaturated coarse soils by stimulating natural processes (DeJong et al., 2006; Whiffin et al., 2007). One of these methods, termed biogrouting, has shown some promise in soil cementation via microbially induced carbonate precipitation (MICP). This approach mimics natural processes by depositing calcite ($CaCO_3$) on the soil grains, thereby increasing the material's stiffness/strength and reducing its erodibility.

In order to address the disadvantages of current coastal countermeasures technique one could look at sustainable or "green" materials and processes using biomimetic in which lessons learned from nature form the basis for evolution of novel technological materials for the development of sustainable materials in the construction industry. As previously mentioned, the confluence of these negative impacts urges the exploration of new alternative countermeasures for coastal erosion protection.

According to the researchers and scientists (Achal and Kawasaki, 2016; DeJong et al., 2010; Ivanov and Chu, 2008), the solutions to this scenario can be potentially achieved through the multi-disciplinary research at the convergence of microbiology, geochemistry and geotechnical engineering. Hence, this study investigates the sustainability and effective techniques for coastal erosion protection methods mimicking natural and bio-geotechnical process i.e., through Bio-mediated Geotechnical Engineering, assessing the complete feasibility towards the real practice.

1.2 Scope and objectives of the study

The objective of the research presented in this dissertation is to assess the viability of using MICP and EICP method as one of the candidates for a new low environmental impact coastal erosion protection. Because of using natural/bio-mediated approach this method is proven as eco-friendly method. From the perspective of bio-geotechnical engineering, yet significant effort has been given on understanding biological responses of the native ureolytic bacteria, cost effective sources of urease enzyme, strength and durability improvement using natural fiber, and treatment strategies to facilitate effective and reliable stabilization process. The scope and objectives of this dissertation is presented in Figure 1. 1.
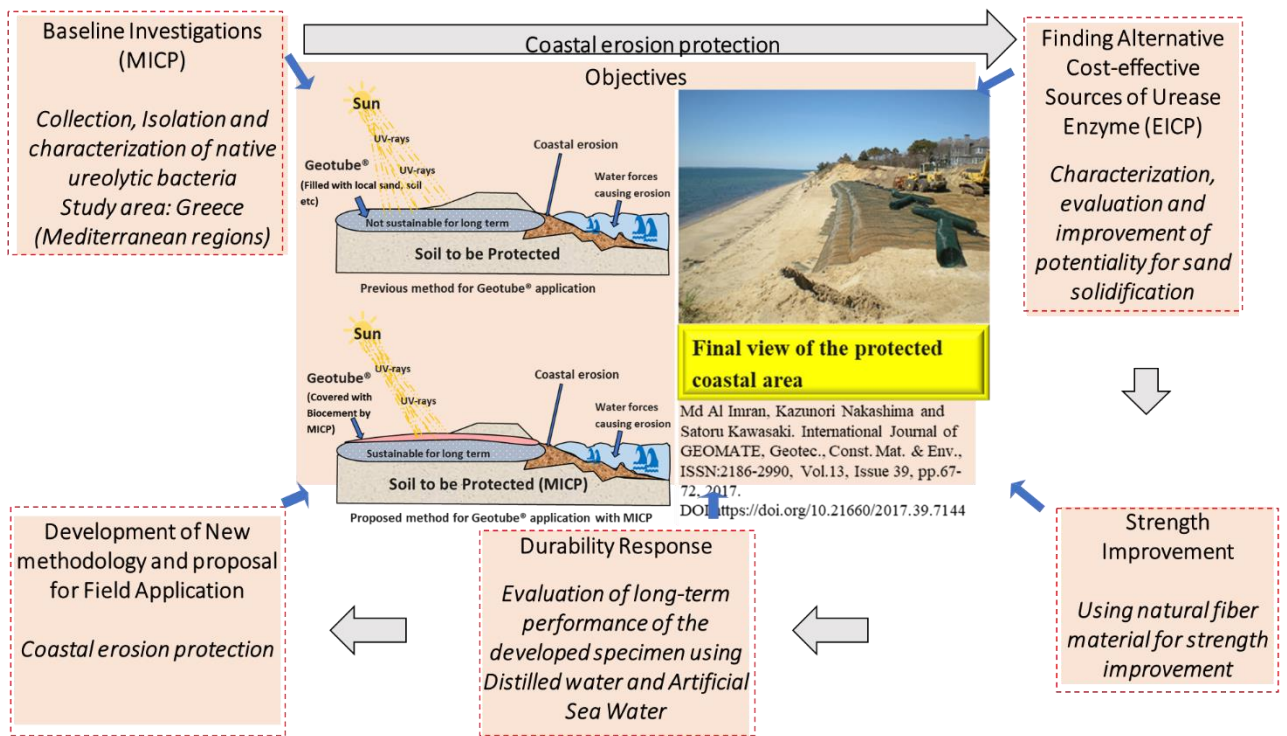
Figure 1. 1: Outline and scope of the research work.

1.3 Arrangement of the dissertation

This dissertation is organized into a total of eight chapters.

☑ **Chapter 1** and **Chapter 2** presented the preface of the research work. Chapter 1 introduced the background, scope, objectives, originality, and significance of the research work.

☑ **Chapter 2** discussed the results of a systematic literature review on various aspects of the bio-mediated technology for coastal erosion protection, mechanism of MICP, EICP process and their subsequent compatibility for coastal erosion protection.

☑ In **Chapter 3**, a baseline investigation and fundamental scientific approach of MICP technique were discussed using native ureolytic bacteria. Isolated native strains were evaluated for urease activity including whole-cell, supernatant and cell pellets and subsequently different environmental parameters (temperature, pH, culture duration etc.) were also investigated. The sand solidification test (syringe) was also performed based on the findings, and the degree of solidification was quantitatively evaluated by the needle penetration test. The

results revealed that urease activity of the identified strains relied on environment-specific parameters and, additionally, urease was not discharged in the culture solution but would discharge in and/or on the bacterial cell, and the fluid of the cells showed urease activity.

☑ **Chapter 4** addressed some of the leading limitations of using microbes for the source of urease enzyme and used alternative sources of urease enzyme that was extracted from watermelon seeds. The carbonate formation process is known as EICP process. Crushed and blended watermelon seeds (both dry and germinated) were used as a source of urease enzyme. Subsequently, their urease activity was also investigated with various environmental parameters (temperature, pH, etc.) and investigated the carbonate precipitation trend. The effect of using magnesium chloride and their subsequent variation to the unconfined compressive strength of the soil was also discussed in this chapter. The results of this study showed that, the lower molar ratio of calcium and magnesium chloride can significantly improve the UCS of the specimen which could be considered a significant outcome for different bio-geotechnical applications.

☑ In **Chapter 5**, a comprehensive study was conducted to investigate the effect of adding plant-based natural jute fiber to the MICP-treated sand and the long-term performance of MICP-fiber treated samples were also investigated followed by wet-dry in distilled water (DW) and artificial sea water (ASW). The results of this study showed that, the added jute fibers could improve the engineering properties of the biocemented sand by MICP method. The durability results showed that the ASW damages were most significant than DW. However, fiber incorporation had a significant role on the strength improvement and long-term performance of MICP treated samples.

☑ In **Chapter 6**, likewise MICP, fiber reinforce EICP method was studied as an alternative countermeasure and to understand their comparative performance in terms of strength and durability improvement. Similarly, to understand the long-term performance of EICP-fiber treated samples the influence of key climatic parameters wet-dry (WD) was also investigated using distilled water (DW) and

5

artificial sea water (ASW). From the non-destructive tests, shear wave velocity tests, XRD and micro-structure analysis (SEM), results showed that, the fiber content significantly affected the engineering properties of EICP-treated soils more considerably than the fiber length. The durability results showed that the ASW damages were most significant than DW. However, fiber incorporation had a significant role on the strength improvement and long-term performance of EICP treated samples. The results of this study could significantly contribute to further improvement of the fiber-reinforced biocemented sand in the geotechnical engineering field applications.

☑ In **Chapter 7**, the significant differences between MICP and EICP method followed by the mechanism of action was discussed. Based on the outcomes of the results discussed above, a novel methodology has been proposed for an effective coastal preservation method.

☑ In **Chapter 8**, each chapter's findings are summarized, along with some suggestions for future work. In addition, based on the outcomes derived from the above works, the application guidelines are outlined regarding optimal MICP, EICP and fiber reinforce recipe, their subsequent implementation strategy, and conditions, along with the evaluation process that would help to ensure the durability performance of MICP and EICP treated fiber reinforce samples for effective coastal erosion protection.

1.4 Originality and significance of this study

Coastal erosion is a significant problem throughout the world and little attention has been paid using MICP and EICP process in a sustainable and eco-friendly way. Figure 1. 2 showing the trend of publication on microbially induced carbonate precipitation. After Stocks-Fischer, Galinat, and Bang (1999) proposed the key principles of MICP, DeJong, Fritzges, and Nüsslein (2006) showed the suitability of MICP to improve the stiffness and the strength of loose sand. However, limited studies have been related to the coastal erosion protection strategies. The majority of the past research has focused on the physical aspects (e.g., 48 %: mechanical behavior,

hydraulic conductivity, etc.) and the biochemical aspects (e.g., 26 %: cell population, pH, kinetics, etc.) of MICP-treated soil, whereas the portion of the published research on erodibility studies of MICP- treated soil is about 5 %. Moreover, 1/3 of the erosion-related work has been related to wind-induced erosion (e.g., Miao et al. 2020; Zomorodian, Ghaffari, and O'Kelly 2019), which renders the research work related to erosion protection at merely 3 % out of entire MICP studies from 1999 to 2018.
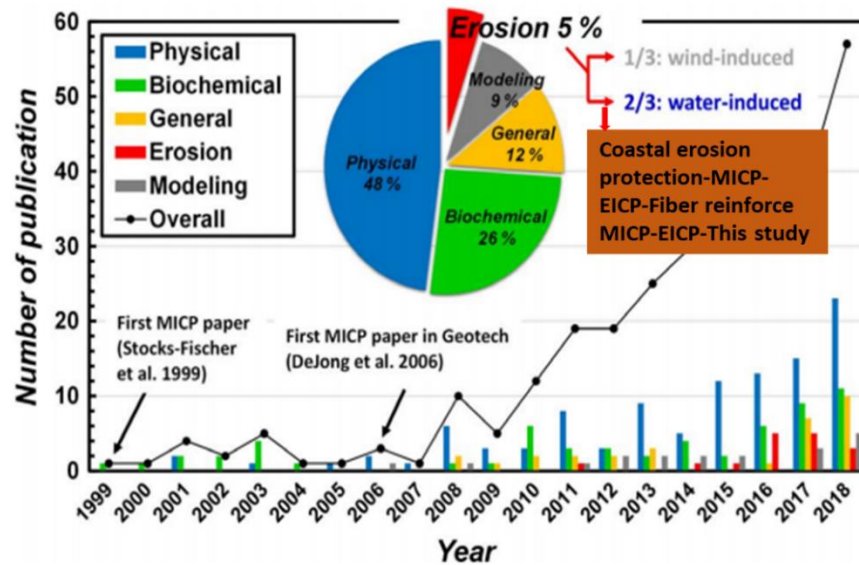
Figure 1. 2: Trend of publication on microbially induced carbonate precipitation (after Do et al., 2020)

Therefore, it's clear that, most of the MICP studies reported to date focused on using foreign bacteria for bio-mediated soil improvement, experienced uncertainties regarding performance and regulatory aspects. The work reported in this dissertation has chosen the pathway utilizing the native bacteria (the pathway that will be more likely to be approved by the public and regulatory).

A new bacterium which was not previously been reported for urea hydrolysis, was isolated from the coastal area in Greece and investigated the potentiality to apply for soil improvement especially on coastal erosion protection.

Plant derived urease enzyme from watermelon seeds (germinated condition) has been used for the very first time as an improved cost-effective-eco-friendly methodology for bio-mediated soil improvement. The studies on fiber reinforce bio-mediated soil improvement are very limited. This studies also focused on using fiber

reinforce MICP and EICP methodology to improve the strength and durability of the treated specimens which will contribute the bio-mediated soil stabilization process nearly to field implementation.

The durability and long-term performance of MICP, EICP and fiber reinforce MICP and EICP methodology are very limited and remaining as a major research gap. As potential indicators of durability, wet-dry tests have been performed deepening the understanding on long-term responses under artificial sea water and fresh water mimicking the real field application. The findings could provide necessary information regarding monitoring, effective lifetime and requirement of re-treatment process adding to knowledge in a way that has not previously been done before.

Finally, field implementation approach has been proposed in combination with geo-tube technology and other cost-effective measure. The significance of this study could play an important source of information for commercial applications in protecting against coastal erosion and for other bio-engineering application in the future.

Overall, the research originality are summarized as follows:-

R. A. N. Dilrukshi et al., 2018 Amarakoon et al., 2014	➡	Investigated EICP method using watermelon seeds with **calcium phosphate** compounds.
This study ➡		Investigated EICP method using **germinated** watermelon seeds to improve the urease activity and strength (soil) with **plant fiber** reinforcement.
Nayanthara, et al., 2019 Daryono et al., 2020	➡	Investigated effects of Mg^{2+} using MICP method.
This study ➡		Investigated effects of Mg^{2+} using **EICP method** and investigated the effects of reaction rate for strength improvement.
Choi, S.-G, et al., 2019 Consoli, N.C et al., 2009	➡	Investigated biocementation method using **synthetic** fiber.
		Investigated biocementation method using **natural plant-based fiber**.

CHAPTER 2 : REVIEW OF THE LITERATURE

2.1 Introduction

The effects of rising sea levels and increasing storm strength make coastal areas more vulnerable to destruction. Large storm surges can be destructive to coastal infrastructure, causing damage to bridges, services, and buildings, as well as putting local residents' lives in danger. Coastal sand dunes serve as a primary barrier against wave action, so their resilience is critical. MICP and EICP method is a potentially long-term alternative to seawall and revetment solutions that damage whole habitats in order to preserve cities or other areas of interest using Bio-cementation approach.

2.2 Traditional methodology for coastal erosion protection

Several mitigation strategies have been employed in various efforts to reduce or avoid coastal erosion over the years. While some of these interventions are successful, they each have their own set of drawbacks Airoldi L et al (2005). Hard structural/engineering options use structures constructed on the beach (seawalls, groynes, breakwaters/artificial headlands) or further offshore (offshore breakwaters). These options influence coastal processes to stop or reduce the rate of coastal erosion Abdul L et al (2012). The following are some examples (Figure 2.1) of conventional shoreline stabilization techniques:

Figure 2. 1: Traditional methodology for coastal erosion protection.

2.2.1 Seawalls

Sea wall is constructed parallel to the coastline to act as a barrier ranging from concrete to sandbags, and can vary in term of design, the major benefit of sea walls is that it can provide a great defense against flooding and erosion while also immobilizing the sand of the adjacent beach. Unfortunately, these structures are expensive, and their effectiveness depends on shape and size. A sloped wall requires more space on which to build. Reflection of a "wave off" of a vertically built sea wall causes turbulence and therefore erodes the sand at the base of the structure. This erosion can weaken the sea wall itself and result in large maintenance costs Bagnold RA (1940).

2.2.2 Revetments

A revetment is, just as a seawall, a shore parallel structure. The main difference is that it is more sloping than a seawall. A revetment has a distinct slope (e.g., 1:2 or 1:4), while a seawall is often almost vertical, the surface of a revetment might be either smooth or rough (a seawall is mostly smooth) and that the height of a revetment does not necessarily fill the total height difference between beach and mainland (a seawall often covers the total height difference). Although revetments provide hard face to cliff Batisha A (2012), easily installed, cheaper than sea wall, deflects and absorbs wave power, but it needs frequent maintenance.

2.2.3 Bulkhead

Bulkheads are normally constructed in the form of a vertical wall built in concrete, stone, steel or timber. The concrete, steel or timber walls can be piled and anchored walls, whereas the concrete and stone walls can also be constructed as gravity walls Borsje BW et al., (2011). The function of a bulkhead is to retain or prevent the sliding of land at the transition between the land, filled or natural, and the sea. Bulkheads are only suitable for low energy protected sites where large waves are not anticipated.

2.2.4 *Dikes and levees*

Sea dikes are onshore structures with the principal function of protecting low-lying areas against flooding. Sea dikes are usually built as a mound of fine materials like sand and clay with a gentle seaward slope in order to reduce the wave run-up and the erodible effect of the waves. The surface of the dike is armored with grass, asphalt, stones, or concrete slabs. The advantages are that they often form the cheapest hard defense when the value of coastal land is low and reduce wave loadings on the structure compared to vertical structures. The disadvantages are the requiring of large volumes of building materials and wide area in order to resist high water pressures on their seaward faces.

2.2.5 Groins

Groins are straight structures perpendicular to the shoreline. They work by blocking (part of) the littoral drift, whereby they trap or maintain sand on their upstream side. Groins can have special shapes; they can be emerged, sloping, or submerged, and they can be single or in groups, the so-called groin fields. Types of groins are wooden groins, sheet-pile groins, concrete groins and rubble-mound groins made of concrete blocks or stones, as well as sand-filled bag groins. The advantages are; building up the beach, makes a wider beach, provides calm water, and encourages tourism Cai F et al., (2009). The disadvantages are; need repairs, suitable with medium waves but strong waves still get to cliff face, and leads to faster cliff erosion down the coast by robbing it of potential beach material.

2.3 Soft defenses

Increasing awareness of the negative side-effects of hard structures on erosion and sedimentation patterns has led to growing recognition of the benefits of „soft" protection and the adaptation strategies of retreat and accommodation which are described below.

2.3.1 Beach fills

Beach nourishment requires the addition of sand to an eroded beach. Sand is imported and spread to increase beach width and elevation. It is used worldwide as a form of soft engineering to protect coastal development from the impacts of unmanaged erosion. It serves to maintain the value of coastal investments and retain the value of beach amenity to tourism and recreation. It allows the sand to shift continuously in response to changing waves and water levels.

The advantages are: reducing the detrimental impacts of coastal erosion by providing additional sediment which satisfies erosional forces, beach nourishment is a flexible coastal management solution, in that it is reversible, and as a result of sediment redistribution by longshore drift, beach nourishment is likely to positively impact adjacent areas which were not directly nourished. The disadvantages: nourishment is not a permanent solution to shoreline erosion, periodic re-nourishments, will be needed to maintain a scheme"s effectiveness. Sediment deposition can generate a number of negative environmental effects, including direct burial of animals and organisms residing on the beach.

2.3.2 Dredging or sand bypassing

Sand bypassing is the hydraulic or mechanical movement of sand, from an area of accretion to a downdrift area of erosion, across a barrier to natural sand transport such as large-scale harbor or jetty structures. The hydraulic movement may include natural movement as well as movement caused by man. Bypassing commonly takes place by two main methods. First, pumping equipment and piping can be constructed that transfers sand from the updrift side of the littoral barrier, and deposits it as a slurry of sand and water on the downdrift side Chapman MG, Underwood AJ (2011).

The second method involves the dredging or excavation of sand from the updrift side, using dredges or heavy machinery, and the placement of this material on the downdrift side by the dredge (water-based transport), or by trucks and other heavy equipment (land-based transport). The advantages are adding to tourist amenity by making bigger beach, attractive, and work with the natural processes of the coast. The disadvantages: needs frequent renewal of more sand and does not protect cliff face from winter storm waves.

2.3.3 *Sand dunes stabilization*

Sand dunes are naturally wind-formed sand deposits representing a store of sediment in the zone just landward of normal high tides. Dune/sand stabilization involves using structural controls and native vegetation to stabilize, build, or repair dunes. Vegetation can be used to encourage dune growth by trapping and stabilizing blown sand. Dunes provide habitat for highly specialized plants and animals, including rare and endangered species. They can protect beaches from erosion and recruit sand to eroded beaches.

As noted above, each method of structural beach protection has its disadvantages. In recent years, several communities have moved away from structural-type protection measures in favor of beach nourishment (Dean, 2003). This leaves sand dunes as the primary line of protection against erosion, upland flooding, and upland damage. Dunes are also excellent for the environment. Sand dunes are the primary location for sea turtle nesting and the home of many other wildlife species. Additionally, dunes and ongoing beach nourishment projects positively impact beach tourism. However, dunes are highly erodible and overall are very susceptible to failure during large-scale storm events. It would be beneficial if there were a sustainable, rapidly deployable mechanism that could be used to strengthen dunes to make them less susceptible to erosion and scour.

2.4 Historical development of MICP

The significant contributions towards the development of MICP techniques are presented in Figure 2.2 in chronological order. Arguably, MICP was first applied for geotechnical applications in 1995 by Gollapudi et al. for controlling leaching of groundwater contaminants in highly permeable channels by packing a mixture of bacteria (*Bacillus pasteurii*) with sand. Note *Bacillus pasteurii* is an outmoded taxonomic name for *Sporosarcina pasteurii*, which is a gram-positive bacterium with the ability to precipitate calcite. Gollapudi et al. observed a maximum of 75% reduction in permeability, which was achieved after 95 h. Stocks-Fischer et al. further investigated the physical and biochemical properties of $CaCO_3$ precipitation via MICP using *B. pasteurii*. They observed that the microorganisms used in the MICP process create an alkaline environment and provide nucleation sites favourable for $CaCO_3$

precipitation. They hypothesized that, at high biomass concentrations, the rate of $CaCO_3$ precipitation decreases possibly due to accumulation of calcium ions (Ca^{2+}) over the surface of the bacteria cells. Later, Fujita et al., while studying the application of MICP as a remediation technique for divalent radionuclides and other contaminants, e.g., strontium[90] ($^{90}Sr^{2+}$) in groundwater, suggested that the rate of $CaCO_3$ precipitation is directly related to the rate of urea hydrolysis in an alkaline environment. MICP was also used by Hammes et al. to facilitate the removal of soluble calcium (Ca^{2+}) from industrial wastewater as an alternative to the use of Na_2CO_3. Their results showed that about 85–90% of Ca^{2+} was removed by using 8.3 mM of urea.

The application of MICP in the improvement of strength and stiffness for soils was first studied in 2002 by Ismail et al. They found an increase in the unconfined compressive strength (UCS) of MICP-treated soil after 5 h of treatment. Several factors were identified that influenced the UCS including the strength of individual grains, soil grain size and shape, density of soil and the presence of pre-existing calcite crystals. Despite earlier applications in soil improvement, little was known about the performance of urease produced by bacterial cells during the MICP process. Whiffin was the first to develop a model called the "Whiffin's conductivity method" to predict the changes in urea hydrolysis during $CaCO_3$ precipitation by measuring the electrical conductivity of the MICP solution. The shear strength and stiffness of MICP-treated soil were later evaluated by DeJong et al., using a series of consolidated isotropically undrained compression (CIUC) triaxial tests. Their results showed that MICP-treated soil specimens exhibited a non-collapse/strain-softening behavior with a higher initial shear stiffness and ultimate shear capacity compared to untreated loose specimens.
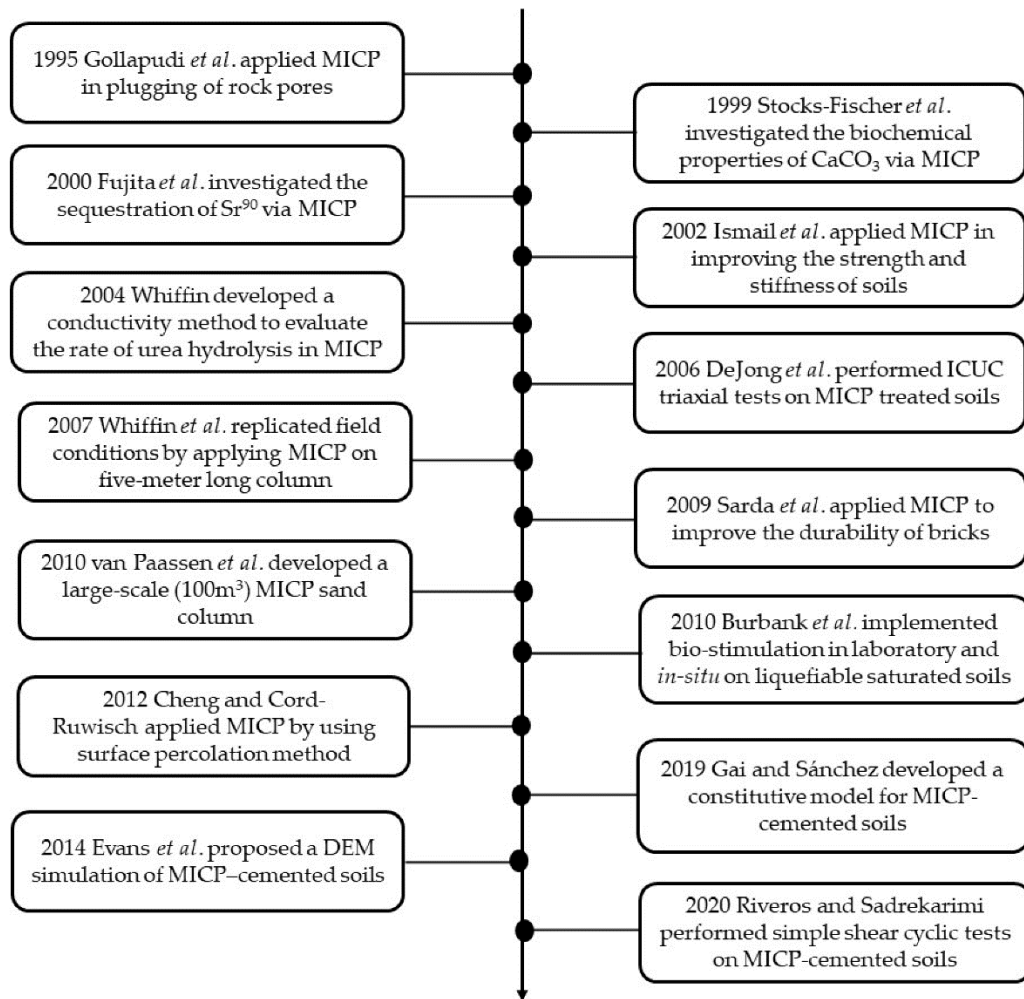
Figure 2. 2: A timeline of the historical development of MICP (After Rahman et al., 2020).

In MICP, biocementation (generation of particle bonding) and bio-clogging (production of pore-filling materials) have notably been explored. Over the last decade, the MICP technique has been applied to enhance the engineering properties (strength and stiffness) of different soils reduce the liquefaction potential of loose sand heal cracks, control erosion and reduce soil permeability via bio-clogging.

Other studies have attempted to investigate the different factors affecting the MICP treatment process. Despite numerous laboratory-scale studies, there have been a lot of uncertainties regarding the overall effectiveness of the technique in large scale applications. Van Paassen et al. reported a large-scale MICP experiment with a 100 m^3 sand specimen. Their results showed that MICP treatment significantly improved the strength and stiffness of granular soils in large-scale applications. However, the

uniform distribution of cementation, especially in large-scale experiments, still proves to be a significant challenge.

Constitutive models are being developed and implemented for the prediction of the soil-cement and stress-strain behavior of MICP-treated soils. Discrete element method (DEM) simulations of MICP-cemented sand have been used to evaluate the micro-scale behavior of the sand-$CaCO_3$ bond.

In recent years, research efforts have grown significantly in terms of investigating various aspects of the MICP process. Figure 2.3 (a) presents a snapshot of the number of publications starting from 1995 to date and shows exponential growth in the number of publications reflecting the growing interest and increased research intensity in the field. While the majority of the research (about 70%) has been conducted in the US and China (Figure 2.3 (b)), researchers from Iran, Australia, Canada, Brazil, India, middle eastern countries, Russia, Europe, south-east Asia and Africa have also stepped in to contribute to the knowledge base.
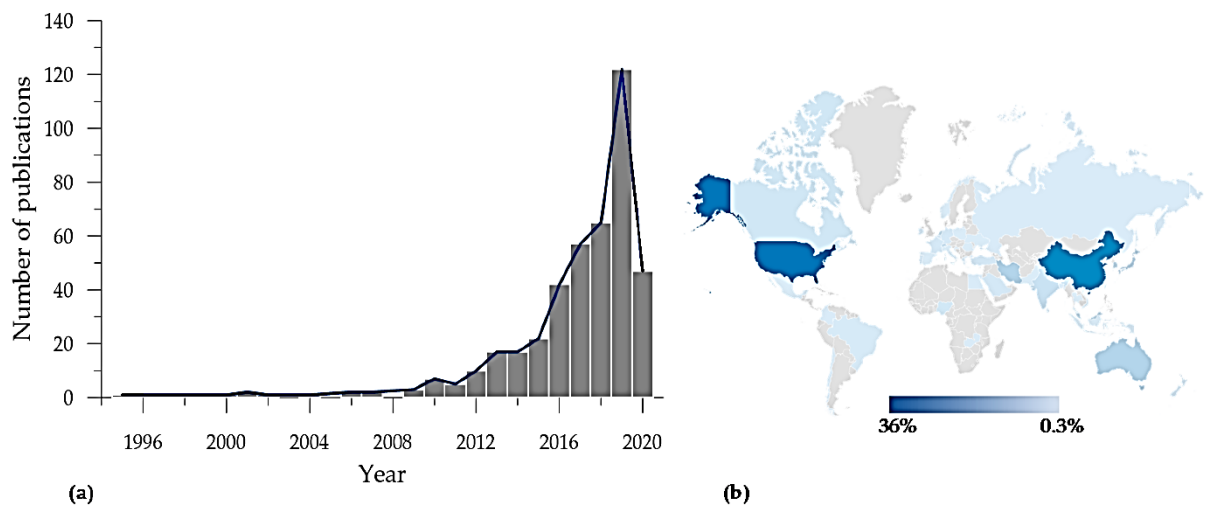
Figure 2. 3: (a) Publications on MICP—a year by year picture (b) country distribution of contributing authors (data source: Web of Science Creative Analytics).

2.5 Biocementation and mechanism of MICP process

Biocementation (or Microbial cementation) is a cementation process (learned from natural beachrock formation mechanism) in which sand particles are coagulated using the metabolic activities of microorganisms. Danjo and Kawasaki (2013) examined a formation mechanism (Figure 2. 4) of beachrock in Okinawa, Japan,

understanding this natural formation mechanism of beachrock is an important step to making artificial beachrock. Microbial cementation is to form soil particle-binding material after introduction of microbes and specific additives into soil. In this method precipitation of carbonate (CO_3^{2-} ion of calcium, magnesium etc. is used to fill the sand voids where CO_3^{2-} ion is produced by bacterial metabolism. Urea producing bacteria are used in this process mainly. It is different from biobinding, which is formation of the particle-binding cellular chains (Ivanov and Chu 2008). Biobinding can be performed by mycelial fungi, actinomycetes, and filamentous phototrophic and heterotrophic bacteria (Ivanov and Chu 2008). In some experiments, the added biomass of some fungal strains binds the sand grains and increases the shear strength of soil (Meadows et al. 1994).
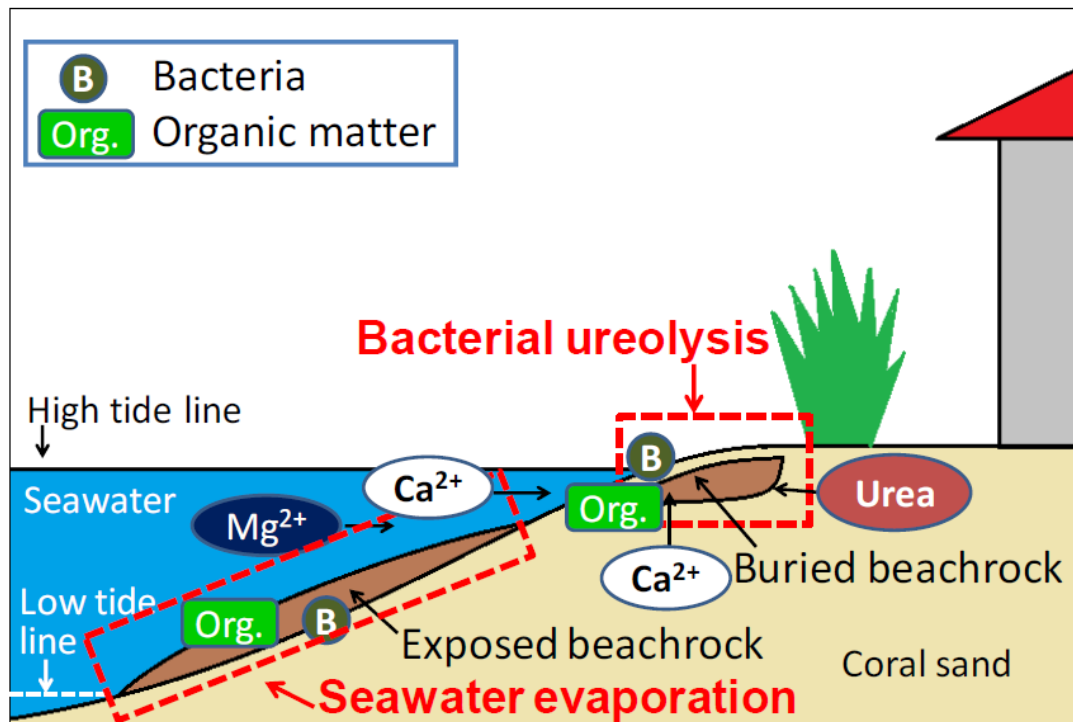
Figure 2. 4: Proposed formation mechanism of beachrock at the study site (Danjo and Kawasaki 2013).

There are various metabolic pathways leading to MICP, and urea hydrolysis is the most prominent for the formation of beachrocks. The reactions occurring in this mechanism are represented by the following equations (Equations (1)–(3)), wherein urea hydrolysis occurs by urease enzyme and produces ammonium ion and carbamate,

mentioned in Equation (1), and subsequently, the carbamate ion is hydrolyzed to form an additional ammonia ion and bi-carbonate, shown in Equation (2).

$$CO(NH_2)_2 + H_2O \xrightarrow{Urease} H_2NCOO^- + NH_4^+ \qquad (1)$$

$$H_2NCOO^- + H_2O \ \rightarrow HCO_3^- + NH_3 \qquad (2)$$

Then, calcium carbonate is formed and finally precipitated, which plays a major role for binding the sand particles. In the presence of Ca^{2+} ions, calcium carbonate is then formed and precipitated, which is effective for the binding of sand particles and for the filling of micro-space:

$$Ca^{2+} + HCO_3^- + NH_3 \rightarrow CaCO_3 \downarrow +NH_4^+ \qquad (3)$$

In the MICP method, precipitation of carbonate minerals is an important factor that occurs through extracellular or intracellular pathways by a sequence of chemical reactions and physiological pathways, which are a key factor for the making of solidified sand that is close to natural beachrock, and could be effective for various bioengineering applications (Sarayu et al., 2014). Therefore, for successful implementation of the MICP method in the bio-geoengineering field, environmental factors such as temperature, pH, duration of bacterial cultivation, and crystal precipitation tendency need to be assessed.

2.6 Suitable microorganisms for MICP process

Various heterogeneous bacterial groups are linked to the pathway for MICP process (Dhami et al., 2014). Braissant et al., (2002) suggested that this pathway might be extremely common in natural environment due to the abundance of low molecular weight acids in soils, especially by fungi and plants. Table 2. 1 summarized the possible pathway and condition for selecting bacteria for MICP process.

Table 2. 1: Possible microbial processes that can lead potentially to biocementation (Source: Chu, 2012).

Physiological group of microorganisms	Mechanism of biocementation	Essential conditions for biocementation	Potential geotechnical applications
Sulphate reducing Bacteria.	Production of undissolved sulphides of metals.	Anaerobic conditions; the presence of sulphate and carbon source in soil.	Enhance stability for slopes and dams.
Ammonifying Bacteria.	Formation of undissolved carbonates of metals in soil due to an increase of pH and release of CO_2.	Presence of urea and dissolved metal salt.	Mitigate liquefaction potential of sand. Enhance stability for retaining walls, embankments, and dams. Increase the bearing capacity of foundations
Iron-reducing Bacteria.	Production of ferrous solution and precipitation of undissolved ferrous and ferric salts and hydroxides in soil.	Anaerobic conditions changed for aerobic conditions; the presence of ferric minerals.	Density soil on reclaimed sites and prevent soil avalanching. Reduce liquefaction potential of soil.

However, the MICP treatment can be achieved by stimulating the growth of indigenous bacteria in situ (bio-stimulation) or by augmenting ureolytic bacterial culture (bio-augmentation). Bio-stimulation is a process of modifying the in situ environmental conditions (e.g., nutrients and pH conditions) to enrich the existing microbial community with required urease capabilities for MICP purpose (Fujita et al., 2000; Gomez et al., 2015). If ureolytic bacteria are present in the subsurface, stimulating the population size and urease activity by supplying suitable nutrients is ideal, because it utilizes native organisms and reduces the engineering challenges of controlling the transport of cells in the subsurface (DeJong et al., 2009). However, there are some drawbacks reported to bio-stimulation process, shown in Table 2. 2.

Table 2. 2: Summary of advantages and disadvantages of MICP pathways (modified from Gowthaman, PhD dissertation 2020).

MICP pathways	Advantages	Disadvantages
Bio-stimulation	i. Elimination of non-native microbial supply ii. Fitness of the microbes, i.e. reliable at native environment iii. Less challenges of controlling transport of cells in subsurface iv. More possibility of approval by public and regulatory agencies	i. Applicable only if the ureolytic bacteria are present ii. Diffuse zone of improvement iii. Risks regarding the stimulation of pathogenic/ harmful strains
Bio-augmentation of exogenous bacteria	i. High initial performance ii. Possible homogeneous cementation at/ around near-surface zones	i. Microbial pollution ii. Uncertainties in long survival iii. Use of exogeneous bacteria is forbidden in some countries iv. Log-linear distribution of bacteria from supply point
Bio-augmentation of indigenous bacteria	i. Elimination of non-native microbial supply ii. Fitness of the microbes, i.e. reliable at native environment iii. Possible homogeneous cementation at/ around near-surface zones iv. More possibility of approval by public and regulatory agencies	i. Hydrolysis of urea relatively at slow rates ii. Log-linear distribution of bacteria from supply point

2.7 Factors affecting MICP process

2.7.1 pH

The pH of the environment controls the survival and the metabolic activity of the microorganisms that indirectly involved in the secretion of the calcite products Hammes *et al*., 2002; Dilrukshi & Kawasaki, 2016). High pH favours the conditions for the formation of CO_3^{2-} from HCO^{3-} which leads to calcification of the generated bicarbonate (Knoll, 2003). Stocks-Fischer *et al*., (1999) stated that the optimum pH for urease ranges between 7.0 to 8.0, which was further supported by the other research findings. Stocks-Fischer *et al*., (1999) also reported that urease activity rapidly increased from pH 6.0 to 8.0, until it reached its peak (pH 8.0) and gradually decreased

when at higher pH. However, Wei-Soon *et al*., 2012; stated that urease activity is still active at pH 9.0. A recent study by (Fujita, *et al*., 2017) showed that urea hydrolysis leads to an increase in the pH of growth medium due to the production of ammonium using *Pararhodobacter* sp.

On the other hand, a study by (Canakci, *et al*., 2015), which focused on the process of bacterial calcium carbonate precipitation in organic soil showed that when soils samples were treated with the bacterial solution, the pH values varied between 9 to 9.4 during the period the sand samples were being treatment. It indicated that this range, that the treatment medium used was appropriate for MICP process as suggested by Mortensen, *et al*., 2011.

2.7.2 Temperature

Enzymatic reactions such as urea hydrolysis by urease are dependent on temperature (Mitchell & Ferris, 2005). The optimum temperature which favours urease hydrolysis ranges between 20 to 37 °C (Okwadha, *et al*., 2010), however, enzymatic reactions for optimum production is influenced by environmental conditions and the concentration of reactants in the system which was studied by Mitchell and Ferris (2005). They also reported that urease activity increased between 5 to 10 times when temperature increased between 10 to 20 °C. Ferris *et al*., 2004 and Dhami, *et al*., 2013 investigated the kinetic rate of urease and temperature on *Sporosarcina pasteurii*. Their findings showed that urease was very stable at 35 °C, but the enzymatic activity decreased by 47% when the temperature increased to 55 °C. However, other studies reported by Lian, *et al*., (2006) on temperature effects on urease activity showed that optimum 60 °C was the optimum temperature for the production of urease. This temperature for urease activity is impractical on site for soil treatment using MICP (Wei-Soon *et al*., 2012).

2.7.3 Bacterial cell concentration

Unlike other multicellular organisms, bacterial population has greatly affected the urease activity because bacteria grow to a fixed size and then reproduce through binary fission, a form of asexual reproduction and under optimal conditions, bacteria can grow and divide extremely quickly, and bacterial populations can double as quickly as every 9.8 min (Siddique & Chahal, 2011). It is also reported that ureolysis rate is linearly

proportional to cell concentration (Lauchnor, *et al*., 2015). Therefore, the type of bacteria which appropriate for MICP application should be able to catalyst the urea hydrolysis. The typical urease positive bacteria used for MICP are aerobic bacteria, are often selected for MICP process because of their ability to release CO_2 which is essential for the rise in pH due to the production of ammonium when urea is being broken down (Wei-Soon, *et al*., 2012).

2.7.4 Nutrients

Nutrients are the energy sources for bacteria, providing sufficient nutrient the ureolytic bacteria is critical for precipitation of calcite. Nutrients are often supplied to the bacteria during culture and soil treatment stages (Kadhim, 2016). The most common nutrients usually provided to bacterial include Potassium, Sodium, Nitrogen, Calcium, Iron and Magnesium (Mitchell *et al*., 2005). The unavailability of organic constituents in soil limits the bacterial growth, hence the supply of sufficient nutrient to soil containing ureolytic bacteria can promote bacterial growth which can enhance calcite precipitation required in achieving the desired level of ground improvement.

2.7.5 Availability of nucleation site

Stocks-Fischer *et al*., (1999) proposed that the bacterial cells served as a nucleation site for MICP occurrence. Their findings showed that about 98% of the initial concentrations of Ca^{2+} were precipitated via MICP. On the other hand, only 35 to 54% of chemically induced calcite was observed. It was then revealed that the bacterial cells provided a nucleation site for calcite precipitation which influences the environment for further calcite to be induced, was responsible for the differences in calcite precipitation via MICP and chemical processes. other studies also showed that the availability of nucleation sites serves as one of the key factors for microbial calcite precipitation which takes place at bacteria cell walls (Knorre and Krumbein, 2000; Lian, *et al*., 2006).

2.8 Potential geotechnical applications of MICP

2.8.1 MICP for liquefaction mitigation

Liquefaction is a phenomenon marked by a rapid and dramatic loss of soil strength, which can occur in weak deposits subjected to earthquake motions. Typically,

the deposits consist of loose, saturated cohesionless soils with insufficient cyclic shear strength are often reported to be susceptible to liquefaction. In the past, several studies have demonstrated that the MICP process could offer a ground improvement method, reducing the liquefaction susceptibility and the damage due to seismic loading.

Montoya et al., (2013) conducted geotechnical centrifuge tests (1-m radius Schaevitz centrifuge) to evaluate the potential of MICP treated soil to increase soil resistance to liquefaction triggering, established the technique as a natural and sustainable solution. The responses of the soil were extensively evaluated at varying cementation levels. Depending on the level of cementation, various failure patterns were observed, when subjected to seismic loading. The failure of the heavily cemented specimens were structural fractures, whereas 23 the lightly and moderately cemented specimens revealed a global soil like failure. Montoya (2012) observed reduced excess pore pressure generation, reduced settlements, and greater peak surface accelerations compared to the untreated loose saturated sands under seismic loading. Burbank et al., (2013) compared cyclic shear test results of sand treated with MICP and Portland cement, and found the cyclic stress ratio (CSR) of the MICP treated soil was higher than the cement-treated soil for similar quantities of cementing agent. Han et al., (2016) found that treating sand with MICP takes less time to improving liquefiable sand than colloidal silica grouting to achieve a similar liquefaction resistance. Considering the dynamic loading from waves and earthquakes, Xiao et al., (2018) studied the liquefaction potential of MICP treated calcareous sands using cyclic triaxial tests. The study indicated that the increase in confining pressure leads to a decrease in the liquefaction resistance for bio-cemented specimens. In addition, they found that the number of cycles to liquefaction increased with increasing cementation content, similar to that observed by Montoya et al., (2013). Zamani et al., (2018) investigated the liquefaction resistance of three silica soils with varying grain sizes treated to moderate level of MICP cementation. The results showed that reduction in grain size and increase in angularity result in a higher resistance to liquefaction after MICP treatment.

2.8.2 MICP for dust control

The various applications of the biotreatment of soils include the control of permeability, improvement of the bearing capacity, strength and stiffness development, and the control of dust due to erosion. The air quality in the majority of cities worldwide

is becoming a grave concern due to the increase in population and urbanization. In this scenario, measures to curb the deterioration of air quality are developed to safeguard the environment. Dust contributes to the deterioration of air quality. According to Watson et al., the major sources of air pollution in the major cities of the U.S. are vehicular emissions and dust from roads. With dust's severe impact on the air quality, methods to reduce dust emission are employed. These methods include using dust suppressants, spraying water, and providing wind shield walls against dust emission. Chang et al. reported that water spraying to control dust serves the purpose for a maximum duration of 4 h. Using water for dust suppression impacts water reserves, since water offers a temporary remedy and needs repeated application. Additionally, chemically activated suppressants for dust control are highly corrosive and hamper the environment. Sustainable and eco-friendly dust control techniques are on high demand. Dust control using biotreatment can be achieved in the same way that sand solidification in the desert can be carried out; potential dust sources with dust particles can be dealt with through biocementation. Sun et al. conducted a study on dust near a quarry site in China by developing a simulation of rainfall erosion and by conducting field tests. Their test methods involved ascertaining surface strength, which is most vulnerable to wind erosion. Surface hardening was obtained by spraying biotreatment solutions on the surface; after spraying a thin and hard calcite on the surface, a crust of soil was formed. Meyer et al. used *Sporosarcina pasteurii* to treat two soil types to control air pollution due to dust. The treated soils were made to pass through a wind tunnel, and the amount of reduction in soil mass after exposure in the wind tunnel was observed to express the amount of wind erosion. The results obtained from this work showed that microbially precipitated calcite was very much effective in controlling soil erosion, as proven by wind tunnel experiments. Naeimi and Chu compared the effectiveness of dust control through the biotreatment method and conventional techniques. *Sporosarcina pasteurii* was used in their study to treat sand against dust emission. The comparison was done on the same sand treated with calcium lignosulfonate, water, and calcium chloride. Their results showed that the biotreatment of soil exposed to wind in the wind tunnel improved erosion resistance, and only 1.5% mass loss was observed.

Most of the conventional methods for fugitive dust control, including the application of water, salt, or synthetic polymers, are reported to be ineffective in arid climates (Hamdan and Kavazanjian, 2016). MICP, as a promising method, has gained

the attention in the recent past. Meyer et al., (2011) studied the applicability of MICP for the dust control by examining the effects of bacterial concentration, temperature and humidity, and fines content on erosion resistance. They found that a higher fines content and higher temperature and humidity helped form the soil crust that resisted fugitive dust emission. Maleki et al., (2016) investigated the erodibility of MICP treated sand in a wind tunnel under wind velocity condition of 45 km/h and shown the maximum weight loss was around 1.29 and 0.16 % for low and high MICP soils, indicating a significant enhancement. Chen et al., (2016) tested the MICP treated desert sand under a wind velocity of 33 m/s for 20 minutes at flat and inclined (30 °C) conditions, observed negligible mass loss from the MICP surfaces even after the exposure of 12 freeze-thaw cycles. Similarly, Zomorodian et al., (2019) demonstrated the stable crust formation on silica and carbonate sands by spraying-MICP, which was found to be reliable at simulated 20 m/s winds.

By using large-scale wind tunnel, Naeimi and Chu (2017) concluded that the required precipitation to control the dust generation by 70% is around 15 g $CaCO_3/m^2$ under a simulated wind condition of 40 km/h (tested to the duration of 6 minutes). Very recently, using the digital imaging technology, Bick et al., (2019) captured the initiation of sporadic and sustained erosions in MICP treated sand and evaluated the shear strength variation timely. Overall, studies confirmed that the MICP have a significant impact on the reduction of wind erosion, reducing the number of airborne particles.

2.8.3 MICP for coastal erosion protection

Among the wide range of MICP applications, attentions have also been given on reinforcing loose sand bodies of nearshore areas and preventing cliffs scouring, thereby improving the responses against erosion from wave action without impairing the intrinsic transient characteristics. Cheng et al., (2014) investigated the feasibility of utilizing the calcium ions dissolved in seawater as the sole source of calcium for MICP. The results revealed that the UCS could increase up to 300 kPa with retained permeability of 30%, suggesting good drainage ability. Salifu et al., (2016) have investigated the erodibility response of the MICP treated small foreshore slopes under tidal wave effects. The results showed that a shallow treatment depth could significantly increase the stability of treated surface against the tidal effects.

Nayanthara et al., (2019) studied the effect of Mg^{2+} availability on the MICP efficacy of coast sand. The results indicated that the formation of needle shaped magnesium carbonate crystals significantly reduced the UCS at higher initial Mg^{2+} concentrations. Results also suggested that the concentrations of Mg^{2+} that naturally exists in coastal environment had negligible effects on the MICP efficiency. Recently, Imran et al. (2019) proposed a sustainable and cost-effective approach, i.e., a combination of geo-tube and MICP for preventing coastal erosion. For instance, Daryono et al. (2020) attempted to compare the geo-physical characteristics of natural and MICP induced artificial beach-rocks, revealing that the formation of natural beach-rocks are governed by several geological factors and marine activities, and are incomparable with MICP materials. Among the soil degradation processes, erosion is one of the most serious degradation processes, and which is primarily persuaded by rainfall and snow melt. Up to now, only few studies have investigated the erodibility of MICP treated deposits through various strategies. By using the simple fume tests, Bao et al., (2017) have conducted sets of flume tests to study the erodibility of MICP treated sands, demonstrated the high surface stability of MICP treated cohesionless sand against scouring. In another study, water jetting erosion test was performed to study the MICP treated sand, showing that the formation of an impermeable stiff crust with thickness of 2.5 cm could markedly increase resistance to erosion (Gomez et al., 2013). Similarly, shallow MICP treatment were also recommended by Salifu et al. (2016) for tidal erosion control. Potential of MICP in controlling seepage-induced internal erosion of gravel-sand mixtures has also been examined by few researchers, suggested that the formation of calcite clusters within the soil is responsible for reduction in erosion (Jiang and Soga, 2019, 2017). Studies also showed that the increase in the predicated calcium carbonate content could increase the resistance to internal erosion. Considering all the above limitations, this study could play an important role for coastal erosion protection measure using MICP method.

2.9 Mechanism of EICP process

EICP offers an alternative for the hydrolysis process by the use of a free water-soluble enzyme derived from an agricultural source used as a catalyst (Hamdan and Kavazanjian 2016; Oliveira et al., 2017; Park et al., 2014). This increases the groutability of the enzyme inside soil pores since there is no need to provide nutrients

or air for bacterial activity, which increases the field applicability for various soil types (Khodadadi et al., 2017). The schematic diagram in Figure 2.5 shows the EICP hydrolysis reaction and the constituents of the EICP cementing solution. Two common approaches are used for the measurement of enzyme properties and activity, namely, discontinuous and continuous approaches. In EICP, the discontinuous approach involves mixing the substrates (urea and $CaCl_2$) and enzyme together and measuring the product ($CaCO_3$) formed after a set period. The chemical equations involved in this reaction are same as MICP. This approach has been widely used in a number of studies to quantify the $CaCO_3$ precipitation ratio (PR). PR is the ratio of the mass of precipitated $CaCO_3$ to the theoretically possible maximum precipitation mass, which depends on the concentrations of various chemicals in the solution. However, the discontinuous approach cannot be used to capture the catalytic properties of the enzyme-catalysed reaction, such as the influence of urease activity and product inhibition. The continuous method of enzyme assay involves the study of the rate of an enzyme-catalysed reaction by mixing the enzyme with the substrate (mostly urea) and continuously measuring the product (e.g., NH_4^+) formed or the dissociation of the substrate over time.
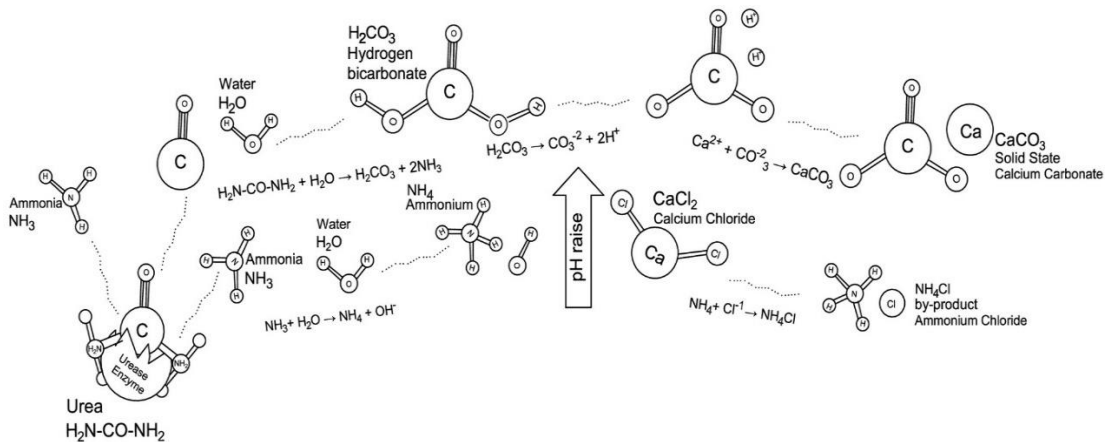
Figure 2. 5: Description of the hydrolysis process catalyzed by the free urease enzyme (EICP) (After Arab et al., 2021).

2.9.1 Potential sources of urease enzyme in EICP process

Enzyme induced carbonate precipitation (EICP) is an innovative ground improvement technique that involves calcium carbonate ($CaCO_3$) precipitation via the hydrolysis of urea ($CO(NH_2)_2$) into ammonium (NH_4^+) and carbonate (CO_3^{2-}) ions catalysed by the urease enzyme. The EICP process has the potential to be applied as

bio-cementation and bio-remediation solutions in many environmental, construction, geotechnical and civil engineering problems, such as improving soil strength, reducing soil liquefaction potential, surface erosion control, reducing permeability, heavy metal contaminant remediation and so forth (Krajewska, et al., 2017; Putra, et al., 2017; Ahenkorah, et al., 2020; Neupane, et al., 2015; Hamdan, et al., 2015). One advantage of EICP is the smaller size of the urease enzyme crystals (typically 12 nm or 120 Å), rendering the process effective for a wider range of soils, including fine-grained soils. From the literature, the most extensively studied urease enzymes are sourced from Jack bean. Other plant species rich in urease include Weeping bottlebrush (*Callistemon viminalis*), Mulberry (*Morus alba*), Palo verde (*Parkinsonia florida*), Pigweed (*Chenopodium album*), Pigeonpea (*Cajanus cajan*), Bitter melon seeds (*Momordica charantia*), Squash seeds (*Cucurbitaceae*), Soybean (*Glycine max*), Sword beans (*Canavalia gladiata*), Watermelon seeds (*Citrullus lanatus*), Cabbage leaves and Soy pulp. Urease is also found in the leaves of same plants listed above and many more including some non-farmed plants common to semi-arid environments such as the *Callistemon viminalis* (weeping bottlebrush) (Hirayama et al., 1983; Hogan et al., 1983). Hogan et al., (1983) showed that simply chopping the leaves of several urease containing plants, rather than chemically extracting the enzyme, was sufficient to induce urease activity in urea solutions. Recent preliminary work using coarsely chopped leaves from *Parkinsonia florida* (palo verde, Fabaceae family) indicates that urease is present in the leaves of this drought resistant tree common to U.S. Southwest. In addition to their broad availability, extraction of the urease enzyme from some crops has been shown to be very simple requiring only basic laboratory equipment (Kayastha & Das, 1999; Srivastava et al., 2001). The fruits, seeds, and beans of most urease containing plants can be readily obtained from local markets and the enzyme can then be isolated following well-established protocol. The leaves of urease containing plants can be obtained as plant litter and enzyme extraction may be pursued through several methods including crude and inexpensive leaf extractions methods. The enzyme can also be acquired from laboratory suppliers since urease has many uses including biomedical applications.

2.9.2 Molecular Structure of urease enzyme and mechanism of carbonate precipitation

Enzymes are highly selective biopolymeric macromolecules that catalyze chemical reactions without being consumed in the reactions. Enzymes have complex 3-dimensional structures based on chemical bonding and electrostatic interactions that can be reversibly or irreversibly altered (denatured) under certain environmental and chemical conditions. There are a number of thermodynamic and chemical mechanisms that contribute to the catalytic power of enzymes. One of the major thermodynamic mechanisms is the decrease in entropy upon formation of the enzyme-substrate complex. The binding of a substrate to its enzyme results in the molecular organization of these two chemical units reducing their ability to freely interact within their chemical environments. A decrease in entropy results in a positive addition to ΔG, a thermodynamically unfavorable condition which promotes the destabilization of the ES complex to EX and thereby pushes the reactants to products, or decouples the ES complex. Desolvation is another mechanism that destabilizes the ES complex. Binding of a substrate removes its waters of hydration which can increase the enthalpy of solvation ($+\Delta H$) and make the substrate more reactive. There are several chemical mechanisms that strongly affect the catalytic power of enzymes that include: (1) structural strain, (2) covalent catalysis, (3) general acid-base catalysis, and (4) metal ion catalysis. Structural strain is a common destabilization mechanism that induces bond strain in the substrate, the enzyme, or both. Covalent catalysis is the formation of covalent bonds between the enzyme and the substrate and is typically driven by a nucleophilic attack of the enzyme by the substrate. General acid-base catalysis is common to nearly all enzyme reactions and can mediate the formation of the ES complex, drive covalent catalysis, and induce structural strains. Metal ion catalysis is especially important to the metalloenzyme urease that requires two Ni atoms to stabilize the enzyme's native state. Metal ions serve as electrophilic centers that activate the substrate by stabilizing increased electron density during a reaction and also assist in coordinating the ES complex.

Urease enzyme is a nickel-containing metalloenzyme synthesized by some plants, bacteria and fungi (Carmona, et al., 2016). Ureases belong to the superfamily of amidohydrolases and phosphotriesterases, which display catalytic mechanisms in their active sites (Figure 2.6). In general, ureases contain two Ni^{2+} ions in their active sites. It has been well-established in the literature that the overall protein scaffold is

conserved among ureases from different sources (Sumner et al., 1926). Urease enzymes in plants and fungi generally consist of homo-oligomeric proteins with identical sub-units compared to the multimeric proteins found in bacterial ureases which are formed from a complex of two (αβ) or three (αβγ) subunits (Mazzei, et al., 2020). These proteins appear to act as urease-specific chaperones required for assembling an active urease (Kafarski, et al., 2018; Follmer, et al., 2008; Mobley, et al., 1995; Sirko, et al., 2000). The mmechanism of $CaCO_3$ precipitation by EICP and MICP has been presented in Figure 2.7.
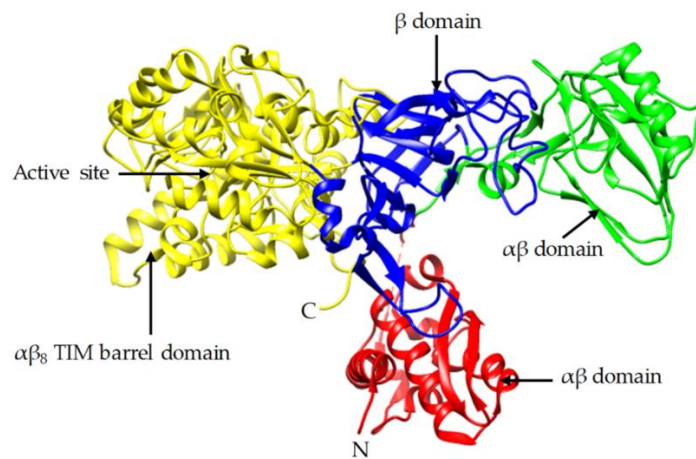
Figure 2. 6: Three-dimensional crystal structure of Jack bean urease (Ahenkorah 2021).
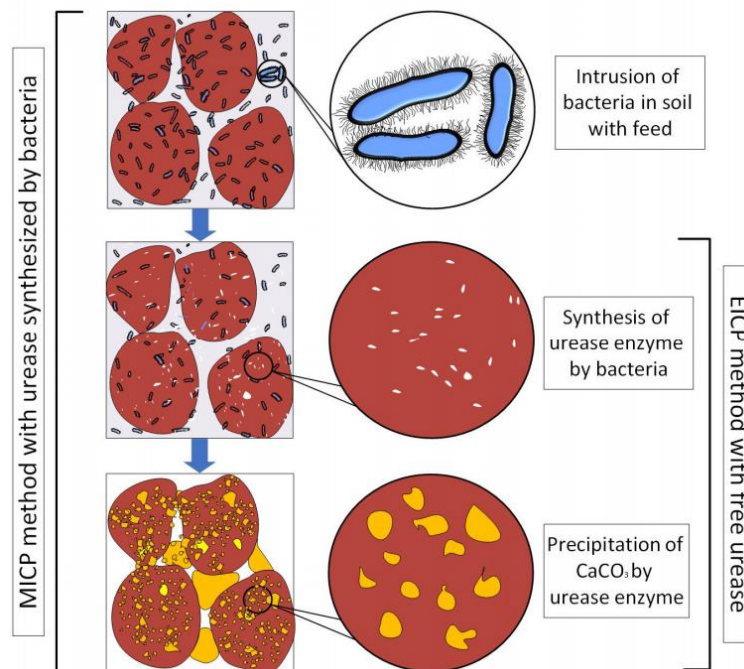
Figure 2. 7: Mechanism of $CaCO_3$ precipitation by EICP and MICP (Almajed 2021).

2.9.3 Use of plant-derived urease in the field of geotechnical engineering

Nowadays, the urease enzyme is widely used in different fields of industries such as medicinal, construction, agricultural, food, etc. Different kinds of ureolytic bacteria and micro algae, soil urease and plant urease have applied for the above fields.

Yasuhara et al., (2011) investigated the use of free urease enzyme to induce calcium carbonate precipitation in sand. They used test tube experiments to provide basic assessments of the influence of concentrations of urea, $CaCl_2$, and urease on carbonate precipitation.

Yasuhara et al., (2012) also conducted unconfined compression tests on toyoura sand samples treated using EICP with two different concentrations of urea to calcium chloride.

Neupane et al., (2013) also conducted test tube tests to find the optimum concentration for EICP for improving soil properties. Their results indicate that higher precipitation efficiency was achieved at lower concentrations of urea and calcium chloride.

Putra et al., (2016) discuss the addition of magnesium chloride to urea, $CaCl_2$, and urease enzyme to modify the precipitation process. The concentration of magnesium chloride to urea, $CaCl_2$ was fixed 0.50 mol/L, and 1 g/L of urease. Poorly graded sand and high-activity urease enzyme (2950 U/g) were used in this experiment.

Knorr (2014) investigated the use of EICP to control fugitive dust through wind tunnel tests. He prepared over 50 pans with three different types of soil and varied concentrations of urea and calcium chloride, from concentrations as low as 0.1 M up to concentrations as high as 2.0 M, but with a fixed concentration of urease enzyme of 0.5 g/L.

Kavazanjain and Hamdan (2015) used free urease enzyme to induced carbonate precipitation in two columns containing different types of soil: F-60 silica sand and Ottawa 20-30 sand. They prepared their samples in 152 mm x 51 mm containers by mix-and compact and injection methods.

Hamdan (2015) and Hamdan et al., (2016) studied the use of xanthan gum, guar gum, and inert polyol-cellulose hydrogels to improve the efficiency of EICP in unsaturated soil via surficial spraying and percolation. They hypothesized that the viscosity of these mixtures would direct the precipitation reaction to the contact points between soil particles. They tested their hypothesis through two experiments. The first

one used 50 mL glass beakers to assess the precipitation of EICP without adding soil. The second experiment involved filling paper cups with F-60 silica sand and pouring the EICP solution with and without hydrogel onto the soil.

2.10 Potential geotechnical applications of EICP

Enzyme induced carbonate precipitation (EICP) potentially has the same applications as MICP over a wider range of soils due to the small size of the urease enzyme and water solubility of the EICP solution. These problems include slope stability, erosion and scour, under-seepage of levees, the bearing capacity of shallow foundations, tunneling in running or flowing ground, and seismic settlement and liquefaction. Research presented herein suggests that among the ground improvement techniques in which EICP can be employed to achieve these goals is formation of cemented columns of soil by infusing cementation solution through a perforated tube or pipe pushed into the ground. EICP-cemented columns can be installed in patterns similar to root piles (*pali radicii*) for slope stability, micro piles for foundation support, and stone columns or soil cement columns to support embankments and restrict lateral spreading in liquefiable soils. Furthermore, the ability to install EICP piles under existing structures without causing heave or settlement make them ideal for remediation of liquefaction potential beneath existing facilities. Columnar stabilization via EICP can also be employed through mix-and-compact methods. Another area where EICP has potential applicability is for the surficial stabilization of soils against wind driven erosion in semi-arid to arid environments. Stabilization of erodible surficial soils, typically fine to medium grain soils, mitigates several important environmental and geotechnical problems associated with soil erosion. In contrast to mass stabilization techniques, carbonate precipitation for surficial soil stabilization has received comparatively little attention in the literature. Both EICP and microbially induced carbonate precipitation (MICP) can potentially be employed to stabilize erodible surficial soils. The rapid carbonate precipitation induced by the EICP process, in contrast to slower microbial methods, makes it well-suited for surface treatments that have a relatively short time frame within which they need to become effective. However, desiccation can the limit the time an EICP reaction can proceed in semi-arid to arid environments and, thereby, reduce the efficiency of carbonate precipitation. Research presented herein also investigates the potential of EICP in a biodegradable hydrogel for

rapid and efficient stabilization of surficial soils in rapidly desiccating environments. EICP applied in a hydrogel offers unique advantages that further improve efficiency by limiting the spatial extent of carbonate precipitation to the surface (or near surface) via the reduction of hydraulic conductivity associated with the ureolytic fluid. In addition, the hydrogel retains water (a necessary component of ureolysis) to extend the temporal frame of ureolysis, especially in semi-arid to arid environments, for greater substrate utilization and reaction time for carbonate precipitation.

CHAPTER 3 : SAND CEMENTATION TESTS BY MICP METHOD

3.1 Introduction

At present, coastal erosion is a major problem all over the world. Traditional measures consisting of hard and soft defense protection systems are adopted to protect from this disintegration. All of these coastal design and structures have been identified as being expensive to build and sustain because of the scarcity of materials, energy, time, cost, and environmental concern. Therefore, sustainable and eco-friendly materials and systems are in demand for the protection against coastal erosion. Countermeasures against coastal erosion protection have been studied by many researchers (Salifu et al., 2016), including hard and soft structures focusing on urea degradation bacteria. However, all these methods have an adverse effect on the surrounding landscape, environment, and ecosystem (Evelpidou et al., 2008); moreover, eco-sustainability is another major concern.

As an alternative method, earlier studies used the microbially induced carbonate precipitation (MICP) technique focusing on ureolytic bacteria within the field of geotechnology and civil engineering (Mujah et al., 2017a). Among them, T. Danjo and S. Kawasaki conducted several studies in Ishikawa and Okinawa, Japan focusing on beachrock formation mechanism. They found significant information to protect against coastal erosion using the MICP method, which they called "artificial beachrock". Moreover, for coastal erosion protection, the attention of using hard and soft structures, such as geo-tube, beach drainage system, vegetation, sand fencing, artificial reefs, and green belts, are dominating with progressive knowledge (Sheehan & Harrington, 2012). Recently, geo-tube technology has converted from being a substitute construction technique to a key solution of choice in a more advanced way for preventing water logging conditions, as well as coastal erosion protection (Ashis, 2015). The traditional geotextile tube technology for coastal erosion protection is not sustainable because of the penetration of UV (Ultraviolet) rays that could accelerate to damage the geosynthetic product very easily; moreover, it is rather difficult to recover or repair, which would be considered as costly (S. C. Lee et al., 2014). Therefore, this technology needs to be improved and, hence, we proposed a novel approach to protect coastal

erosion through a combination of MICP and geotube, which is more eco-friendly, cost-effective, and more sustainable.

There are various metabolic pathways leading to MICP, and urea hydrolysis is the most prominent for the formation of beachrocks. The reactions occurring in this mechanism are represented by the following equations (Equations (1)–(3)), wherein urea hydrolysis occurs by urease enzyme and produces ammonium ion and carbamate, mentioned in Equation (1), and subsequently, the carbamate ion is hydrolyzed to form an additional ammonia ion and bi-carbonate, shown in Equation (3-5).

$$CO(NH_2)_2 + H_2O \xrightarrow{Urease} H_2NCOO^- + NH_4^+, \qquad (3)$$

$$H_2NCOO^- + H_2O \rightarrow HCO_3^- + NH_3. \qquad (4)$$

Then, calcium carbonate is formed and finally precipitated, which plays a major role for binding the sand particles. In the presence of Ca^{2+} ions, calcium carbonate is then formed and precipitated, which is effective for the binding of sand particles and for the filling of micro-space:

$$Ca^{2+} + HCO_3^- + NH_3 \rightarrow CaCO_3 \downarrow + NH_4^+. \qquad (5)$$

In the MICP method, precipitation of carbonate minerals is an important factor that occurs through extracellular or intracellular pathways by a sequence of chemical reactions and physiological pathways, which are a key factor for the making of solidified sand that is close to natural beachrock, and could be effective for various bioengineering applications (Sarayu et al., 2014). Therefore, for successful implementation of the MICP method in the bio-geoengineering field, environmental factors such as temperature, pH, duration of bacterial cultivation, and crystal precipitation tendency need to be assessed.

In the MICP method, most of the earlier studies addressed ureolytic bacteria as a specific foreign microorganism, and there was a major concern about the adverse effects (for example, competition for nutrients with other species, survival capacity in the new environment, dormancy or sudden shock) on the surrounding environment due to the presence of a large number of foreign species. Therefore, creating artificial beachrock using local ureolytic bacteria by the MICP method can be an alternative for coastal erosion protection, which is a sustainable and eco-friendly biological ground

improvement technique. Most of the research on MICP have been confined to land ureolytic and little attention has been paid to marine ureolytic bacteria for the measurement of urease activity and subsequently, their various environmental effects were not investigated. Marine ureolytic bacteria (e.g., *S. pasteurii*) are able to grow in a variety of freshwater conditions and in saline conditions equivalent to 100% seawater (Mortensen, *et al*., 2011) but land bacteria have low survival capacity. Thus, considering the MICP application it needed to characterize the ureolytic bacterial species (land or marine). Therefore, to overcome the adverse effect, this study aimed to reduce the impact on ecosystems by isolating urea degradation bacteria from local marine sand (Greece), targeting for coastal erosion protection in that specific area (Greece), and later on we will focus on other areas where coastal erosion is a major problem. Isolated native strains were evaluated for urease activity as whole-cell, supernatant and cell pellets and subsequently different environmental parameters were investigated. On the basis of the results, the sand solidification test (syringe) was also performed, and the degree of solidification was quantitatively evaluated by the needle penetration test. Furthermore, for the practical use of this technology, we proposed a novel approach that is sustainable and eco-friendly, one we aim to apply in future for coastal erosion protection in the targeted area.

Moreover, most of the research on MICP has been limited to land ureolytic bacteria, focusing on the urea hydrolysis mechanism and on the efficacy of calcite production, and little consideration has been drawn for marine ureolytic bacteria and their subsequent application. However, some of the previous studies and scope of these studies are mentioned in Table 3.1. Nonetheless, in the present study, we selected marine ureolytic bacteria isolated from a coastal region in Greece, which has the most comprehensive coastlines among the Mediterranean countries and coastal erosion in this region is severe. In order to protect this long coastal shoreline from erosion, the application of the proposed MICP method was suggested towards the creation of artificial beachrock using native ureolytic bacteria because of its long-term sustainability, considering the local coastal climatic environment. Previously, it was revealed that the formation mechanism of beachrocks is greatly influenced by marine ureolytic bacteria, which show a great affinity for $CaCO_3$ precipitation and can be sustained for a long time, which is a key factor for the MICP method. Hence, we isolated three ureolytic bacterial species (16s rDNA analysis) from the Greek coastal

36

area: *Micrococcus* sp., denoted as G1; *Pseudoalteromonas* sp., denoted as G2; and *Virgibacillus* sp., denoted as G3. We selected native ureolytic bacteria (from Greece) due to their sustainability (considering the temperature, pH, etc.) and high urease activity, which is very important for the making of artificial beachrock by the MICP method.

Table 3. 1: Microorganism studied for microbially induced carbonate precipitation (MICP).

Ureolytic Bacteria	Type	References
Sporosarcina pasteurii	Land	Adams, 2015
Bacillus cohnii	Land	Cheng, 2019
Bacillus subtilis	Land	Crone, 2004
Micrococcus sp.	Marine	This study
Pseudoalteromonas sp.	Marine	This study
Virgibacillus sp.	Marine	This study

The effects of temperature, pH, and culture duration, urase distribution as well as the trend of carbonate precipitation of marine ureolytic bacteria that are isolated from local coastal regions in Greece have been investigated in this study. The results in this study revealed that the urease activity of marine ureolytic bacteria species relies on some environmental parameters, which are very important for successful sand solidification. In future, we aim to apply these findings for coastal erosion protection as well as for bio-mediated soil improvement.

3.2 Objectives

The successful application of MICP to coastal erosion protection, the type of bacteria, bacterial cell concentration, reaction temperature, cell culture duration, carbonate precipitation trend, the pH of the media that control the activity of the urease enzyme etc., are necessary to be evaluated. The aim of this study was to improve the understanding of the relevant phenomena (different environmental factors) that affect urease activity on isolated bacterial species. Current study mainly focused on isolating and characterizing of urea decomposing bacteria species and subsequently evaluating their performance which could be suitable for soil improvement considering urease

activity, cell growth, pH and temperature dependency, urease distribution and $CaCO_3$ precipitation trend.

3.3 Materials and methods

3.3.1 Study area and sample collection

The ureolytic bacterial (G1, G2 and G3) species were isolated from the coastal area of Porto Rafti and Loutraki in Greece (Figure 3.1). There is a very limited report found on the screening and exploitation of microbial diversity, specially ureolytic bacteria from these regions. To date, there have been no recorded studies in Greece on the isolation of urease producing bacteria from coastal regions. So far, this is the first study to isolate ureolytic bacteria from coastal regions in Greece. This research gap enhances the possibility to isolate certain ureolytic bacteria that might contribute to ground improvement and coastal erosion protection in the respective coastal regions. The soil samples were (around 100 g) collected using conical bottle-shaped plastic tubes and stored in a thermos cool box (at the sampling site) before being transported to the laboratory for further analysis. The sample transported using a polystyrene container from sample collection sites to laboratory. The samples were then preserved in a refrigerator (4 °C) prior to culture. After having received the permission from the Ministry of Agriculture, Forestry and Fisheries, we imported the soils from Greece based on the plant protection law of Japan.
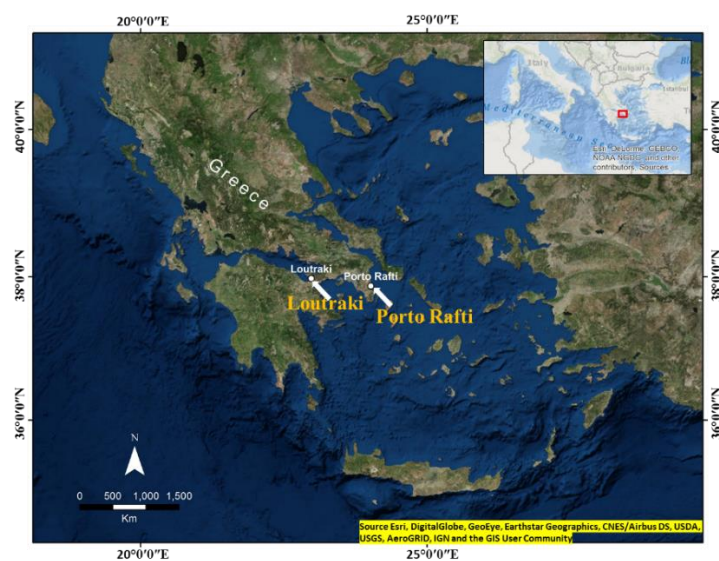
Figure 3. 1: Map of Greece showing the sample collection site (Porto Rafti: N 37° 52′ 57.1″, E 24° 00′ 51.1″ and Loutraki: N 37° 57′ 02.3″, E 22° 57′ 37.7″).

3.3.2 Screening, isolation and cultivation of ureolytic bacteria

At the laboratory condition, 5 g of soil was taken and diluted serially (up to six-fold) with sterile distilled water and 0.1 mL aliquot of serially diluted samples were inoculated in a petri dish which contains nutrient agar (5.0 g/L polypeptone, 1.0 g/L yeast extract, 0.1 g/L FePO$_4$ and agar 150 g/L). The sample plates were then incubated under aerobic conditions at 30 °C for 48 hrs. Upon the growth of bacterial colonies, sub-culturing was performed until single bacterial colonies were obtained. After screening, the bacterial species were identified by 16s rDNA gene analysis. The genome extraction was done using 100 μL of Mighty Prep reagent taken into a 1.5 mL microtube. From the colonies on the plate, the cells were removed with a sterilized platinum loop, suspended in the microtube, heated at 95 °C for 10 minutes, and then centrifuged at 12000 rpm for 2 minutes. The supernatant of the suspension centrifuged was transferred to another tube and used as a template for PCR (polymerase chain reaction). After successful PCR amplification, DNA extraction was carried out by an extraction kit (Nippon Genetics Co. Ltd.). The six types of primers used in this experiment were 9F, 515F, 1099F, 1541R, 1115R, and 536R. Finally, for the identification of the isolated bacterial species 16s rDNA, base sequence analysis (about 1500 bp) was performed. Finally, BLAST (Basic Local Alignment Search Tool) analysis was performed by the database DB-BA12.0 (Techno Suruga Laboratory, Japan). ZoBell2216 culture solution (hi-polypeptone 5.0 g/L, yeast extract 1.0 g/L, and FePO4 0.1 g/L mixed with artificial seawater (Table 3.2), maintained at pH 7.6–7.8) was used as the main culture medium for the growth of the species. The bacterial cells were pre-cultured (5 mL) in the ZoBell2216 solution at 30°C for 24 h by shaking at 160 rpm. The preculture (1 mL) was inoculated into 100 mL of fresh ZoBell2216 medium and incubated at 30°C with shaking at 160 rpm. Subsequently, it was continuously cultivated for 10 days. During the cultivation, the bacterial cell growth was determined (OD$_{600}$) by a UV-VIS spectrophotometer (V-730, JASCO Corporation, Tokyo, Japan).

Before further using the isolated species the urase activity of the isolated species was conducted by a simple colourimetric method (Colour change due to variation in pH; yellow to purple) have been used (Danjo and Kawasaki, 2014). In the clean bench, the isolated and cultured microorganisms were added to the urease activity measurement solution (cresol red) in a 20 mL screw bottle. A toothpick was used for

each new microbe inoculation carefully to prevent contamination. After adding the microorganisms, cover the styrol screw bottle and stir it about 20 times. Thereafter, it was allowed to set in an incubator set at 45 °C and observed with time (until 48 hrs).

Table 3. 2: Composition of artificial seawater

The composition of artificial seawater (Yashima chemical, Japan) [g / L] (solvent: distilled water)	
Elements	**[g / L]**
$MgCl_2 \cdot 6H_2O$	222.23
$CaCl_2 \cdot 2H_2O$	30.70
$SrCl_2 \cdot 6H_2O$	0.85
KCl	13.89
$NaHCO_3$	4.02
KBr	2.01
H_3BO_3	0.54
NaF	0.06
NaCl	490.68
Na_2SO_4	81.88

The reason for setting 45 °C at the incubator was to promote the activity of microorganisms. Continuously after 48 hrs, the color change was confirmed, and pH was measured. The composition of cresol red solution (Table 3.3) and composition for measuring the urease activity (Table 3.4) of the isolated bacterial colony sample has shown below. The urease activity test was conducted through visual observation for colour changes. The ureolytic isolated bacterial species can change the colour of the cresol red solution from yellow to pink with time. Finally, glycerol stock (Fortier and Moineau 2009) was used for long-term storage of the isolated bacterial species at -80 °C for further study. The overall procedure for isolation and identification of ureolytic bacterial species is presented in Figure 3.2.

Table 3. 3: Composition of cresol red solution.

The composition of cresol red solution (100 mL, per solvent: distilled water)	
Cresol red (Powder)	0.1 g
Ethanol (95%)	20 mL

Table 3. 4: Composition measurements of urease activity.

Composition measurements of urease activity (100 mL, per solvent: distilled water)	
Urea	2.5 g
Cresol red solution	2 mL
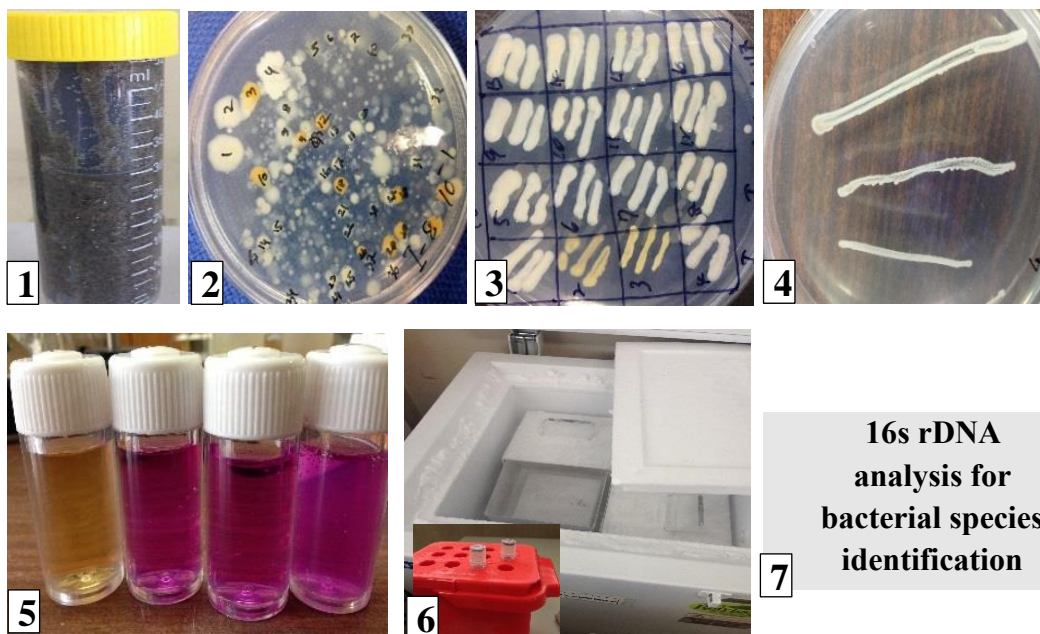
1. Collected soil sample.
2. Various colony formation on an agar plate.
3. Screening of selected colonies.
4. Isolation of colonies for urease activity check.
5. Urease activity check by cresol red solution.
6. Long term storage in glycerol stock solution (at -80 °C).
7. 16s rDNA analysis for bacterial species identification.

Figure 3. 2: Procedure for isolation and identification of ureolytic bacteria.

3.3.3 Urease activity tests

Urease activity of the cultured bacterial cells was assessed at different pH and temperature levels following the indophenol method (Natarajan, 1995) where ureolysis occurred directly by the bacterial cell in a solution. The collected sample solution (1 mL) from the cell culture was added to 100 mL of the stratum solution containing 0.3 M urea and 0.1 M EDTA (Basic Local Alignment Search Tool) buffer with phenol-

nitroprusside. The reaction composition was stirred using a water bath and kept at a steady temperature and pH. At the sampling point, 10 mL solution was sampled and 0.1 mL of 10 M NaOCl was added to the solution to prevent quick enzymatic hydrolysis. The composed solution was incubated subsequently for 10 min at 50–60 °C. The urease activity test was carried out to evaluate the effect of the reaction solution conditions, by 48 h cultured cells at distinctive temperatures ranging from 10 to 60 °C, and the pH was 6, 7, and 8 (adding EDTA buffer solutions at 30 °C). The urease activity of the discharged urease from the culture supernatants was also investigated. Cultured bacteria cell culture (1.2 mL) was centrifuged by 10,000 rpm for 5 min at 10 °C, and then the supernatant (1 mL) was used to examine urease activity as per the following method (Figure 3.3). Urease activity of the sampled supernatant would correspond to the discharge of urease.
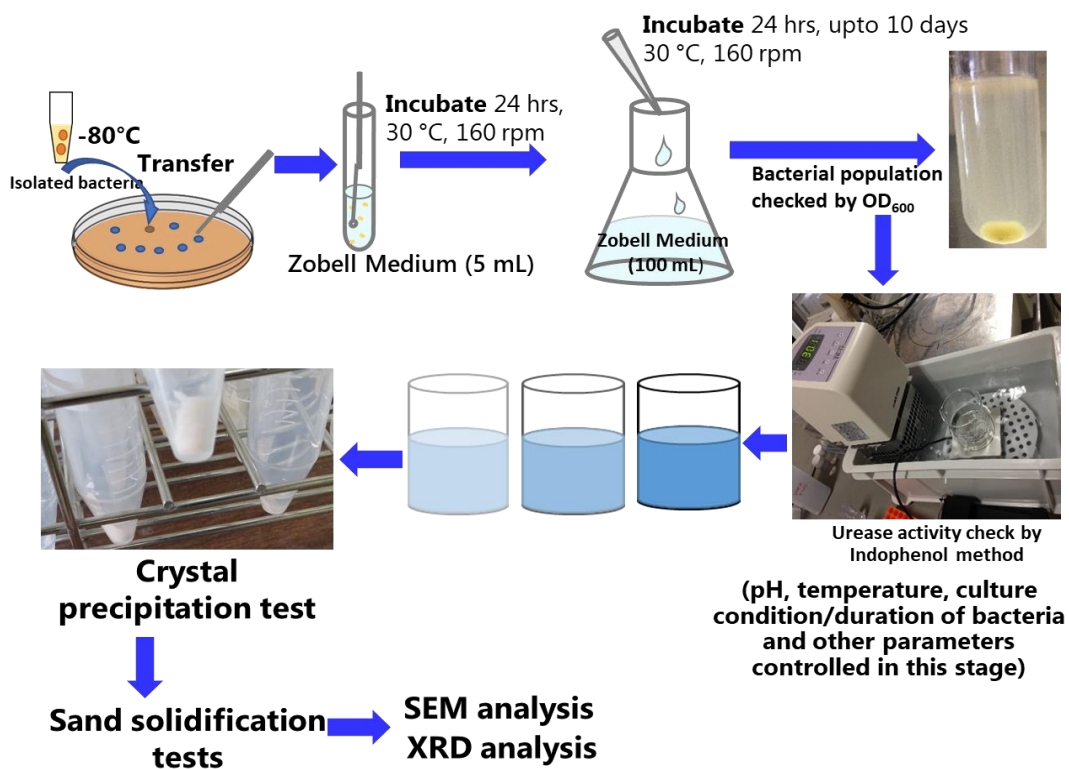
Figure 3. 3: Schematic illustration of the experimental procedures.

3.3.4 Distribution of urease

The activities of the culture supernatants were examined to investigate the secreted urease. To remove the supernatant, a 40 mL sample was collected from the bacterial

cell culture tube and centrifuged by 10,000 rpm, for 5 min at 10 °C. To get a solution from the resuspended bacterial cell, the cell pellet was washed by 0.1 M Tris and HCl buffer for repeated times. The urease activity assessment was conducted considering different OD_{600} values. The urease activity of the cell lysate, soluble and insoluble portion of the cell lysate, and finally the whole bacterial cell was also investigated. After 48 h culture of the cell, 10 mL sample solution was collected and centrifuged by following the same procedure as mentioned earlier. The sample solution was resuspended to remove the culture supernatant with 500 mL sonication buffer (0.1 M NaCl, 20 mM Tris/HCl, and 1 mM EDTA) and was named as the whole-cell. The soluble cell lysate was prepared using the disrupted bacterial cell using ultrasonication for 5 min with 130 W, and time interval was 1 min. Remaining bacterial cell-debris was also collected by centrifugation for 20 min at 4 °C with 8000 rpm, which was insoluble to the solution (Figure 3.4). The urease activity assessment was also conducted for both soluble and insoluble cases, followed by the indophenol method.
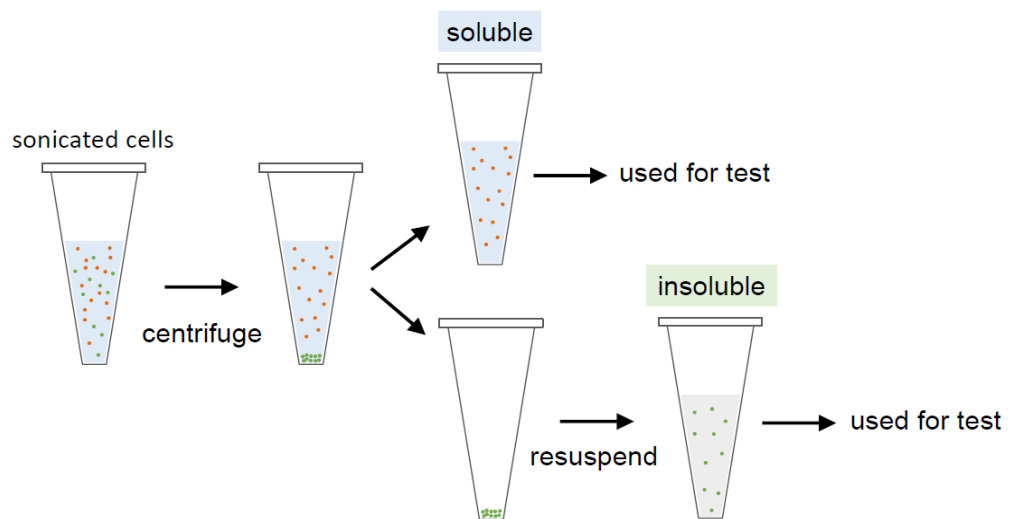
Figure 3. 4: Schematic illustration for segregation of cell pellets.

3.3.5 Microbial CaCO₃ precipitation tests

The selected bacterial strains were cultured with a ZoBell2216 solution (1.0 g/L of yeast extract, 5.0 g/L of hi-polypeptone, and 0.1 g/L of $FePO_4$) mixed with artificial seawater (Table 2) with a controlled pH of 7.6-7.8, until the maximum cell growth was

observed. The cell growth (OD_{600}) was measured by a UV-VIS spectrophotometer (V-730, JASCO Corporation, Tokyo, Japan). In the meantime, 0.5 M $CaCl_2$ and 0.5 M urea were put in a test tube up to 10 mL. The bacterial culture solution was centrifuged (12,000 rpm) for 10 min. The supernatant and cell pellets were divided, and the bacterial cell concentration (OD_{600}) was adjusted using distilled water. The adjusted bacterial cell concentration was then added to the test tube and put in a shaker at 30 °C for 48 h. Finally, the precipitation (white crystals) was observed and the precipitated crystals (centrifuged at 12,000 rpm for 10 min) was separated from the culture solution by a filter paper. The testing condition for $CaCO_3$ precipitation is shown in Table 3.5. The precipitated crystal tubes were kept in an oven drier for 24 h at 100 °C and then the final weight was taken to calculate the total crystal precipitation amount.

Table 3. 5: Testing condition for $CaCO_3$ precipitation tests.

Used Species	Temperature (°C)	Urea-$CaCl_2$ (M)
G1		0.3
	25	0.5
		0.7
G2		0.3
	25	0.5
		0.7
G3		0.3
	25	0.5
		0.7

3.3.6 Sand solidification tests

In order to check the ability of sand solidification of the isolated strains, a small-scale sand syringe solidification test was conducted. First, the isolated strains were grown in ZoBell2216E culture medium and shaken continuously at 30 °C for 2 days.

Then, 40 g of dried (110 °C for 2 days) Mikawa sand (particle size distribution shown in Figure 3.5) was loaded in a 35 mL syringe (height: 7 cm and diameter: 2.5 cm). physical properties of mikawa sand used in this study is shown in Table 3.7. Subsequently, 16 mL of the bacterial culture solution (ZoBEll2216E) and 20 mL of the consolidation solution (Table 3.6) was serially injected into the syringe showing in Figure 3.6. The syringe was flushed after 2 h, leaving approximately 2 mL of the solution close to the surface of the sand. The consolidation solution was injected and

drained every day for 21 days. The testing conditions are presented in Table 3.8. The pH values and Ca^{2+} concentrations from the outlet were measured afterwards. After 21 days, the UCS of the sample was measured by a needle penetration device (SH-70, Maruto Testing Machine Company, Tokyo, Japan).
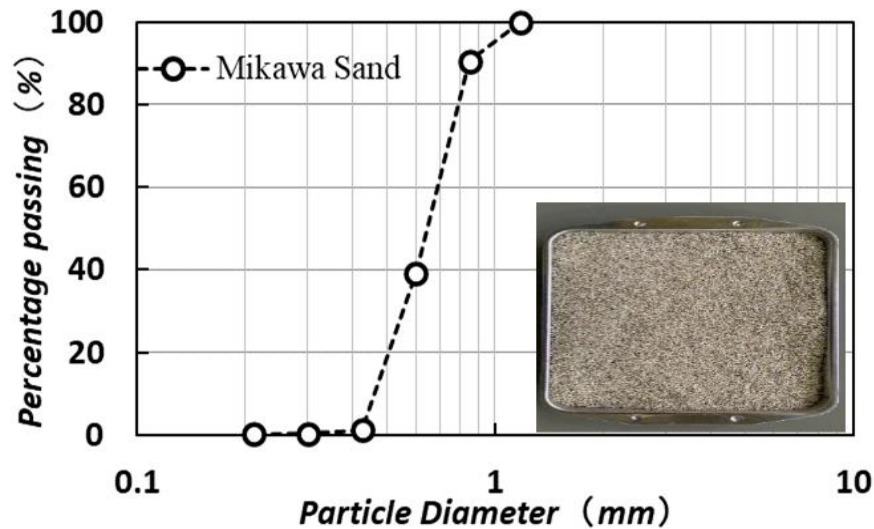
Figure 3. 5: Particle size distribution of Mikawa sand.

Table 3. 6: Composition of sand solidification solution.

Composition	Concentration (g/L)
$CO(NH_2)_2$	30.0
$CaCl_2$	55.5
Nutrient broth	3.0
$NaHCO_3$	2.12
NH_4Cl	10.0

Table 3. 7: Physical properties of "Mikawa" sand used in this study.

Physical property	Mikawa sand
Maximum Density (g/cm^3)	1.476
Minimum Density (g/cm^3)	1.256
Particle Density (g/cm^3)	2.66
Mean Diameter (mm)	0.870
pH	7 ± 01
C_u (coefficient of uniformity)	1.5
C_C (coefficient of curvature)	0.92
G_s (specific gravity)	2.66

Table 3. 8: Testing conditions for sand solidification tests.

Used Species	Testing Case	Bacterial Injection Interval (Days)	Temperature (° C)	Concentration of solidification solution (M)	Incubation time	Used portion
G1	1 (control)	-	25	0.5	21 days	-
	2	7	25	0.5	21 days	Whole cell
	3	7	25	0.5	21 days	Supernatant
	4	7	25	0.5	21 days	Cell pellet
G2	1 (control)	-	25	0.5	21 days	-
	2	7	25	0.5	21 days	Whole cell
	3	7	25	0.5	21 days	Supernatant
	4	7	25	0.5	21 days	Cell pellet
G3	1 (control)	-	25	0.5	21 days	-
	2	7	25	0.5	21 days	Whole cell
	3	7	25	0.5	21 days	Supernatant
	4	7	25	0.5	21 days	Cell pellet
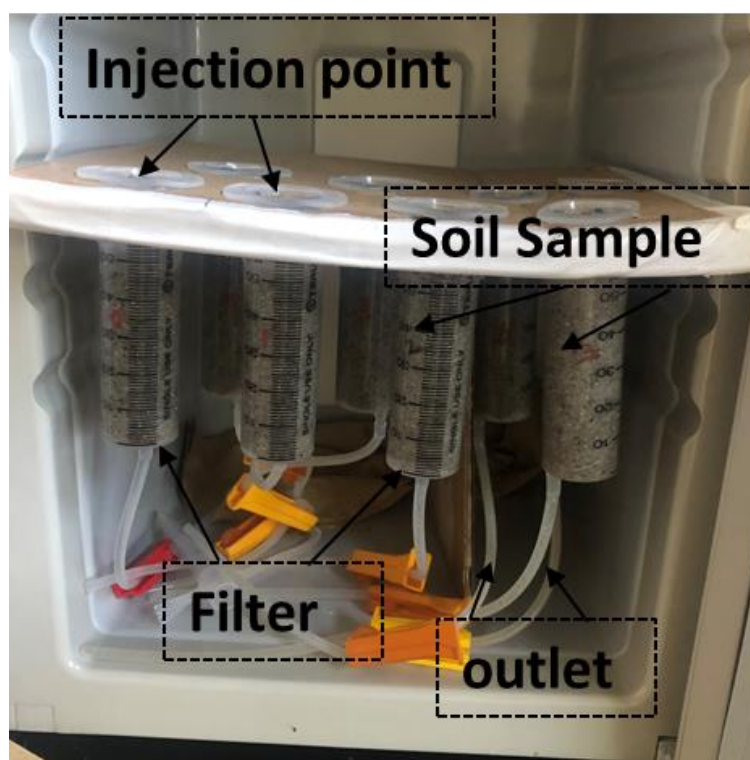
Figure 3. 6: Appearance of sand solidification tests.

3.3.7 Measurement of calcium carbonate content

Carbonate content was determined by the simplified device (Figure 3.7) developed to measure the pressure of CO_2 gas released when the cemented specimen is treated with HCl in closed system under constant volume and temperature (Fukue et al., 2001). Mass of the oven dried (105°C for 48 h) sample was measured, and the sample was placed into the flask. HCl (2 mol/L) was placed in small plastic vials and set into the flask without spattering the specimen. Subsequently, HCl was allowed to react with specimen in the closed system until the digital manometer (connected with the system) read a constant pressure. From the calibration curve developed between the pressure and $CaCO_3$ content, the carbonate content was estimated, hence the percentage of mass of $CaCO_3$ was determined using the following equation:

$$CaCO_3 \, content \, (\%) = \frac{Weight \, of \, CaCO_3 \, (in \, the \, specimen)}{Weight \, of \, the \, oven \, dried \, specimen - Weight \, of \, CaCO_3}$$
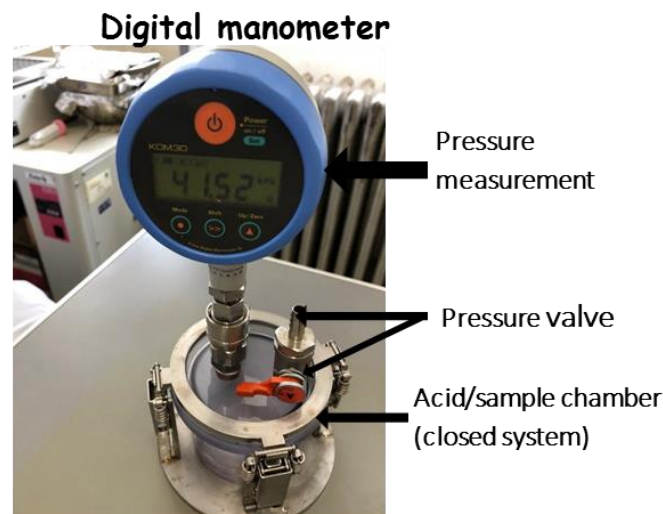
Figure 3. 7: Digital manometer set up for measuring $CaCO_3$ content.

3.3.8 Needle penetration tests for estimation of UCS

The unconfined compressive strength (UCS) of the cemented specimens were estimated using needle penetrometer (SH-70, Maruto Testing Machine Company,

47

Tokyo, Japan, shown in Figure 3.8(a) according to JGS 3431-2012 (JGS 3431-2012, 2012). The equipment was developed in Japan for predicting the UCS of soft, weak, very weak rocks and cemented soil specimens, and recently, ISRM has recommended the method for indirect estimation of mechanical properties of the soft rock materials (Ulusay, 2014). This penetration is a non-destructive test, and that has a great potential to be used as a sound technique for MICP field assessments. The penetration depth (mm) of the needle attached to the device and the penetration resistance (N) were measured during the test. Using the regression relationship (Eq. 4) developed by analyzing 114 natural soft rock samples and 50 cemented soil samples, the UCS of the specimen was estimated.

$$log\ (y)=0.978\ log\ (x)+2.621 \qquad\qquad (4)$$

where, x is penetration gradient (ration between penetration resistant (N) and penetration depth (mm)); y is corresponding UCS.

The load is applied to the specimen perpendicularly and slowly. The specimen should be fixed to prevent its movement during the application of load (Figure 3.8 (b)).
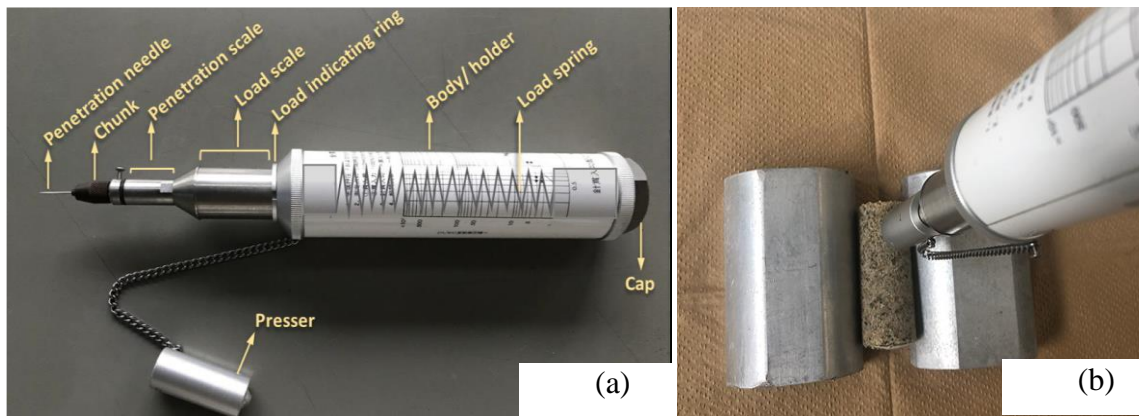
Figure 3. 8: (a) Needle penetration tests device (b) and mode of action.

3.3.9 SEM observation (SEM)

To study the microstructural changes in the specimens, SEM analysis was performed using Miniscope TM 3000 (Hitachi, Tokyo, Japan) (Figure 3.9). The representative samples were carefully taken from the samples and observed through SEM after the oven dry at 60 °C.

Low vacuum SEM instrument

Figure 3. 9: SEM instrument.

3.3.10 X-ray diffraction (XRD) analyses

X-ray diffractometer patterns of the powdered beachrock samples were analysed using an X-Ray generator (MiniFlex™, Rigaku Co., Ltd., Tokyo, Japan) (Figure 3.10). The analysis was carried out in room temperature using the XRD machine with CuKa radiation at a rate of $6.5°2\theta$/min ranging from 10 to $80°2\theta$. Qualitative mineralogy of the samples was determined with the standard interpretation procedures of XRD using Match! software for phase identification from powder diffraction as described to the previous sections.
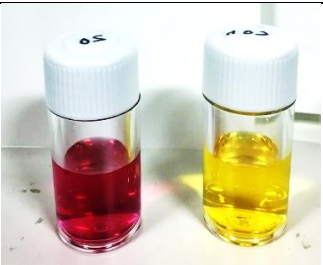
XRD instrument

Figure 3. 10: XRD instrument.

3.4 Results and discussion

3.4.1 Results of indigenous isolates and selection of a suitable ureolytic bacteria

The isolation of the ureolytic bacteria was done successfully and the urease activity of the locally isolated ureolytic bacteria was calculated and compared to a control strain. If the sample to be investigated is a urea-degrading bacterium, the hydrolysis of urea in the solution proceeds and the pH in the solution rises. From the results (Table 3.9) it is showed that the colour and pH was changed with incubation time. In general, the cresol red solution colour changed immediately with higher pH which is a sign of high urease activity (Danjo & Kawasaki, 2016). The presence or absence of urea-resolving ability was judged from the difference between the colour difference between the control and the measured value of pH. From the results, it is observed that the colour change (yellow to pink) of the treated sample is varied with incubation time.

Table 3. 9: Simple urease activity tests (cresol red solution).

Sample No.	Result	Time/Duration	pH	Picture (discoloration)
G1	Activity found immediately: after 02 hrs	Incubated until 72 hrs @ 45 °C	G1 (11) Sample-9.0	
G2	Activity found immediately: after 02 hrs	Incubated until 72 hrs @ 45 °C	G2 (12) Sample-9.0	
G3	Activity found immediately: after 02 hrs	Incubated until 72 hrs @ 45 °C	G3 (11) Sample-8.98	

Among the isolated colonies, only two strains showed the pH increase and colour change in cresol red indicator, suggesting the urease potential. The experimental finding in this study suggests that G1 samples had the highest urease activities when compared to the G2 species. The strains were characterized as *Micrococcus* sp. (*G1*), *Pseudoalteromonas* sp. (*G2*) and *Virgibacillus* sp. (G3) by the 16s rDNA analysis and the result was confirmed using a third-party company (DB-BA12.0, TechnoSuruga Laboratory) compared to the result using DDBJ/ENA(EMBL)/GenBank, Japan. As far as is known, this is the first attempt to isolate and characterize the efficiency of ureolytic bacteria that can be applied to protect coastal erosion areas such as those of Greece and other Mediterranean regions.

From the previous results, it was found that the *Micrococcus yunnanensis* is a gram-positive, non-endospore forming bacteria and its temperature and pH tolerance ranges for growth are 4–45°C and pH 6–8, respectively (G. Z. Zhao et al., 2009a). *Pseudoalteromonas* sp. is a gram-negative, rod-shaped bacterium, motile by a polar flagellum which helps it move back and forth between solid surfaces. It requires sodium ions for growth and has an oxidative metabolism (Vera, et al., 1998). It has also been found that bacterial cell growth is closely related to cell culture duration (Okwadha et al., 2010). Moreover, it has been concluded that the rate of urea hydrolysis is directly proportional to the concentration of bacteria, which is an important factor for the success of the MICP application (Lauchnor, et al., 2015). Figure 3.11 shows the cell growth with culture duration of the isolated species. As shown in Figure 3.11, that initially the cell concentration increased and thereafter decreased with time producing a bell-shaped profile for each species.
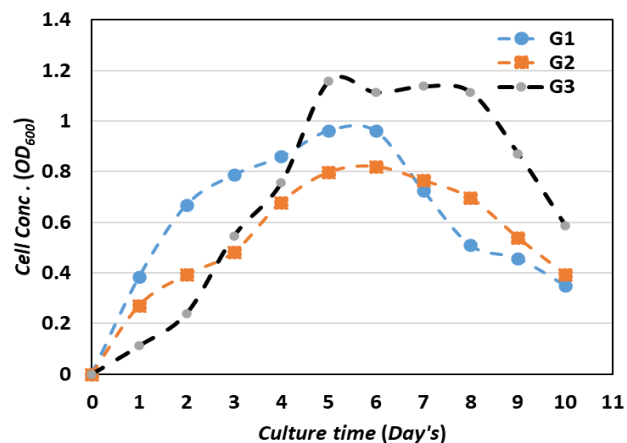
Figure 3. 11: Growth profiles of the isolated species.

3.4.2 Results of urease activity influenced by environmental factors

I. *Urease activity: Temperature dependency*

Urease activity with various temperature conditions is shown in Figure 3.12 for the G1, and G2 and G3 species. High urease activity was observed at a temperature above 30 °C (G1 species) and then gradually decreased and showed an almost bell-shaped profile because of cell denaturation at a higher temperature, except in the case of G2 and G3 species. The divergent tendency of urease activity (nearly 40–60°C) was also observed by Fujita et al., 2017. However, there are few data about the urease activity of marine ureolytic bacteria in Greece. Even though the urease activity of G1, G2, and G3 species are lower than that of *Pararhodobacter* sp., the results obtained in this study would be innovative and adventitious information for the sand solidification method through microbial carbonate precipitation because the use of native ureolytic species (isolated from marine area). In future, it may be possible to use G1, G2, and G3 species for sand solidification, which could help to manufacture artificial beachrock following the MICP technique. This result could also be adventitious in Greece for coastal erosion control purposes by increasing bacterial population either by centrifugation and/or urease enzyme extraction by ultrasonication and/or adding bacterial populations several times during the sand solidification process before urease activity completely declined. Similar results were also found for the strains such as *Deleya venusta* and *Pararhodobacter* sp. Previously, it was also found that urease activity influenced to $CaCO_3$ precipitation at temperatures from 10 to 60 °C, which is similar to the findings of this study. However, the effectiveness of environmental factors on urease activity of the negative species with variation temperatures was not examined. Therefore, on the basis of these experimental findings, the G1, G2, and G3 species showed high urease activity in the different range of temperatures that could reflect the importance of isolating the ureolytic bacterial species from the local environment and their subsequent application for sand solidification and soil improvement.
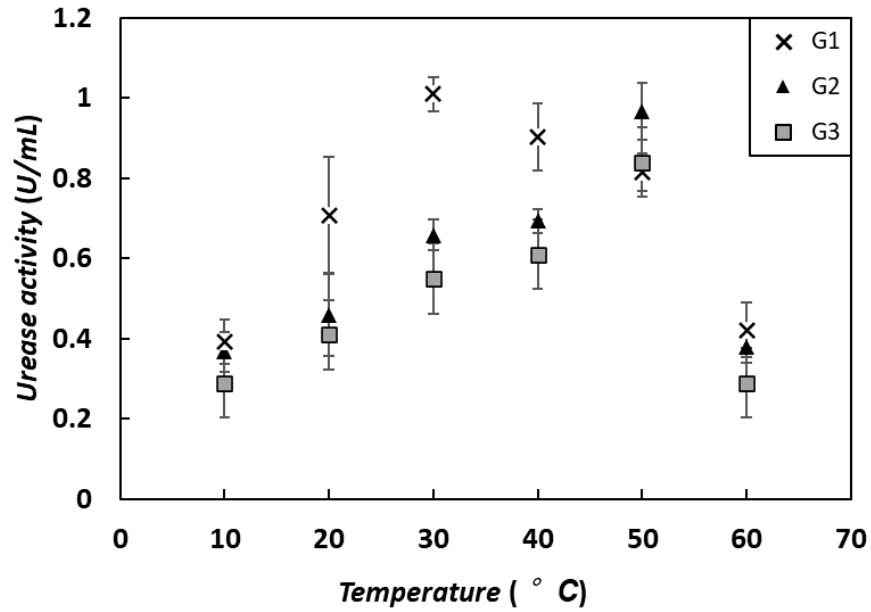
Figure 3. 12: Urease activity of different temperature conditions.

II. *Urease activity: pH dependency*

Figure 3.13 represents urease activity with different pH conditions at a certain temperature (30 °C) for G1, G2, and G3 species. The results exposed a nearly bell-shaped outline showcasing the maximum activity around pH 7 for all of the three species. Following the same conditions, the G1 species showed the highest urease activity compared to the G2 and G3 species. Previous research showed that the MICP process favored an initial pH environment of 6.5–9.3 (neutral to basic condition). Additionally, it was revealed that, in the case of some species such as *Pararhodobacter* sp., considerable loss of urease activity was observed with acidic (lower than pH 6) and alkaline (higher than pH 9) conditions attributed to denaturation of protein. It was also reported that the urease activity of some ureolytic bacterial species favored lightly alkaline conditions. Consequently, the pH value played an important role for the bacteria transportation and adhesion to obtain homogeneously improved strength of treated soils. Therefore, the results of this study could also be useful information for obtaining a successful sand solidification process for identifying the optimum pH condition for native species.
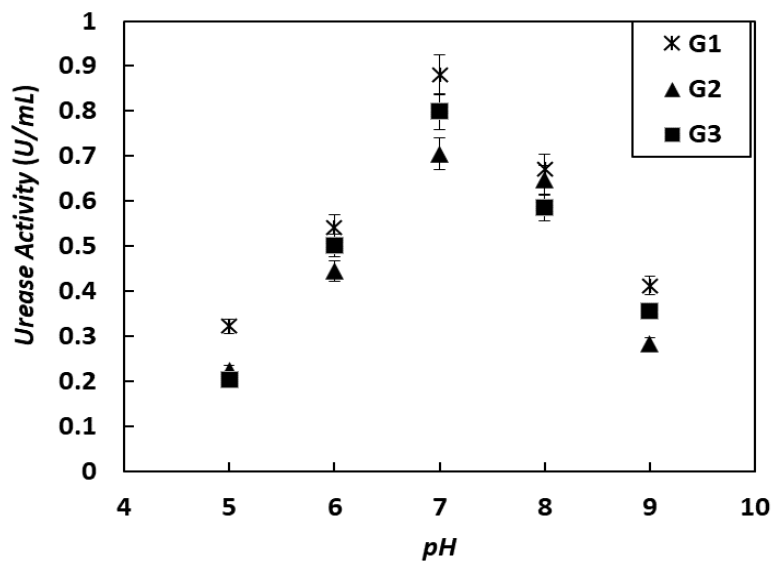
Figure 3. 13: Urease activity of different pH conditions.

3.4.3 Urease distribution results

Urea hydrolysis is a very significant pathway during the MICP process as the urease enzyme is directly used during the MICP process as a whole-cell during the biomineralization process (Danjo & Kawasaki, 2016; Al-Thawadi & Cord-Ruwisch, 2012). The evaluation of urease distribution in the cell (secretion or non-secretion, cytoplasm or cell membrane) is substantial information for an effective solidification process because complicated bi-/tri-phase reactions occur in the mixture of solution, cells. and sand particles during urea hydrolysis (Fujita, et al., 2017). However, insufficient information is available regarding specific secretion pathways of urease enzymes for ureolytic bacteria. Thus, we investigated the secretion pathway of the urease enzyme using the soluble fraction of the cells of the ureolytic bacteria (using the G1, G2, and G3 species).

The total cell culture (supernatant and cell-pellet) and the urease activity is shown in Figure3.14 for the isolated species. Figure 3.14 shows that considerably lower activity was observed (G2 species) in the culture supernatant compared to the supernatant of the cell culture. However, substantial urease activity was found on the supernatant and cell pellet for both the G1 and G3 species. This indicates that urease would not be secreted to the extracellular medium but would likely have urease enzymes on the cell membrane, similar to urease from *Helicobacter pylori* (Phadnis et

54

al., 1996) where it is localized on the cell membrane. Because the enzyme likely accumulated in/on the cell membrane, quite low enzymatic activity was found in the culture supernatant. The urease enzymes (proteins) are released by autolysis linked with the cell surface by reabsorption and secretion of the urease enzyme (protein) relying on selective bacterial species as investigated during the growth phase in this study. However, the findings in this study can be useful information to determine the phase of the reaction/mixture in a culture medium and for treating soil improvements using the MICP method either by enzymatic extraction and/or centrifugation of the cell or modification of the injection pattern (Chang et al. 2016). These results showed that the variation of urease activity depended on cell lysate, cell membrane, and whole-cell by focusing on the urea hydrolysis by native bacterial strain. The results showed that, urease could exist as a soluble protein or likely as a soluble membrane protein. We found that the protein was not released into the culture solution but was separated from the bacterial cell membrane into the solution during ultrasonication because the crystal precipitation was greatly influenced by the bacterial cells. Therefore, the findings in this study support in figuring out the urease accumulation characteristic and extraction of the enzyme by sonication, which could be effective for the efficacy of the soil treatment/ground improvement by MICP and/or enzymatic process in practical field application for coastal erosion protection, especially in the coastal area of Greece and Mediterranean regions.
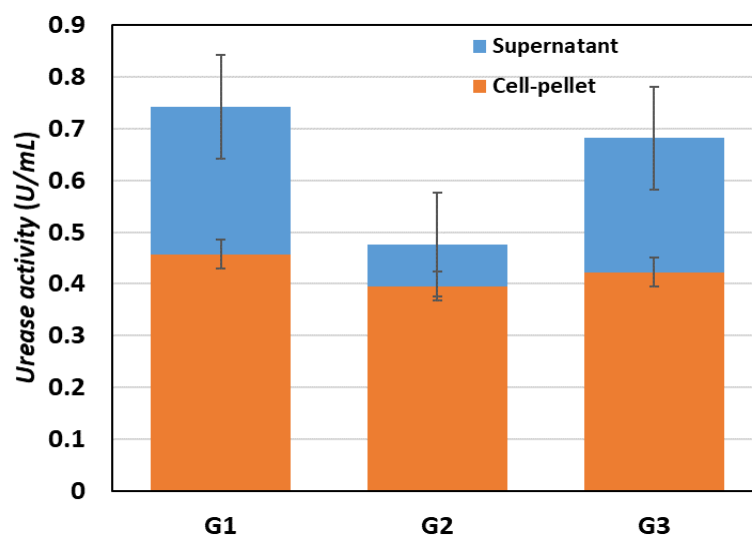
Figure 3. 14: The results showing the (a) cell growth and (b) urease activity of the isolated strains including the (c) cell pellets and supernatant.

3.4.4 Results of CaCO₃ precipitation tests

Earlier studies showed that it is possible to control the strength of the treated sand by regulating the amount and/or volume of precipitated minerals. It has also been reported that various environmental factors, including temperature, pH, bacterial size, and cell concentration, control the amount of calcite precipitation during the MICP process. Therefore, it is very important to investigate the trend in $CaCO_3$ precipitation for individual bacterial species because the $CaCO_3$ acts as the main binder material between the substrate particles for soil improvement during the MICP process. The $CaCO_3$ precipitation trend for the G1, G2, and G3 species is shown in Figure 3.15. Figure 3.15 indicated the trend of $CaCO_3$ precipitation at different $CaCl_2$-urea concentration. Results showed that, higher concentration of $CaCl_2$-urea leads to precipitate higher amount of $CaCO_3$ crystal. From the figure, it is clear that $CaCO_3$ precipitation is closely related to the $CaCl_2$-urea concentration values, which supports previous studies (Jawad Kadhim & Zheng, 2016). From our studies, was also observed that higher $CaCl_2$-urea concentration influenced the $CaCO_3$ precipitation amount. Under the same conditions, the G1 and G3 species had the advanced ability of precipitating a higher amount of $CaCO_3$ compared to the G2, leading to a higher possibility of sand solidification (Figure 3.16). At the same time, the rate of the precipitated $CaCO_3$ decreased and tended to be constant with a further increase of the $CaCl_2$-urea concentration. However, this study suggests that the variation in the $CaCO_3$ precipitation trend was related to the $CaCl_2$-urea concentration with individual species, which supports earlier studies.
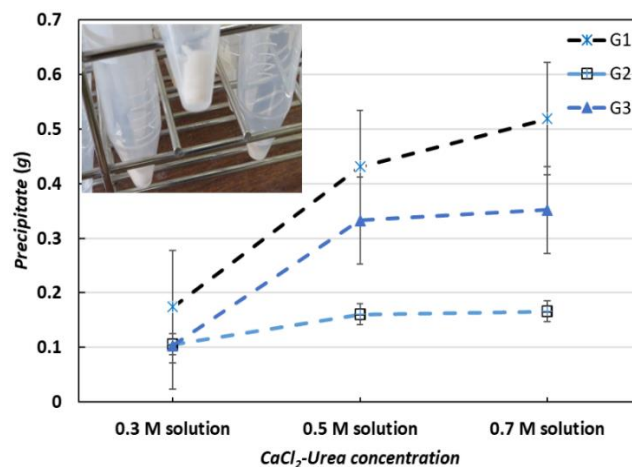
Figure 3. 15: Crystal's precipitation pattern.
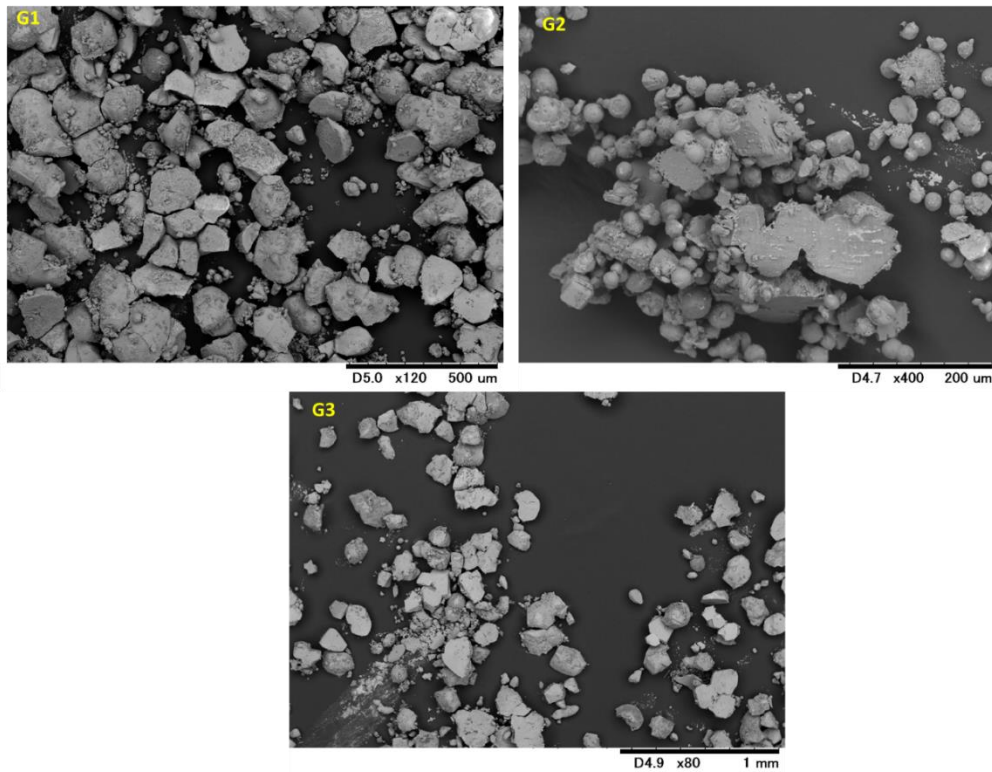
Figure 3. 16: SEM images of precipitated crystals.

3.4.5 Sand solidification test results

Small scale syringe sand solidifications tests were conducted under to evaluate the effect of variations biological solution by MICP. One sand column was treated with whole cell culture and another with cell pellets and supernatant by keeping all other factors constant. The strength was measured using a needle penetration device. The outcomes of the needle penetration test are summarized individually and shown in Figure 3.17. From the figure, it was observed that maximum USC around 1.6 MPa was obtained for G1 species (Figure 3.18) in case of whole cell used. Irrespective of the lower strength was observed, in the top and middle parts of the sample treated with supernatant and cell with cell pellets. Similar tendency was observed for G2 (Figure 3.19) and G3 cases (Figure 3.21). The treated sand profile is shown in (Figure 3.20 for G2) and Figure 3.22 for G3. One major factor that influences the efficiency of MICP process is how well urease enzyme or the cells of urease producing bacteria is adsorbed on to the sand grains. The primary controlling factors of bacterial cell adsorption and movement include grain size, surface properties of the cells and sand grains (surface charge and hydrophobicity) along with concentration of ions in the extracellular

57

environment. It is possible that the adsorption properties of the cells might have changed after centrifugation, washing and resuspension steps and had an effect on the sand solidification. From the results, it is revealed that bacterial cells have been well adsorbed onto the sand grains and filtered out along the sand column when the intact culture was injected thereby facilitating better calcium carbonate bridge formation between the grain contacts. For the column treated with cell pellets, it seems adsorption of cells on sand grains has not been efficient thus allowing cells to be flushed out along with the cementation solution. However, that has eventually caused lesser pore filling and clogging of voids by calcium carbonate cement on top resulting in a more homogeneous vertical strength enhancement. However, further investigation is required to improve the solidification condition.
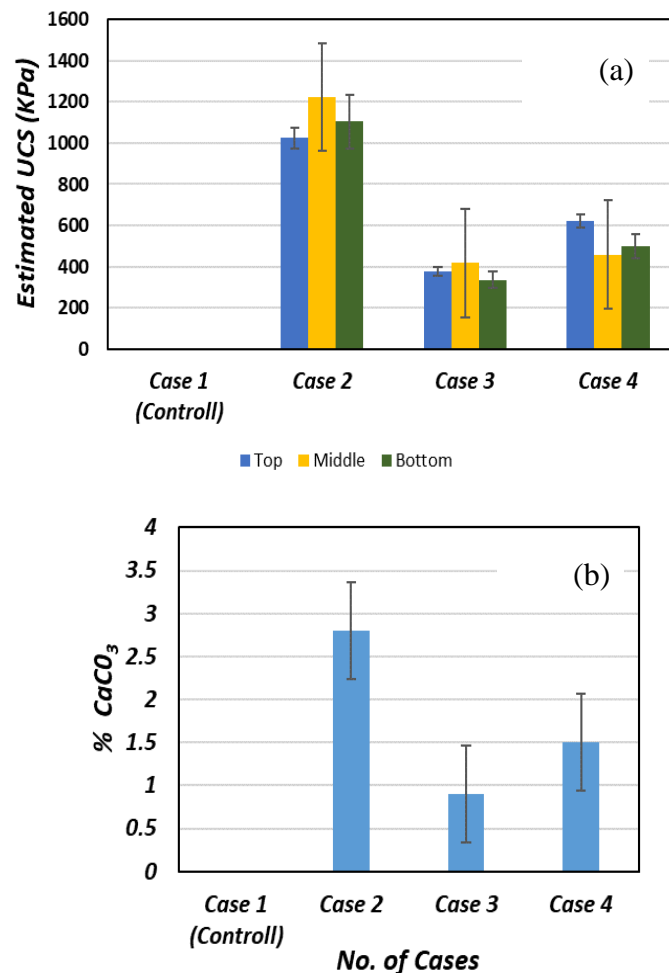
Figure 3. 17: (a) variation of UCS and (b) calcium carbonate content of G1.
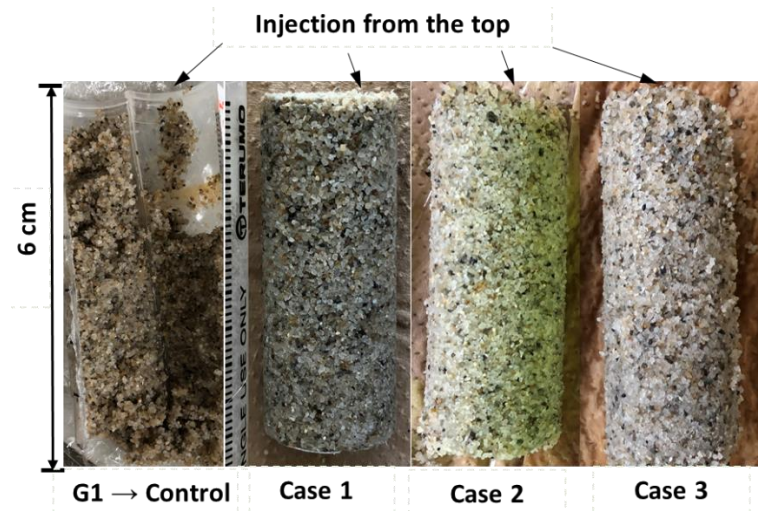
Figure 3. 18: Sand profile after MICP treatment.
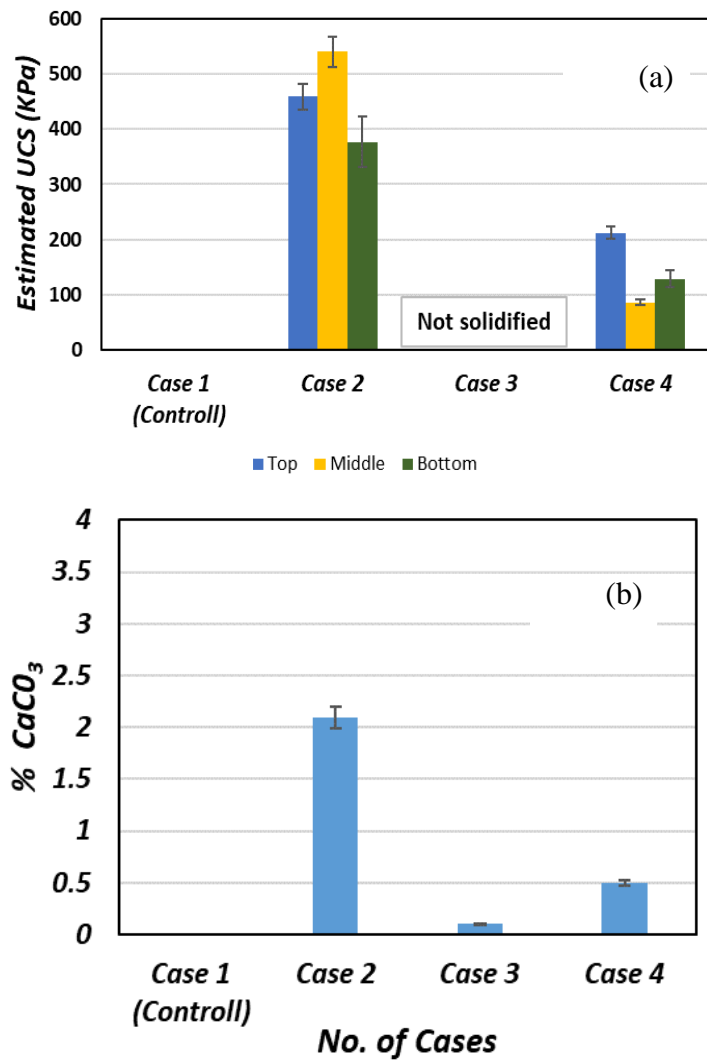
Figure 3. 19: (a) variation of UCS and (b) calcium carbonate content of G2.
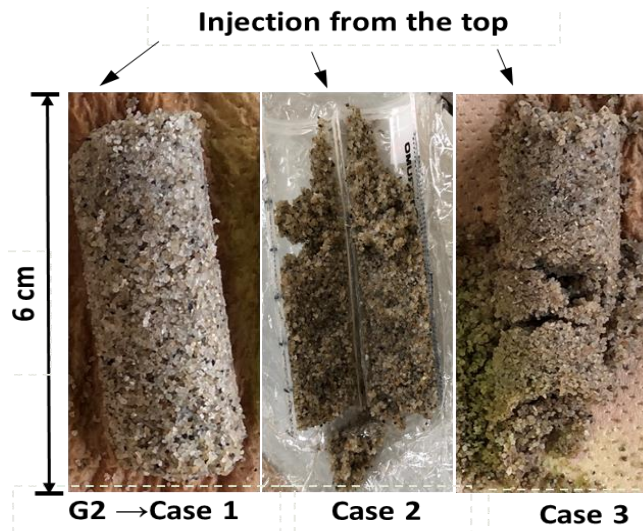
Figure 3. 20: Sand profile after MICP treatment.
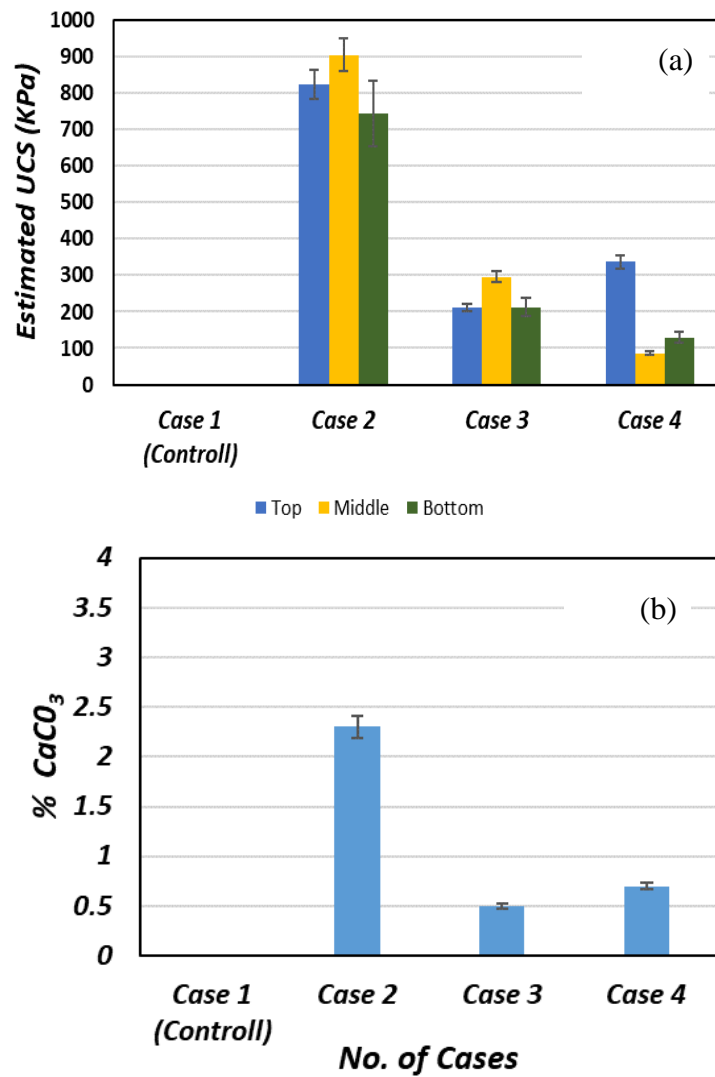
Figure 3. 21: (a) variation of UCS and (b) calcium carbonate content of G3.
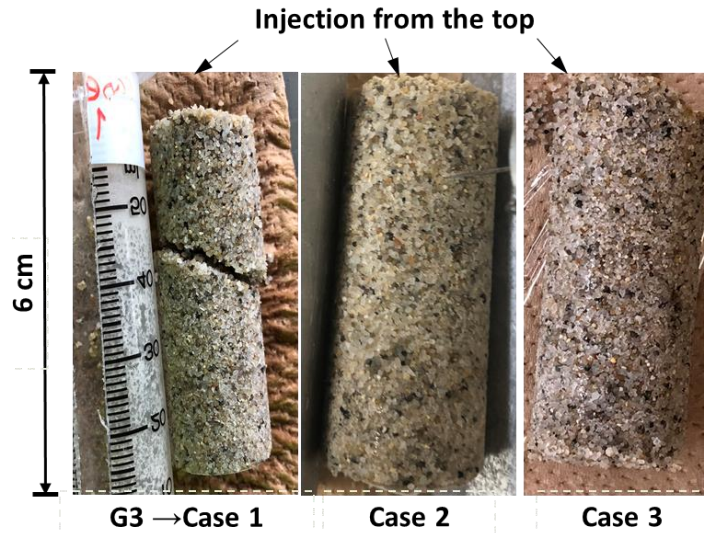
Figure 3. 22: Sand profile after MICP treatment.

3.4.6 Microscale analysis results of the MICP treated samples

The SEM images of the MICP treated sands are shown in Figure 3.23. The images demonstrate that the calcium carbonate preferentially precipitated at particle contacts (contact cementing). Generally, bacteria cells prefer to position themselves in smaller surface features (such as near particle-particle contacts) compared to the particle surface due to the reduced shear and a higher availability of nutrients at the particle contacts (DeJong et al., 2010), which leads to the precipitates at the particle contacts. Also, the matrix support (i.e. grow from particle surface into pore space to create bridges between particles) is barely observed in sands treated herein by percolation. Another interesting observation that should be noted here is the local strength variation along the sand column. The column strength improvement shows a gradual decline from top to bottom in all cases possibly due to better filtering and accumulation of bacterial cells on top than far away from injection point. Further, the initially precipitated crystals closer to injection point may interrupt the nutrient transport to the bacteria and may slow down the flow of cementation solution due to blockage of the pore spaces. This results in depletion of reactant concentration as they are being readily consumed for biocementation. The other pertinent reason is the inhibition of the activity of the aerobic bacterium as the availability of oxygen diminishes from top to bottom. However, Dhami et al., (2016) stated that availability of oxygen plays the governing role than particle size distribution thus efficacy of MICP reduce with depth irrespective of the

grain sizes. However, combination of these phenomena is suspected to impair the efficiency of MICP far away from the injection point.
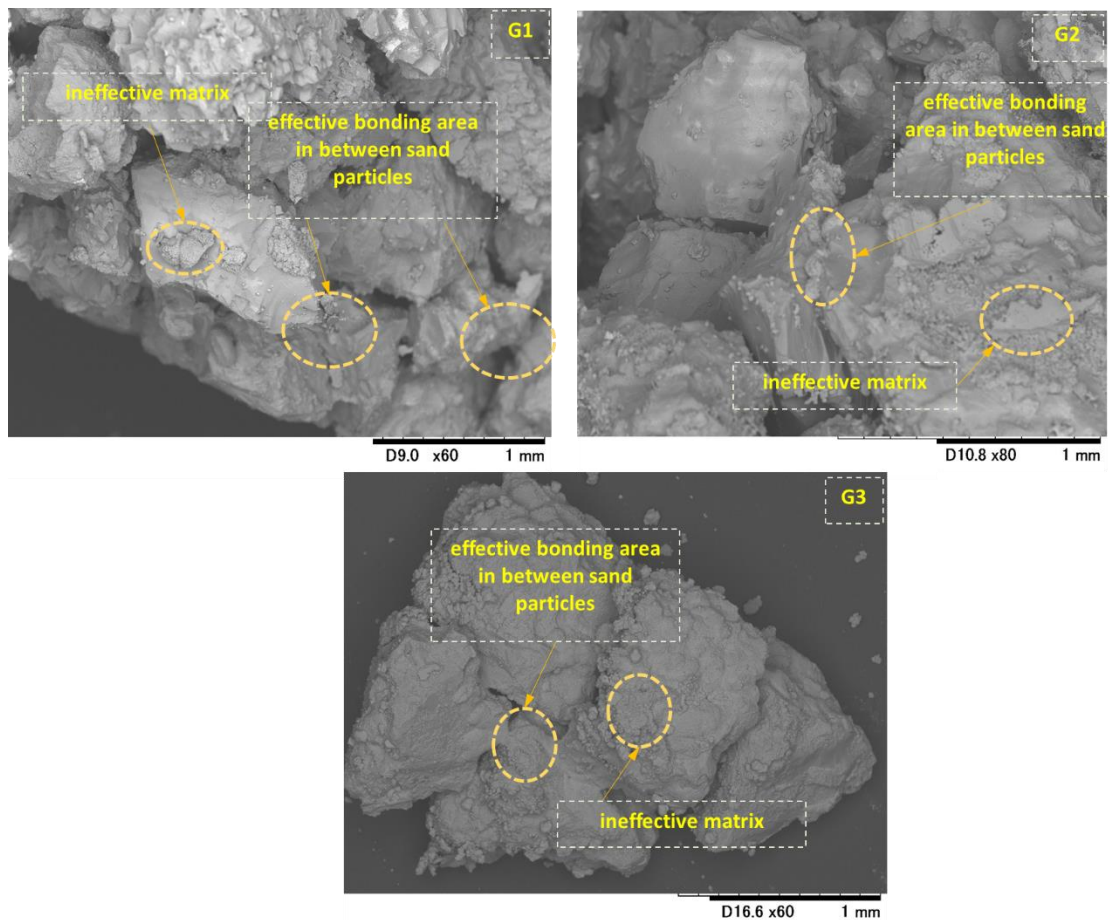
Figure 3. 23: SEM images of the MICP treated sand.

3.5 Conclusions

MICP is a sustainable and eco-friendly technique that must be improved both at laboratory and field scales. MICP technique must be optimized to find out the best conditions (pH, soil, temperature, the concentration of cementation media etc.) for each bacterial activity, and to reach a homogeneous distribution in the soil as well as prerequisite to improve the UCS. This study discussed about the characteristics of ureolytic bacterial species isolated from the coastal area of Greece. The findings in this thesis suggested that the isolated ureolytic bacteria (G1, G2, and G3 species) have the potential to be used as alternative microbial MICP agents for biocement applications, especially in coastal areas. The findings of our study provide insight into the factors

that influence urease behavior in local ureolytic bacteria species, as well as the possibility of effective sand solidification. The effects of various cultural conditions on urease behavior for isolated bacterial species are also presented in this report, which could be used to solve problems in environmental biotechnology, civil engineering, and geotechnical engineering. Furthermore, the isolated ureolytic bacteria identified in this study may have additional potential in the field of MICP and can be used as a useful reference resource for microbial biotechnology and construction microbial biotechnology researchers.

The main results obtained in this study are as follows:

1. Three kinds of urea-degrading bacteria were newly discovered by screening from coastal soil collected from Greece.

2. The effect of culture duration on the bacterial cell growth and urease activity has been reflected in this study suggested that cell growth and urease activity is correlated with the cell culture duration. The results indicated that bacterial cell viability is very important for optimum urease activity that can enhance sand solidification process.

3. This study indicated that the pH had a significant effect on the urease activity of individual species. In a higher pH bacteria species is still viable for urease activity. These findings could also be applied to the alkaline soil treatment.

4. The urease secretion ration which indicates that urease would not be secreted to the extracellular medium but would likely have urease enzyme on the cell membrane which is revealed in this study. The experimental results in this study, also suggested that the urease enzyme (proteins) is released by autolysis linked with the cell surface by reabsorption and secretion of urease enzyme (protein) relies on selective bacterial species.

5. From these studies it is also observed that higher OD_{600} values influence the $CaCO_3$ precipitation amount which leads to the higher possibility of sand solidification.

CHAPTER 4 : SAND CEMENTATION TESTS BY EICP METHOD

4.1 Introduction

Enzyme-induced carbonate precipitation (EICP) is an innovative, bio-inspired soil stabilization technique (Hamed Khodadadi et al., 2017; Putra et al., 2020) in which calcium carbonate ($CaCO_3$) crystals are enzymatically precipitated and bind the soil particles and enhancing the soil engineering properties. In recent years, soil improvement through calcium carbonate ($CaCO_3$) precipitation by a biological approach (bio-calcification, bio-grouting, biomineralization, bio-cement) has emerged as a potential strategy for soil stabilization and has been studied intensively throughout the world over the last two decades. Most of the previous work published on the microbial induced carbonate precipitation (MICP) method is based on microorganisms (ureolytic bacteria, fungi, etc.) that precipitated $CaCO_3$ via urea hydrolysis in the presence of Ca^{2+} ion at favorable conditions (e.g., pH, temperature, bacterial culture/duration/population, the interval of injection, etc.). These minerals of carbonate ($CaCO_3$) serve as the main binding agent inside the pores of the soil, bridging the particles of the soil and giving complete cohesion to the soil structure and thus enhance the soil stability. However, bacteria's cultivation and its storage at a large scale is a complex process that challenges the use of MICP (Putri et al., 2020) in real field application. The enzyme is the most expensive component of the EICP solution. It has a size of 12 nm per subunit and is soluble in water, facilitating its transport within the pores of soils (Blakely and Zerner, 1984). As the $CaCO_3$ precipitation reaction through EICP does not employ living organisms, it is not limited by oxygen availability as when using MICP for deep soil treatment. Furthermore, MICP requires nutrients for bacterial activity, is subject to competing effects of other microorganisms, or rely upon cell attachment to soil particles. For these reasons, EICP possesses many practical advantages over MICP. Another advantage of EICP over MICP in some cases is that the reaction process in EICP occurs more rapidly than MICP, making it particularly useful for some applications in arid and semi-arid environments. In recent years, soil improvement through calcium carbonate ($CaCO_3$) precipitation by a biological approach (bio-calcification, bio-grouting, biomineralization, bio-cement) has emerged

as a potential strategy for soil stabilization (Kavazanjian & Hamdan, 2015; Miftah et al., 2020) and has been studied intensively throughout the world over the last two decades. Most of the previous work published on the microbial induced carbonate precipitation (MICP) method is based on microorganisms (ureolytic bacteria, fungi, etc (De Muynck et al., 2010; Mujah et al., 2017b) (e.g., pH, temperature, bacterial culture/duration/population, the interval of injection, etc.). These minerals of carbonate ($CaCO_3$) serve as the main binding agent inside the pores of the soil, bridging the particles of the soil and giving complete cohesion to the soil structure and thus enhance the soil stability (Al-Salloum et al., 2017; C.-S. Tang et al., 2020). However, bacteria's cultivation and its storage at a large scale is a complex process that challenges the use of MICP (Putri et al., 2020) in real field application. Nevertheless, the screening, isolation, cultivation and controlling of ureolytic bacteria, physical non/homogeneity, oxygen availability and their enzymatic activity, bacterial cell attachment to soil particles, and their interaction between other species in the soil is a complex process (Arias et al., 2017) and their large-scale preservation is also a challenging method that threatens the use of MICP in actual field application. However, some researchers have tried to overcome some of these challenges (Osinubi et al., 2020), but some inconclusive issues related to MICP still persist, for instance survivability of the bacteria, culture and nutrition supply to the bacteria, etc. (Y. S. Lee & Park, 2018). Additionally, the use of urease enzymes obtained from non-microbial sources such as jack bean seeds, watermelon seeds, etc., is also known as enzyme-induced carbonate precipitation (EICP). In recent years, EICP has drawn the interests of numerous researchers (Putra et al., 2017) to a successful investigation and explored the feasibility of using this method on a laboratory scale. At present, commercially available urease enzyme is expensive, because it is produced in small quantities at high levels of purity for use in sensitive applications (e.g., food and medical applications). To overcome some of the above leading limitations, this study focused on using an EICP method which is considered a low cost, sustainable, and eco-friendly method in improving the geotechnical properties of soil. Using crude extract from different plant urease, considered a promising alternative to microbial urease. Considering cost effectiveness and waste utilization, this study focused on using watermelon seeds (*Citrullus lanatus*) because watermelon seeds are considered "food waste material" and a promising alternative to other plant derivative urease (Nam et al., 2015).

However, under a controlled laboratory condition and soil improvement technique using the EICP method (extracted crude urease from watermelon seeds) urea hydrolysis reaction rate, various in situ factors (temperature, pH) that can influence the urease activity and morphology of calcium carbonate crystals (considering Mg^{2+}/Ca^{2+} ratios) were not investigated extensively, since Mg^{2+} is one of the most vital modifiers of $CaCO_3$ morphology (Davis, 2000) found in the natural environment. In contrast to previous research work available for soil improvement by carbonate precipitation, no attention has been paid to understanding the effect of magnesium modified $CaCO_3$ crystals on the variation of the unconfined compressive strength of the soil. Hence, considering the limitations in the previous understanding of magnesium modified calcium carbonate precipitation for soil improvement, this study tried to evaluate the following parameters as discussed below considering different Mg^{2+}/Ca^{2+} ratios (from 0 to 1).

4.2 Objectives

- Extraction and evaluation of urease activity of the crude enzyme (dry condition and germinated condition) and their subsequent effects on temperature and pH.
- Evaluation of urea hydrolysis rate with time considering different Mg^{2+}/Ca^{2+} ratios.
- Mineralogical and morphological characterization of precipitated carbonate crystals by X-ray powder diffraction test (XRD) and scanning electron microscopy (SEM).
- Finally, evaluation of the unconfined compressive strengths (UCS) of the soil specimens treated with EICP solution at various Mg^{2+}/Ca^{2+} ratios and subsequent evaluation of the effective bonding patterns in between the sand particles.

4.3 Materials and methods

4.3.1 Extraction procedure of crude enzyme from watermelon seeds

Dry and germinated (0–4 days) watermelons seeds (0.5 g) were finely crushed with a kitchen blender using 10 mL of distilled water (concentration 50 g seeds/L) and then stirred at 500 rpm for around 1 h. One portion of the collected crude extract was used

directly to measure the urease activity and the other portion of the crude extract was filtered and centrifuged at 10,000 rpm for 5 min at 25 °C and the collected supernatant was used to assess the urease activity considering several environmental parameters (temperature and pH, etc.) followed by the indophenol method (Natarajan, 1995a). The effects of pH were studied at room temperature (25 °C) and the effects of temperature were studied at neutral pH condition (pH 7). The flow chart of the extraction procedure of crude urease solution from watermelon seeds is presented in Figure 4.1. The urease activity of the enzyme (crude extracts) solution was calculated (absorbance at OD_{630} nm) by measuring the released NH_4^+ ions (described by indophenol method) as a result of urea hydrolysis. The measuring time interval for urease activity was 0 min, 5 min, 10 min and 15 min. The overall experimental procedure illustrated in Figure 4.2.
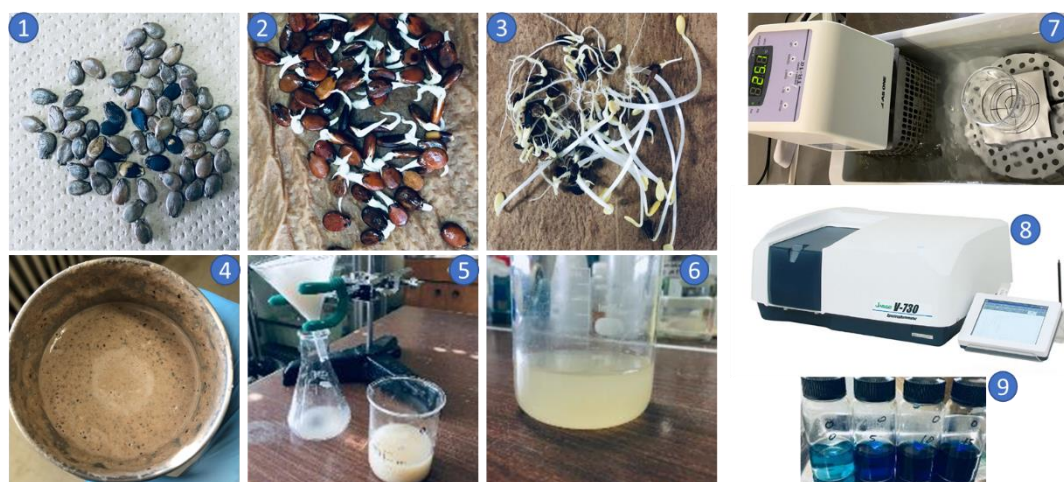
Figure 4. 1: Extraction procedures of crude urease solution from watermelon seeds. (1) Dry seeds, (2) germinated seeds at 48 h, (3) germinated seeds at 96 h, (4) crushed and blended watermelon seeds, (5) filtration of the crude extract, (6) after subsequent filtration translucent crude extract obtained, (7) constant temperature water bath for urease activity investigation, (8) UV-vis spectrophotometer, (9) intensity of dye-solution measured at OD_{630}.
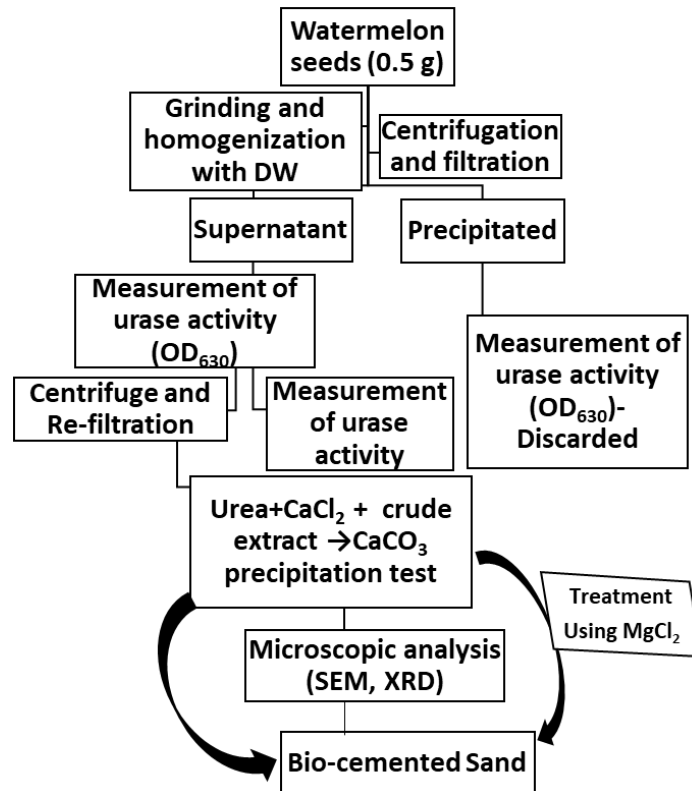
Figure 4. 2: Experimental procedure used in this study (DW—distilled water; SEM—Scanning Electron Microscope; XRD—X-ray Diffraction).

4.3.2 Potentiality assessment of EICP process with various environmental factors

I.   *Materials and equipment for urease activity tests*

Indophenol method was used to measure the urease activity of the crude extract of watermelon seeds. Following materials and equipment were used for the indophenol method.

   I.   Phosphate buffer with pH 7.01: Buffer solution was prepared using 0.1 M potassium phosphate buffer containing 1 mM EDTA).

  II.   Substrate: 0.1 M urea solution in phosphate buffer was used as the substrate.

 III.   Urease enzyme: The crude urease solution was prepared using watermelon seeds extracts.

 IV.   Phenol-Nitroprusside: The solution was prepared by dissolving 23.5 g of analytical grade reagent phenol in 500 mL of deionized water containing 30 mg

of sodium nitroprusside and stored in a brown bottle at 4 °C. The reagent is stable for 3 months.

V.   Hypochlorite Reagent: Dissolve 2 g of sodium hydroxide in 100 mL of deionized water containing 7.5 mL of commercially available bleach (5% NaOCl) and store in a brown bottle at 4 °C.

VI.   Visible spectrophotometer: Visible spectrophotometer was used to measure the intensity of color at 630 nm (OD_{630}).

VII.   pH and Ca^{2+} meter (Eutech Instruments Pte., Ltd., Singapore).

VIII. Reagents: Calcium chloride ($CaCl_2$) and urea ($CO(NH_2)_2$) was used as reagents.

A quantitative value for urease activity was obtained using indophenol method (Natarajan, 1995). In this investigation, the enzyme urease is used to catalyze the hydrolysis of urea into CO_2 and NH_3. The formed NH_4^+ ions react with phenol in the presence of hypochlorite to give the blue dye, indophenol. Intensity of the color produced is proportional to the concentration of NH_4^+ ion in the sample and is measured at 630 nm. NH_4^+ ions released as a result of urea hydrolysis is determined by referring to a previously prepared standard curve with relating absorbance at 630 nm for 0.1, 1 and 10 mg/L NH_4^+ ion solutions prepared from 1000 mg/L NH_4Cl stock solution (Figure 4.3).

The chart shows a plot of OD_{630} versus NH_4^+ ion (mg/L) with equation:
$$OD_{630} = 0.2131(NH_4^+ (mg/L)) + 0.2227$$
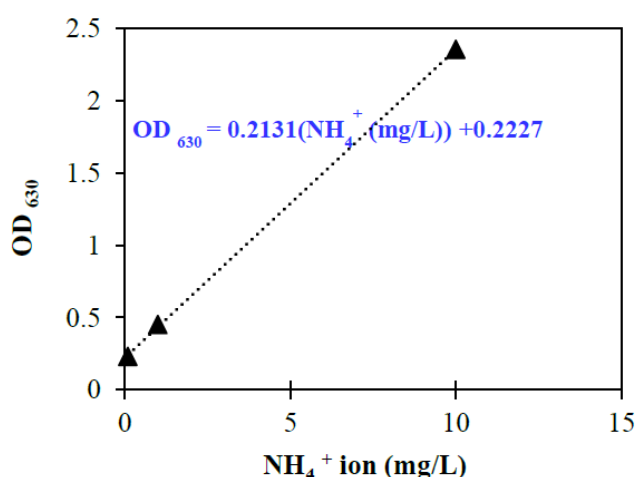
Figure 4. 3: Standard curve for OD_{630} obtained for known NH_4^+ concentrations.

At the indophenol method, 0.1 M urea solution was prepared using 100 mL of phosphate buffer with pH 7.01 and was heated up to required temperature in a water bath. 1 mL of urease solution was added into urea solution that was kept in the water bath. 2 mL from the urea-urease reaction mixture was taken out at 0 min, 5 min, 10 min and 15 min after the addition of urease solution. Sampling at 0 min. was done just after adding urease solution into the urea solution. The reaction was terminated by quickly adding 4.0 mL of phenol reagent followed by 4.0 mL of alkaline hypochlorite reagent into each sample. After that, the final mixture (10 mL) was incubated at 45° C for 10 min after vortexing. The absorbance at 630 nm was measured after diluting with distilled water as required. The rate of NH_4^+ generation and urease activity were calculated using the following formula.

The rate of NH_4^+ generation (mg/L/min) = r_1
Rate of NH_4^+ generation-µmol NH_4^+/min= r x 0.1 x 1/18 x 103= r_2
Urease activity = µmol urea hydrolyzed/min = [U/mL] = r_2 x ½

4.3.3 Enzyme catalyzed reaction rate and CaCO₃ precipitation test

To evaluate the urea hydrolysis reaction rate and to confirm the morphology of $CaCO_3$ precipitation and its precipitation trend, a series of experiments were conducted by various combinations of $CaCl_2$–urea and urease directly in transparent polypropylene tubes. Subsequently, the rate of $CaCO_3$ precipitation in combinations with $CaCl_2$–urea and crude urease was measured directly by evaluating Ca^{2+} concentration with time. The concentration of the crude urease was 50 g seeds/L. $MgCl_2$ was mixed with $CaCl_2$–urea–crude urease solutions counting various molar ratios from 0 to 1 (Table 4.1). The adjusted solution was then added to the test tube and kept in a shaker at 30 °C for 48 h. The obtained precipitation ($CaCO_3$) was separated from the solution using filter paper and kept in an oven drier for about 24 h at 100 °C. Finally, precipitated $CaCO_3$ was weighed to determine the total carbonate precipitate mass. To check the reproducibility of the test three samples of each condition were evaluated. Scanning Electron Microscope (SEM) (TM3000, Hitachi, Tokyo, Japan) and X-ray diffraction (XRD) (MiniFlex™, Rigaku Co., Ltd., Tokyo, Japan)-analysis were also conducted to investigate the morphology of the precipitated carbonates. Calcium Ion Meter (Horiba LAQUAtwin, CA-11, Maine, USA) was used to measure calcium ion concentration (Figure 4.4).

Table 4. 1: Testing conditions for the CaCO₃ precipitation test.

Urea (mol/L)	CaCl₂ (mol/L)	MgCl₂ (mol/L)	Mg^{2+}/Ca^{2+} Ratio
0.50	0.50	0.00	0.00
0.50	0.45	0.05	0.11
0.50	0.40	0.10	0.25
0.50	0.35	0.15	0.43
0.50	0.30	0.20	0.67
0.50	0.25	0.25	1.00

Figure 4. 4: Calcium ion meter with standard solutions for calibration.

4.3.4 Sand solidification (Syringe) tests: Effects of adding Mg^{2+} ion

The majority of the bio-stabilization studies carried out so far has assessed the change in soil properties with calcium carbonate precipitation. However, the real field conditions are such that it is likely to contain other impurities and cations that may interact with the precipitation process. For implementation of the EICP for the desired application in near shore environments, attention has to be paid to the fact that target treatment environment will consist of a considerable amount of magnesium ions. Therefore, a set of experiments were conducted incorporating both Mg^{2+} and Ca^{2+} ions with various Mg^{2+}/Ca^{2+} molar ratio from 0 to 1. Anhydrous magnesium chloride (MgCl₂) was used as the Mg^{2+} source. Dried "Mikawa" sand (commercially available) was placed at 110 °C for 1 day and then transferred (85 g) into a 50 mL syringe (diameter, φ = 3 cm, height h = 7.1 cm) and compacted gently. The physical properties of "Mikawa" sand used in this study are outlined in Table 4.2. Prepared samples were

placed in an incubator (30 °C). Subsequently, 26 mL of prepared urea–CaCl$_2$–urease solution (maintaining Mg^{2+}/Ca^{2+} ratios) was added to the syringe and the final level of the solution maintained above the top surface of the sand sample. A new solidification solution was injected into the samples (48 h intervals) with the same volume and concentration and drained the previously injected solution gradually. To avoid clogging and considering the fast reaction rate, the crude urease injection interval was decided (48 h). To investigate the temporal variations of these parameters within the specimen, the concentration of Ca^{2+} and the pH of the outlet was observed regularly (48 h intervals). The experimental protocol used in this study illustrated in Figure 4. 5. Finally, using a needle penetration device, a value for approximate UCS (unconfined compressive strength) was measured after 14 days of curing. The microstructure and morphology analysis were conducted by SEM and XRD analysis. The condition of the syringe solidification test outlined in Table 4.3.

Table 4. 2: Physical properties of "Mikawa" sand used in this study.

Physical property	Mikawa sand
Maximum Density (g/cm^3)	1.476
Minimum Density (g/cm^3)	1.256
Particle Density (g/cm^3)	2.66
Mean Diameter (mm)	0.870

Table 4. 3: Testing conditions for sand solidification.

Mg^{2+}/Ca^{2+} ratio	Curing days	Temp (°C)	Injection Interval (h)	Level of Saturation
0.00	14	30	48	Saturated
0.11	14	30	48	Saturated
0.25	14	30	48	Saturated
0.43	14	30	48	Saturated
0.67	14	30	48	Saturated
1.00	14	30	48	Saturated
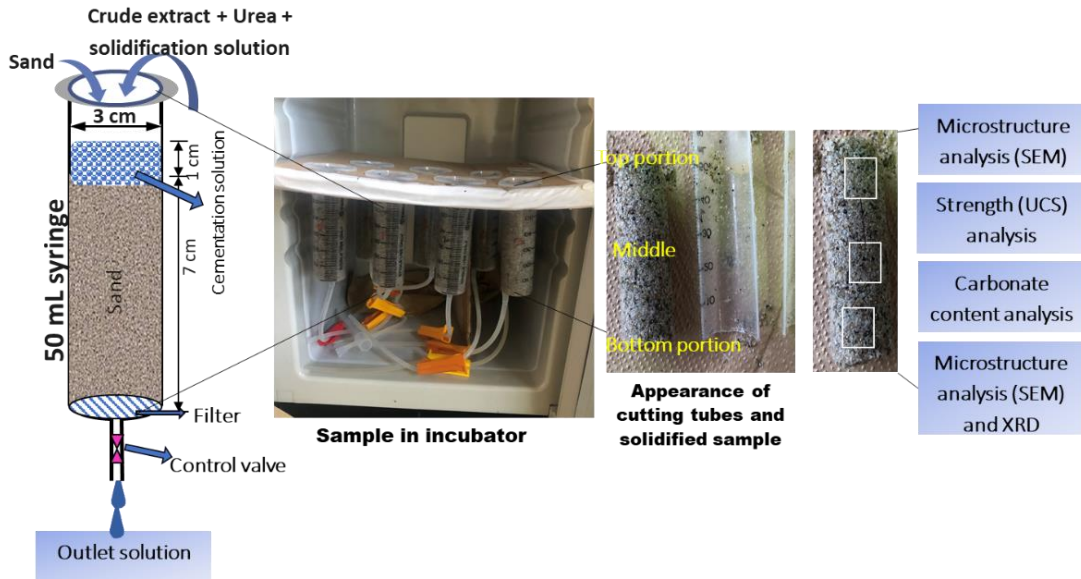
Figure 4. 5: Schematic experimental protocol used in this study.

4.3.5 Needle penetration tests for estimation of UCS

An estimated UCS was obtained from the needle penetration (NP) value given by the needle penetration device (SH-70, Maruto Testing Machine Company, Tokyo, Japan) as described to the previous sections.

4.3.6 SEM observation (SEM)

To study the microstructural changes in the specimens, SEM analysis was performed using Miniscope TM 3000 (Hitachi, Tokyo, Japan). The representative samples were carefully taken from the specimens and observed through SEM after the oven dry at 60 °C as described to the previous sections.

4.3.7 X-ray diffraction (XRD) analyses

X-ray diffractometer patterns of the powdered beachrock samples were analysed using an X-Ray generator (MiniFlex™, Rigaku Co., Ltd., Tokyo, Japan). The analysis was carried out in room temperature using the XRD machine with CuKa radiation at a rate of $6.5°2\theta/min$ ranging from 10 to $80°2\theta$. Qualitative mineralogy of the samples was determined with the standard interpretation procedures of XRD using Match!

software for phase identification from powder diffraction as described to the previous sections.

4.4 Results and discussion

4.4.1 Results of urease activity: Crude urease

Urease activity (U/mL) of the extracted enzyme from watermelon seeds is shown in Figure 4.6 corresponding with dry seed condition and germinated seed condition with time. Results showed that, for the case of dry seed crude extract solution, the urease activity was 6 U/mL and gradually increased with time (germinated condition). After several consecutive days (48 h) the urease activity reached to its peak (9 U/mL) and then the urease activity declined (5 U/mL) after 96 h and showed a bell shape curve. The fluctuation of the urease activity was influenced by some metabolic factors, biological reactions and functional proteins (Abas Wani et al., 2006; Wani et al., 2011) which triggered the enzymatic activity of the seed. The obtained urease activity (in the case of dry seeds) in this study was equivalent to some previous studies that mainly focused on crude solution extracted from crushed watermelon seeds (Dilrukshi et al., 2018; Javadi et al., 2018). In addition, this study also revealed higher urease activity extracted from germinated watermelon seeds, which allows gaining of an additional 50% urease activity from the same mass of seed used (Table 4.4), for improving the enzyme-induced bio-cementation method and its application. Therefore, germinated seeds (48 h) were used for rest of the study.
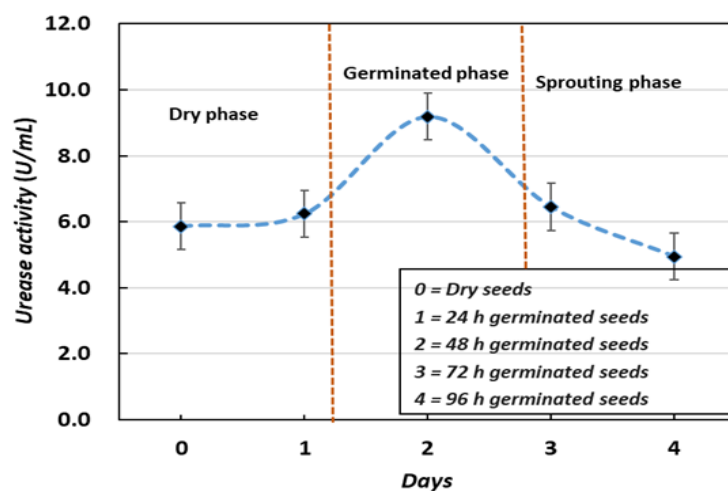
Figure 4. 6: Urease activity of different conditions of seeds.

74

Table 4. 4: Crude urease extraction results with their purification percentage.

Product	Urease activity (U/mL)	Volume of extraction (mL)	Total Units (U)	Specific activity (U/mL)	Purification fold	Loss of enzyme (%)
Wako pure enzymes	15	100	150	10	0.67	0
Non-treated	10	100	100	10	1	33
Treated	8	100	80	10	1.25	47

* Loss of enzyme = [Sum of crude extract (U) – Total Units after treatment) / Sum of crude extract (U)]

I. *Urease activity: Temperature dependency*

The successful implementation of the EICP technique for soil improvement was likely dependent on several environmental factors including urease activity, temperature, pH, etc. (Feder et al., 2021), which were also evaluated in this study. Figure 4.7 showed the interdependent changes of urease activity from the initial phase to the declining phase (10 °C to 60 °C) and the fluctuation of urease activity was temperature dependent. From the results (Figure 5), the urease activity was lower at 10 °C and increased progressively with increasing temperature for both non-treated and treated cases (before centrifuge and after centrifuge). Subsequently, the urease activity reached a stable phase at 30 °C and the urease activity dropped with further increase in temperature. Compared with some of the previous studies, the maximum urease activity was obtained at 65 °C (jack bean seeds) and was deactivated at 70 °C (Blakeley & Zerner, 1984; Feder et al., 2021). It was reported that, at low temperature (below 10 °C) and at high temperature (above 70 °C), the free enzyme easily denatured (Dixon et al., 1975). The possible reason was that the molecules of the enzyme exceed the barrier of energy and the breakage of the hydrogen and hydrophobic bonds (Weber et al., 2008) that were responsible for maintaining the structure of the enzyme (EL-Hefnawy et al., 2014). Finally, because of the broken structure of the enzyme, further ureolysis potentiality also dropped. From this study, it is obvious that, to obtain maximum urease activity from crude extract, i.e., plant sources (watermelon seeds), retaining moderate temperature is recommended.
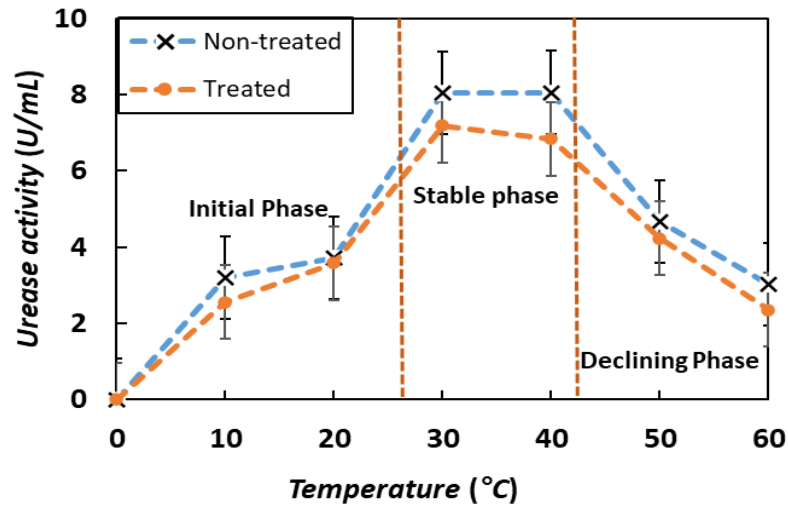
Figure 4. 7: Urease activity with different temperature conditions.

II. *Urease activity: pH dependency*

The pH values played an important role in the urease activity of crude urease. Previous research reported that the pH of the reaction medium is a significant abiotic factor that affects the urease activity during urea hydrolysis (Labana et al., 2005). In this study, the urease activity of the extracted crude urease from watermelon seed was found to yield maximum activity at pH 7.5 (Figure 4.8), which means that the watermelon urease may belong to the category of basic urease. The pH value of the test condition was set from slightly acidic (pH 5) to slightly alkaline (pH 9). The results of pH dependency showed that variation of pH was evidently sensitive for urease activity. The urease activity was below 1 U/mL at pH 5. The maximum urease activity (7.5 U/mL) was observed with increasing pH (7.5) and with further increase in pH (9), the urease activity declined (2 U/mL). Similarly, several other studies reported basic pH as an optimum value for the urease activity of extracted crude urease (Neupane et al., 2013). These findings may be clarified by the fact that the acidic or alkaline pH inhibits the enzyme, decreasing its activity. The presence of active sites in amino acids can also be affected by changes in pH, which may alter their ionization and consequences on urease activity (Cui et al., 2021). Studies also observed that an acidic reaction medium delayed the EICP reaction rate (Rohy et al., 2019), which was also consistent with the results from bio-treated soil stabilization (Cheng et al., 2017).
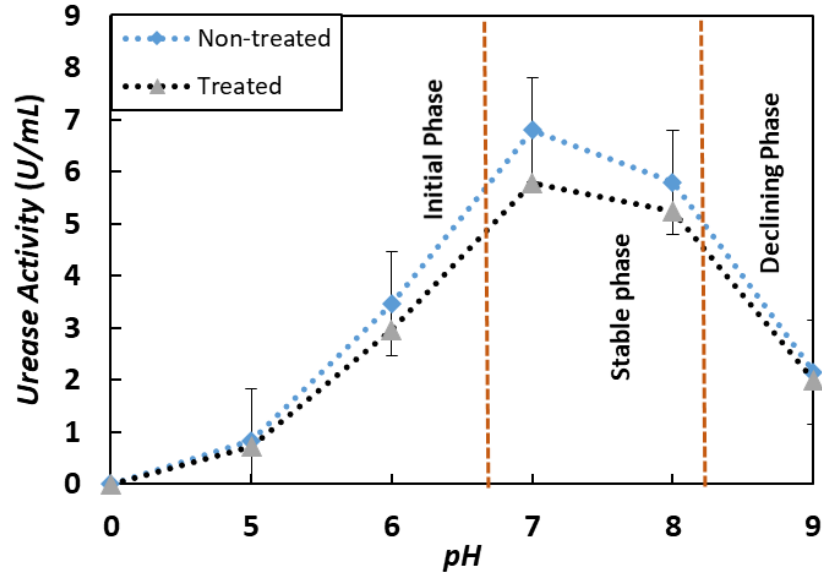
Figure 4. 8: Urease activity with different pH conditions.

4.4.2 Results of CaCO₃ precipitation test

It is reported that, CaCO$_3$ acts as the main binding materials in between the sand particles to stabilize the soil for producing artificial beach rock and bio-cemented sand (Wani and Shivhare et al., 2011; Mobley and Hausinger 1989). In EICP process, the crystal precipitation amounts closely related with CaCl$_2$-urea concentration, and the CaCO$_3$ crystals started to form immediately because of the accessibility of free urease enzyme (Figure 4.9), which was also reported by previous studies (Baiq and Johan et al., 2020). Figure 4.9 showed the evidence of forming and enlargement of CaCO$_3$ crystals.
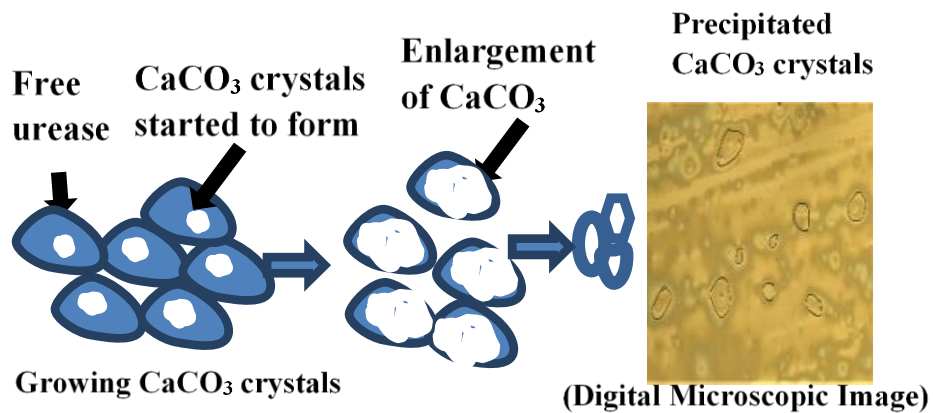
Figure 4. 9: Growing of CaCO₃ crystals

It's well established that $CaCO_3$ serves as the primary binding materials in between the sand particles to stabilize the soil (Khodadadi Tirkolaei et al., 2020). The effects of different Mg^{2+}/Ca^{2+} ratios and subsequent hydrolysis with time were studied and the results are shown in Figure 4.10. Figure 4.10 showed that the urea hydrolysis rate of among the different Mg^{2+}/Ca^{2+} ratios demonstrated a significant difference. Notably, when the $Mg^{2+}/Ca^{2+} = 0$ the urea hydrolysis rate was very fast, the urea hydrolysis mostly occurs in between 0 and 5 h. With increase in Mg^{2+}/Ca^{2+} ratios, the urea hydrolysis rate tends to be slower and delayed the urea hydrolysis rate up to 24 h. The variation of the reaction rate was determined by the Mg^{2+}/Ca^{2+} ratios (Katz, 1973). Since Mg^{2+} ion has a greater solubility than Ca^{2+} ion (Katz, 1973), therefore, during the urea hydrolysis process, the supersaturation of calcium carbonate occurred by interfering with the nucleation sites (Doner & Pratt, 1969), resulting in formation of calcite, aragonite and/or vaterite depending on the Ca^{2+} and Mg^{2+} reaction equilibrium.
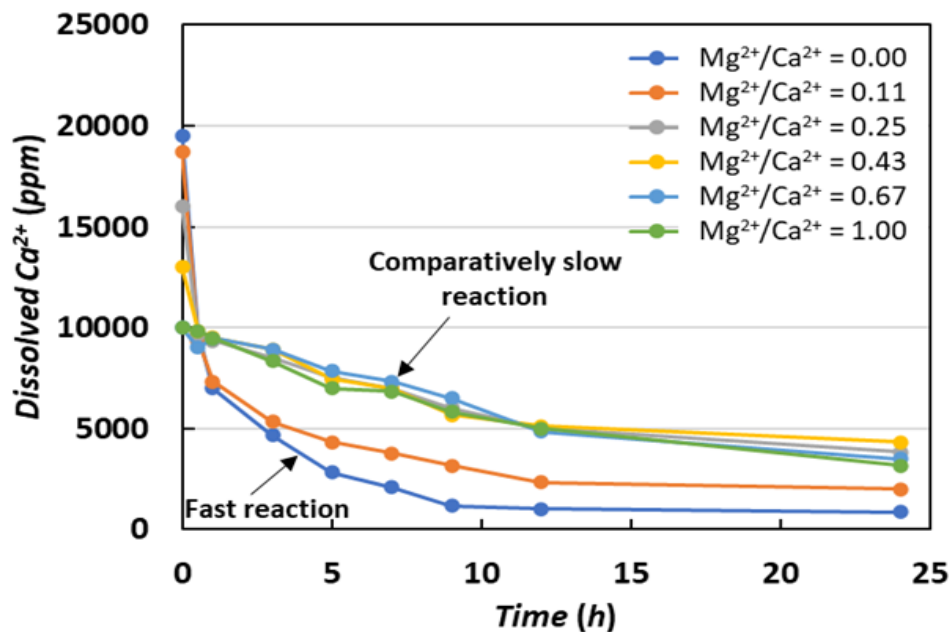
Figure 4. 10: Urea hydrolysis rate with time.

Furthermore, the amount of formed $CaCO_3$ precipitated crystals were also highly influenced by Mg^{2+}/Ca^{2+} ratios. Based on the results of test-tube experiments, Figure 4.11 illustrates the effect of various Mg^{2+}/Ca^{2+} ratios on the formed $CaCO_3$ crystals. The results showed that, as the Mg^{2+}/Ca^{2+} ratios increased, the $CaCO_3$ crystals were

decreased. The possible reason for varying $CaCO_3$ precipitation was unstable pH and the duration of urea hydrolysis which occurred. Under a certain pH change or during the hydrolysis process, the shape of precipitated crystals changed and extended through the crystallization or re-crystallization process until a more stable form was obtained (Chandra & Ravi, 2020). The re-crystallization process triggered the system to lose energy by forming an unstable crystal structure (Xia et al., 2020), which could be one of the reasons for the decreased $CaCO_3$ precipitation amount. The result of this study is in accordance with some of the previous studies as well.
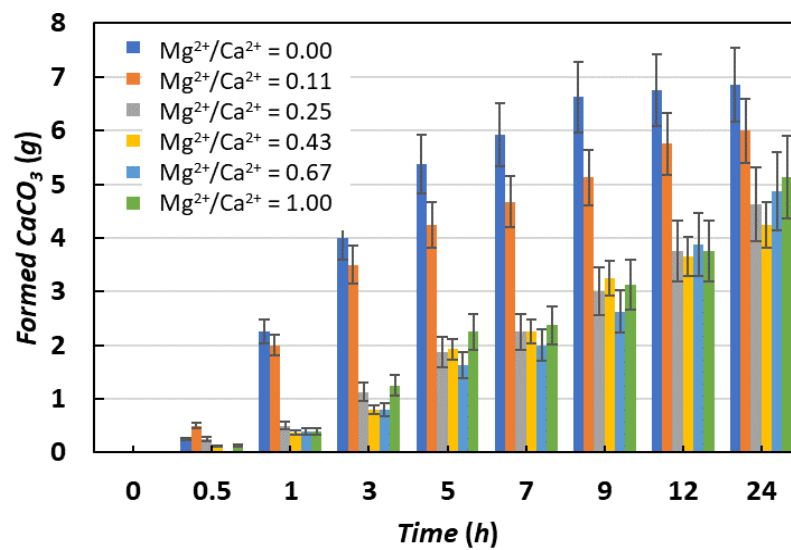
Figure 4. 11: Amount of $CaCO_3$ precipitated with time.

The size and morphology of the precipitated crystals has serious implications on the successful bio-stabilization technique. Therefore, microstructure and mineralogy of the precipitates from the experimental cases were determined. The evolution of the crystals' morphology and shapes obtained from the SEM and XRD analysis is shown in Figures 4.12 and 4.13. The crystal structure of the image showed a rhombohedral shape without the magnesium ($Mg^{2+}/Ca^{2+} = 0$), which is also confirmed as calcite (20.3%) and vaterite (79.7%) by XRD analysis. With increasing Mg^{2+}/Ca^{2+} ratios, the precipitation tendency and crystal morphology were also observed to change from rhombohedral (vaterite) to hexagonal (calcite) and orthorhombic (aragonite) (Sun et al., 2019; Xu et al., 2020). When $Mg^{2+}/Ca^{2+} = 0.11$ and 0.25, results showed an effective transformation of calcite (85%) and vaterite (15%) (Figure 4.12-b-B). Furthermore, due

to metastable nucleation and increased Mg^{2+}/Ca^{2+} ratios (Mg^{2+}/Ca^{2+} = 1) orthorhombic (aragonite) crystals are evident from figure (Figure 4.13-f-F). The overall mechanism of transformation of crystals is illustrated in Figure 4.14.
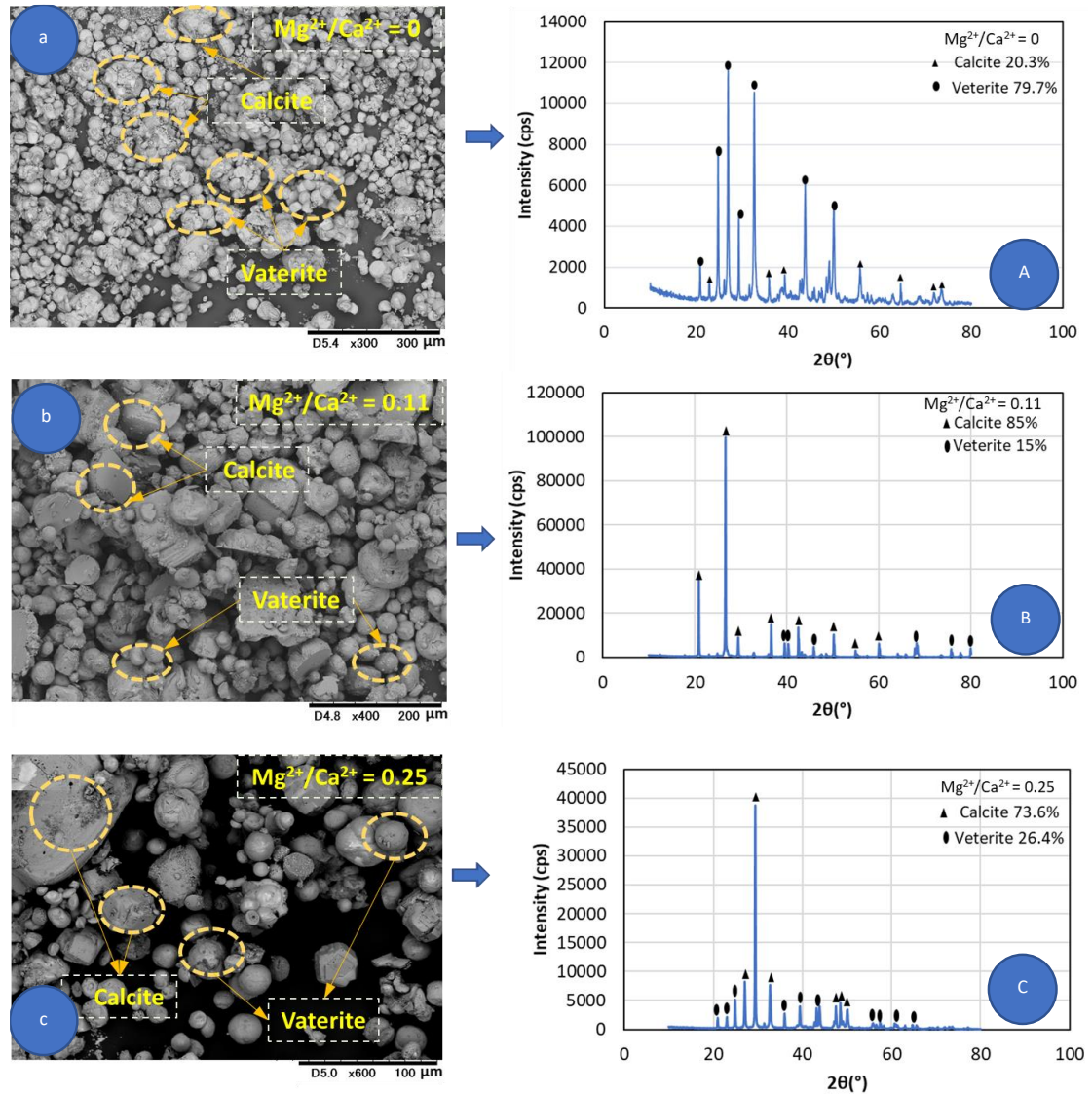
Figure 4. 12: SEM images of the precipitated $CaCO_3$ crystals with different Mg^{2+}/Ca^{2+} ratios (**a**–**c**) and their subsequent XRD analysis to confirm the polymorph of the crystals (**A**–**C**).
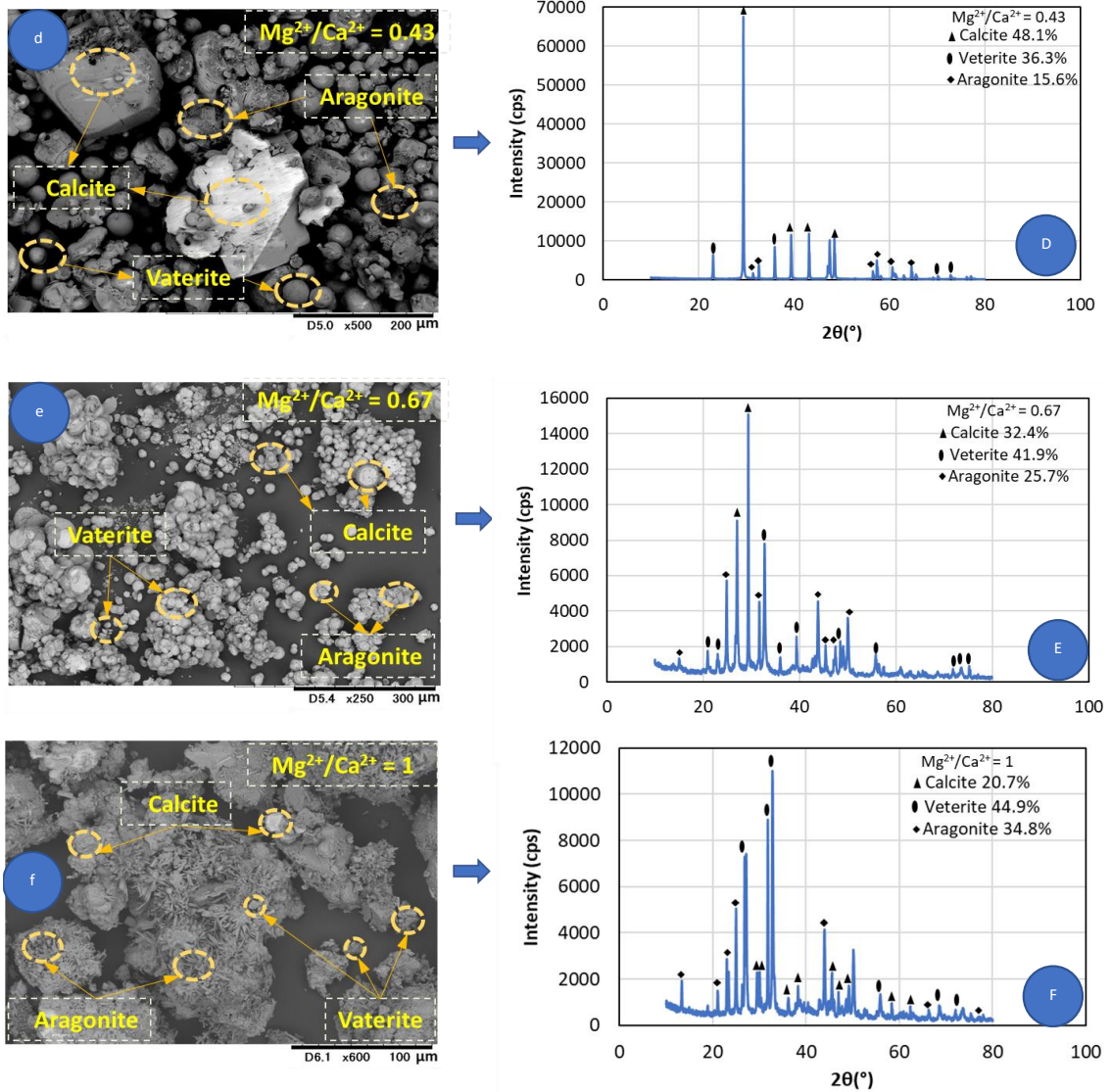
Figure 4. 13: SEM images of the precipitated CaCO₃ crystals with different Mg²⁺/Ca²⁺ ratios (**d**–**f**) and their subsequent XRD analysis to confirm the polymorph of the crystals (**D**–**F**).
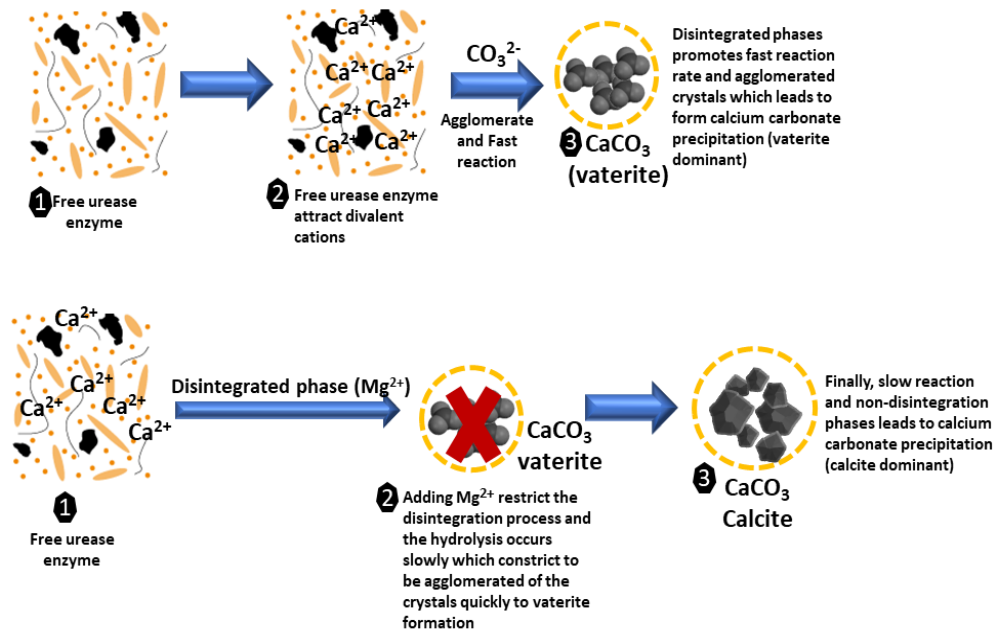
Figure 4. 14: Schematic illustration of the $CaCO_3$ formation mechanism (calcite and vaterite) in contract with Mg^{2+}/Ca^{2+} ratios.

4.4.3 Results of sand solidification test: Effects of adding Mg^{2+} ion

To better understand of the bonding effect in between the sand particles syringe sand solidification tests were conducted. Figure 4.15 shows the UCS value resulting from the specimens of soil treated with crude extract solution containing various Mg^{2+}/Ca^{2+} molar ratios. According to the UCS results, a moderate UCS (1.2 MPa) was obtained using only crude extract enzyme solution ($Mg^{2+}/Ca^{2+} = 0$). Moreover, a higher UCS (2.5 MPa) was obtained when Mg^{2+}/Ca^{2+} ratios increased at 0.11 and cured for 14 days. After subsequent increase in $Mg^{2+}/Ca^{2+} = 0.43–1.00$, the UCS values declined gradually and reached a lower UCS (1.5 MPa) value compared to other testing cases.
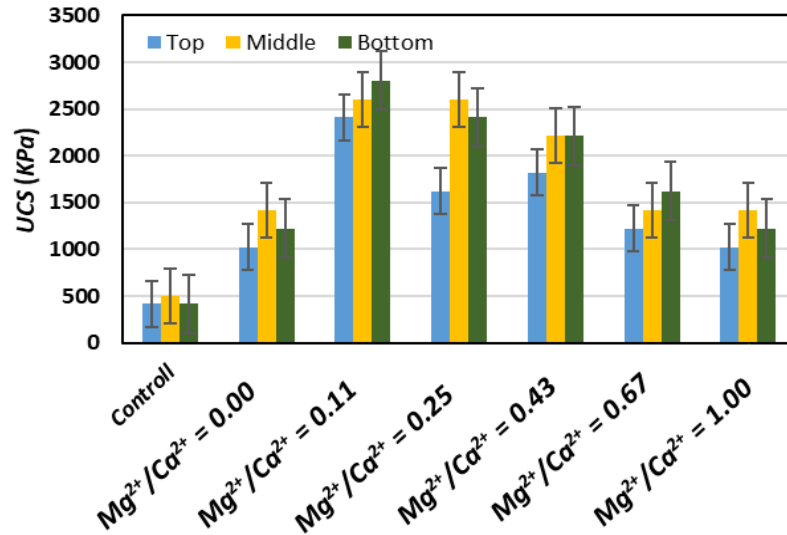
Figure 4. 15: UCS of the solidified sand.

Figure 4.16 shows the overall improvement tendency of using Mg^{2+}/Ca^{2+} ratios over estimated UCS. The results showed that Mg^{2+}/Ca^{2+} ratios are a significant factor for EICP treated sand improvement. Minimal performance observed at higher ($Mg^{2+}/Ca^{2+} = 1$) or lower Mg^{2+}/Ca^{2+} ratios ($Mg^{2+}/Ca^{2+} = 0$). Optimum Mg^{2+}/Ca^{2+} ratios were favored to obtain an effective treatment of the EICP-treated specimens.
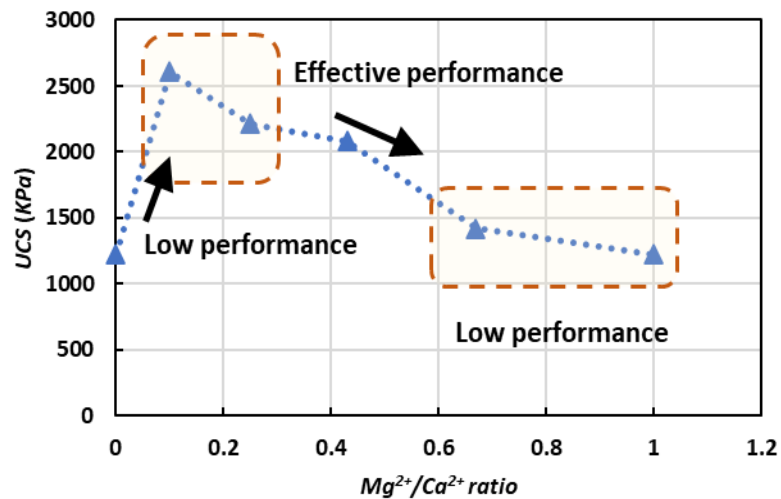
Figure 4. 16: Improvement tendency of the solidified sand (UCS) with different Mg^{2+}/Ca^{2+} ratios.

4.4.4 Microscale observation results (SEM and XRD)

From the SEM observation results, it is obvious that, in the case of only crude extract enzyme–$CaCl_2$–urea solution, the crystals (mostly vaterite) remained on the sand particles, and their bonding capacity between the sand particles remains very weak (Figure 4.17). The grain surfaces are fully covered with crystals of average size 10 μm and the matrix is supported by relatively larger crystals. Crystals are very well interweaved and crosslinked at the grain contact points thereby effectively bonding the loose sand particles together. Furthermore, the promotion of the newly added solution (depending on the Mg^{2+}/Ca^{2+} ratios), the transformation of the crystal occurred (mostly calcite) and the strength of the sand sample was significantly increased. From the SEM images, it's also clear that the precipitated crystal morphology changes from rhombohedral to spherical and then to needle shape when Mg^{2+}/Ca^{2+} ratio gradually advanced from 0 to 1. The effectiveness of the bonding pattern and agglomeration of $CaCO_3$ crystals in between the sand particles shown in Figure 4.17 (A–F). The results clearly reflect the presence of calcite in between the sand particles and void space which is mainly responsible for the increase in the strength of the treated samples. The results of this study are in accordance with (Arab et al., 2021; Cuccurullo et al., 2020; Sulistiawati Baiq, 2020).
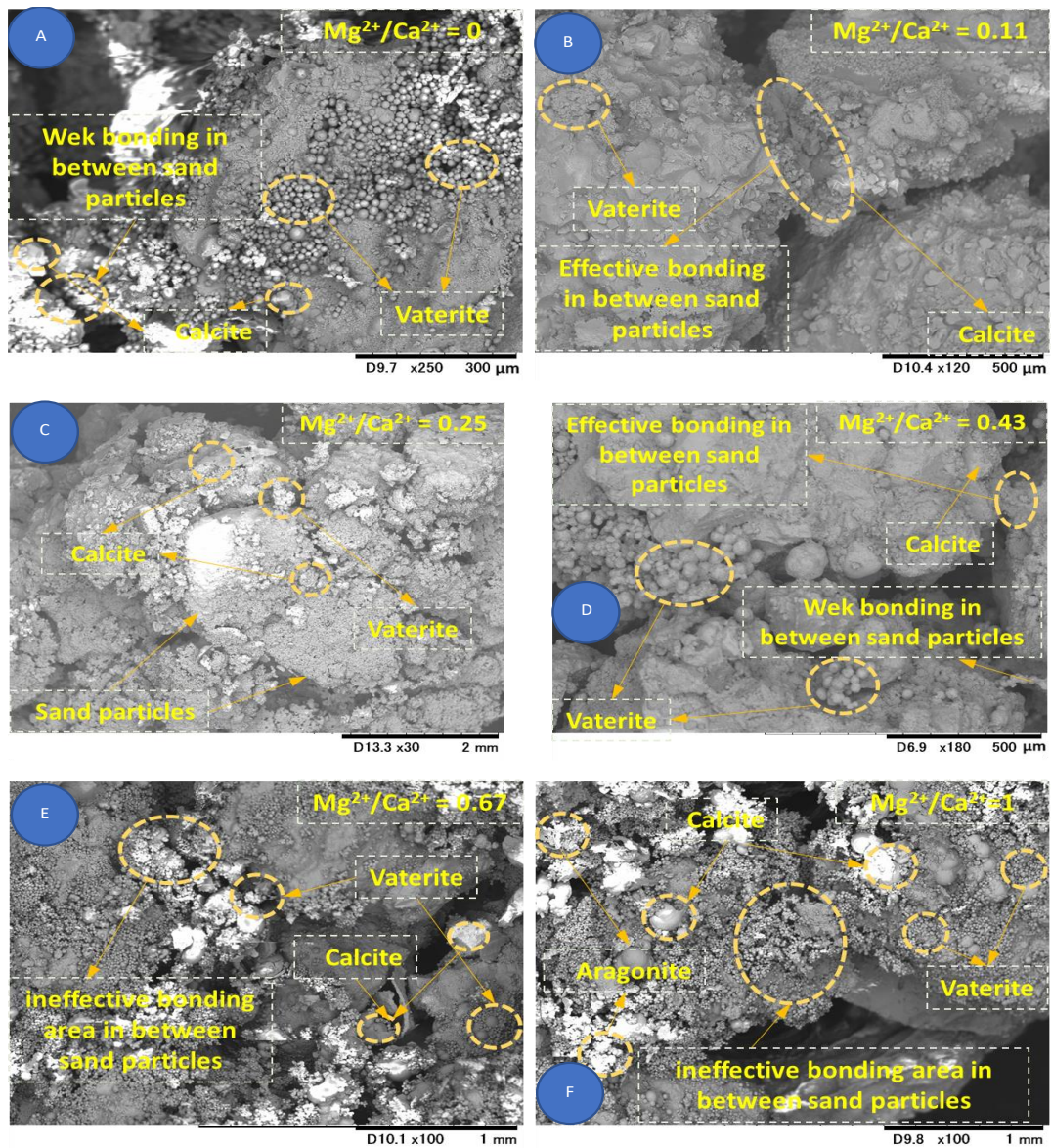
Figure 4. 17: SEM images showing the efficacy and bonding patterns of $CaCO_3$ crystals in between the sand particles (**A–F**).

4.5 Conclusions

The prospect of using the enzyme induced carbonate precipitation (EICP) method as an effective bio-inspired technique has been evaluated in this study using natural source of urease enzyme (watermelon seeds). The development of alternative sources for urease enzymes which are economical and easy to regulate in the natural world was a major problem in the feasibility of calcite precipitations strategies. Through extracting the enzyme from watermelon seeds (upto 60% purity level) in a sustainable, cost-

effective, and eco-friendly way, this research successfully addressed a feasible solution. Moreover, this study also explained the effects of Mg^{2+}/Ca^{2+} ratios on carbonate precipitation and their morphology and described the overall process of soil improvement methods using sustainable, cost-effective, and environmentally friendly bio-mediated techniques. Considering the results performed in this study, the following conclusion can be drawn:

i. Crude extracts from seeds germinated for two days showed a 50% higher urease activity than that extracted from dry seeds.

ii. It was detected that the Mg^{2+}/Ca^{2+} ratios are a significant factor influencing both the amount of carbonate precipitation and the ratios of the calcium carbonate polymorphs (calcite, vaterite, aragonite) in EICP process.

iii. The Mg^{2+}/Ca^{2+} ratios influence the UCS value of the treated samples. For Mg^{2+}/Ca^{2+} ratios $= 0.11$, an improvement of UCS of 50% compared to $Mg^{2+}/Ca^{2+} = 0$ could be demonstrated.

iv. Our results suggest that calcite is more efficient in binding the sand particles compared to vaterite. Adding a small amount of $MgCl_2$ has a significant effect on the $CaCO_3$ precipitation pattern and bonding between the sand particles during EICP, as it increases the proportion of calcite. However, some major challenges for field implementations of this EICP method still remain in this novel area.

v. Nevertheless, the findings of these studies could play a significant role for sand stabilization and other applications in the geotechnical sectors.

CHAPTER 5 : STRENGTH AND DURABILITY IMPROVEMENT OF THE BIO-CEMENTED SAND BY MICP METHOD

5.1 Introduction

Recently significant interest in bio-mediated soil improvement has been highlighted as an innovative and effective approach for soil and ground improvement. Among the various bio-mediated soil development approaches, Microbial Induced Carbonate Precipitation (MICP) has been recognized as a promising approach for soil improvement in recent years. The microbial urease hydrolyzed the urea $[CO(NH_2)_2]$ and produced ammonium and carbonate ions and consequently increased the pH during the MICP (Gowthaman et al., 2019; Mwandira et al., 2017) immobilization and strength improvement using several types of soil materials; the capability of microorganisms to form calcium carbonate within the sand particles and pores; the relationship between the precipitated calcium carbonate content and the strength of MICP-treated sand; studying the engineering properties of the MICP-treated sand such as volume, permeability, strength, and compressibility, introductory numerical simulations (Omoregie et al., 2019). However, many recent experiments demonstrated the mechanism of calcium carbonate deposition and improvement of soil strength after curing MICP. Earlier research also found non-uniformity of precipitation of calcium carbonate and brittle failure behavior of MICP-treated soil (Mortensen et al., 2011). Studies showed that, the MICP-treated soil tends to fails at a low axial strain in unconfined and triaxial compression tests and the axial stress drops rapidly after peak stress because most of the calcium carbonate precipitated non-uniformly close to the influent of the specimen column and hindered the biocementation process in the deeper location of the specimen (Martinez et al., 2013).

To improve this shortcoming, few studies have been conducted to improve the ductility and toughness of sand after curing of MICP-sand. Although the sand solidified by microorganisms can reach a high strength, it mainly performs as brittle failure of the substances and the strength lost immediately with a threaten of safety hazard problems. Therefore, the development of new mechanisms to improve the toughness, ductility,

and durability of MICP treated soil becomes a critical need for research which can be improved by addition of fibrous materials. Earlier studies showed that, using fibrous materials increased bacterial interaction with the cementation solution and facilitated the uniform calcium carbonate precipitation within the sand pores with MICP treated soil (L. Li et al., 2014). Several studies also revealed that, adding of fiber materials can significantly improve the shear strength and the ductility of soils and less postpeak loss of strength and improved the brittle failure behavior and improved the internal friction and stiffness of the soil (Qiu et al., 2019). However, to address these challenges most of these previous studies focused on using synthetic polymer-based fiber materials like non-woven geotextile fiber, steel fiber, polypropylene fiber, glass fiber, carbon fiber, etc. which associated with the relatively high cost, health concern and environmental hazards (H. J. Chen et al., 2019). Moreover, to date, only a few experiments have concentrated on the improvement of the engineering properties of soils treated with MICP method using fiber materials. Therefore, developing a new approach and identifying cheap, readily available fiber content in view of safety, environmental considerations and sustainability required further investigations. A detailed analysis to improve the drawbacks of MICP-treated sand by the inclusion of fibers was inspired by the current deficiencies in the traditional MICP process. This study considered to use natural jute fiber (*Corchorus capsularis*) because of it's excellent physical mechanical properties, high resistance capacity (temperature, pH, salinity) easily available, inexpensive, low energy required, light weight, sustainable and eco-friendly (Choi et al., 2016; Gowthaman et al., 2018b).

Among the wide range of potential applications of fiber reinforce MICP treated biocemented sand, coastal erosion protection is gaining a great deal of interests among geotechnical engineers (Rangel-Buitrago et al., 2015; Khan et al., 2016). The coastal areas are typically exposed to several climatic changes such as rainfall, evapotranspiration, wet-dry cycles etc. Cyclic wet-dry (WD) is another core weathering agent, and that has been a serious concern in geotechnical and geological engineering especially for coastal erosion protection. Due to the direct contact with the atmosphere, the surface undergoes periodical WD cycles during (i) diurnal changes in rainy-sunny weathers (Tang et al., 2011) and (ii) subsequent processes of rainfall evapotranspiration (Tang et al. 2016). Several studies demonstrated that the WD cycles caused substantial irreversible deformations in the fabric of geomaterials. For example, it has been

discovered that the presence of swelling minerals causes temporal changes in soft soils during WD, resulting in desiccation cracking, shrinkage, and volumetric changes (Tang et al., 2011; Zhang et al., 2013). The microstructure of soil aggregates is dramatically altered by the WD operation, resulting in a decrease in shear strength and compressibility (Tang et al., 2016). Fracture energy reduction and chemical corrosive behavior are the most commonly recorded degradation mechanisms in sedimentary materials. Several research works evidenced that WD process significantly deteriorates the mechanical properties of calcarenite rocks and sandstone materials (Ciantia et al., 2014, 2015; Khanlari and Abdilor 2015). Since the responses of MICP-treated soils (cemented by $CaCO_3$) are often comparable with natural carbonate/sandstone sediments (Daryono et al., 2020), treated samples may more likely undergo similar deterioration during prolonged exposure to repeated WD process. It is worth noting that the available information on weathering effects of MICP treatment under repeated WD actions are very limited A performance assessment with respect to durability is therefore necessary and recommended prior to the field applications.

5.2 Objectives

I. The primary objectives of this work were to improve the strength of the fiber reinforced MICP treated samples by investigating the effects of natural fiber (jute) on the MICP treated soil considering fiber length, content (ratio); carbonate precipitation patterns and interaction with the microorganisms to improve the engineering properties (ductility, toughness and brittleness behavior) of the biocemented sand specimen. The mechanical properties of the MICP treated sand, microstructure of the specimen, interaction between the fiber and microorganisms were investigated and analyzed using unconfined compressive strength (UCS), scanning electron microscopy (SEM), and fluorescence microscopy.

II. Another core objective was to investigate the influence of WD cycles on the physical and mechanical characteristics of the fiber reinforce MICP treated sand, using distilled water (DW) and artificial sea water (ASW) to compare the efficiency of treated samples.

89

5.3 Materials and methods

5.3.1 Strength Improvement

I.   Fiber used in this study

Previous research studies indicated that jute fibers, with appropriate length and content, could increase substantially (Sivakumar Gowthaman et al., 2018a; Wen et al., 2018) Moreover, jute fibers consisted of high initial modulus, high consistency in tenacity and tensile strength, high rigidity, and a lower percentage of elongation during breakage, which lead to their use in soil improvement widely and motivates to use in this study. The locally available jute fiber (100% natural) was used in this study (Figure 5.1) without any chemical treatment. The jute fiber was purchased from "DCM Homac CO., LTD.", Japan and the fiber was collected by "Hayase Industries, LTD", Japan. Microstructure of jute fiber was examined through scanning electron microscope images. SEM images of cluster and single filament of jute fiber presented in Figure 5.1.

The key features of the jute fiber used in this study shown in Table 5.1. It was studied that, the efficiency of the fibers used to soil improvement highly dependent on the properties of the fibers, such as the nature of fibers, fiber length, and fiber ratio (Hejazi et al., 2012). The jute fiber was cut into three different lengths (5 mm, 15 mm, and 25 mm) and several percentages (content) by weight (0.5%, 1.5%, 3%, 5%, 10% and 20%) were used for mixture with mikawa sand particles. The physical appearance of the prepared jute fiber samples shown in Figure 5.2. All the jute fibers used in this study were placed in a dryer at 60 °C for 24 h before mixing with the sand and MICP treatment.

Table 5. 1: The key features of the jute fiber used in this study.

Fiber type	Thickness	Length (Total)	Weight	Type	Moisture content	Colour
Jute	2 mm	510 m	900 g	Roll	3.4%	Golden-brown
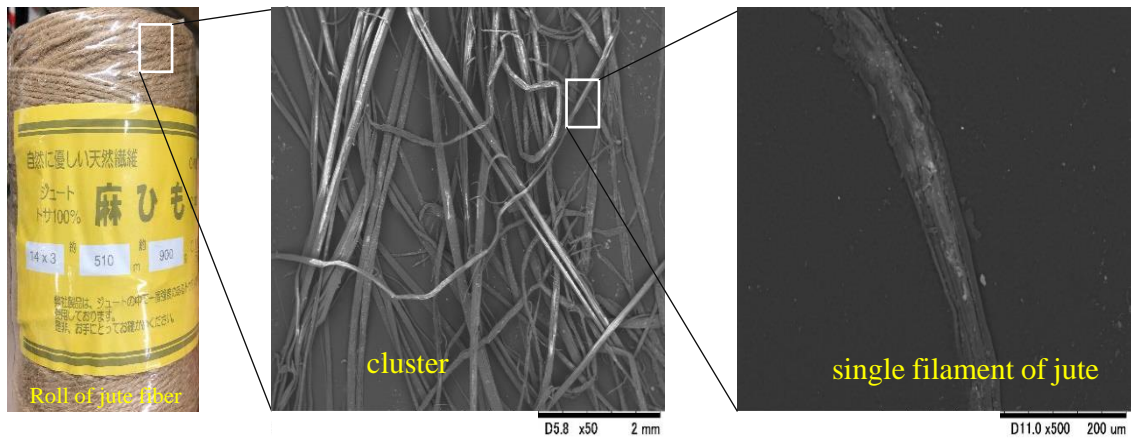
Figure 5. 1: Apparency of jute fiber and microstructure images of jute fiber obtained by SEM.

Figure 5. 2: Physical appearance of jute fiber cut into different length used in this study.

II.   *Used microorganisms and soil properties*

The bacteria used in this study was *Micrococcus yunnanensis* (hereafter denoted as G1), isolated from the coastal area of Porto Rafti, Greece (Imran et al., 2019). The key features of this bacteria (Figure 5.3) were known to exhibit comparatively high urease activity with salt-tolerant properties, could survive for an extended period of time at various temperatures and pH conditions, and in nutrient-deficient conditions (G. Z. Zhao et al., 2009b). Liquid ZoBell2216 medium were used as culture solution for the selected bacterial species. The culture medium was dissolved with hi-polypeptone (5.0 g/L), FePO4 (0.1 g/L), and yeast extract (1.0 g/L). The components were mixed with artificial seawater and maintained pH at 7.6–7.8. The bacterial cells were

precultured (using the ZoBell2216 medium) for 24 h at 30 °C in a shaker at 160 rpm. The precultured bacterial cells were then transferred (1 mL) to a 100 mL of fresh ZoBell2216 medium and incubated at 30 °C at 160 rpm. Prepared bacterial culture solution was used for the MICP process. During the cultivation, the bacterial cell growth (OD600) was determined and adjusted (approximately 6) by a UV-VIS spectrophotometer (V-730, JASCO Corporation, Tokyo, Japan) and urease activity (1.5±3 U/mL) was measured by indophenol method (Natarajan, 1995b).
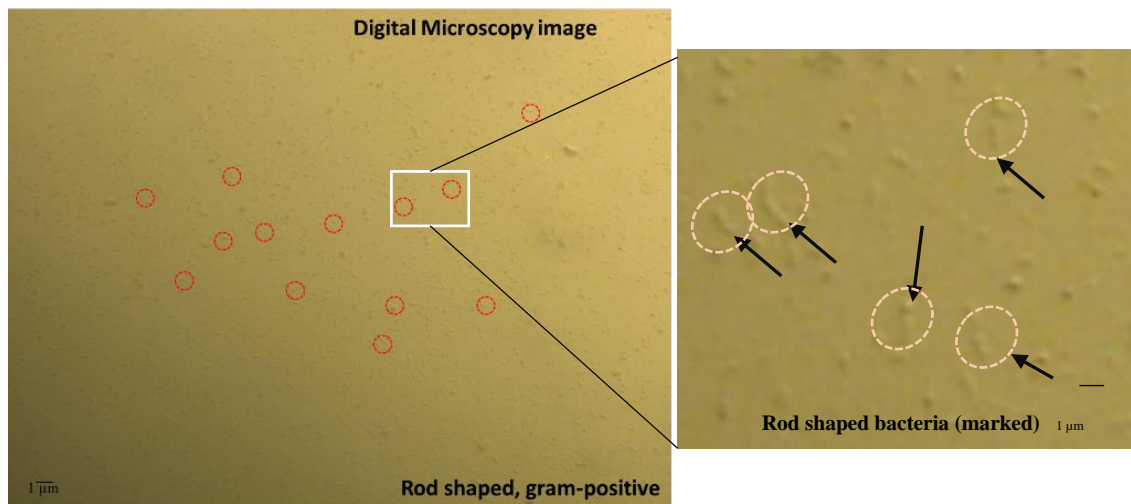
Figure 5. 3: Digital microscopic image of the microorganism used in this study.

The soil used in this study was commercially available "Mikawa" sand. The maximum and minimum dry densities of the sand were 1.476 and 1.256 g/cm^3. Particle density and mean diameter was 2.66 g/cm^3 and 870 μm, respectively. The grain size distribution of "Mikawa" sand presented in Figure 5.4. Before using for MICP process, the sand was dried in an oven dryer at 110 °C for 24 h.
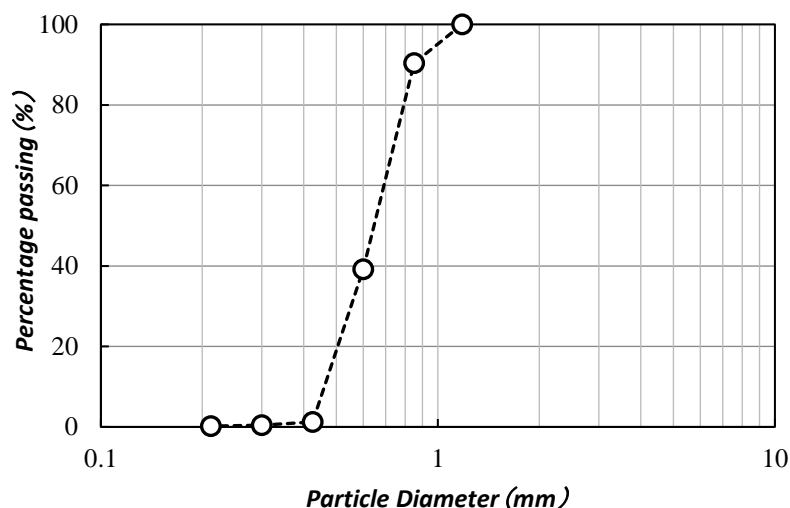
Figure 5. 4: The grain size distribution of "Mikawa" sand.

III.   *CaCO₃ precipitation tests with fiber*

To investigate the interaction between jute fiber and $CaCO_3$, same concentration (0.5 mol/L) of $CaCl_2$ and urea solutions were used for the precipitation test in a test tube with and without fiber. The total volume of the mixers was adjusted up to 10 mL using distilled water and samples were kept in the shaker for 48 h at 30 °C, and the rpm was 160. The testing condition showed Table 5.2 and Table 5.3, considering fiber content and length, respectively. After 48 h, the reaction mixture was centrifuged to collect the crystal precipitate, and supernatant of solutions from the tube was removed separately by using filter paper (whatman filter paper, 11μm). Both of the filter papers and the tubes with the precipitate were oven dried for 24 h at 110 °C and subsequently, the dry weights of the crystals were measured. The weight of the precipitated crystal was determined by contracting the empty weight of the tube from the dry weight of the tube and the filter paper's dry weight. Using a scanning electron microscopy (SEM; MiniscopeTM3000, Hitachi, Tokyo, Japan), the morphology of crystals with jute fiber was analyzed. All the experiments were done in triplicate, and mean value was plotted accordingly. Standard deviation was used to represent the error bars.

Table 5. 2: Testing conditions $CaCO_3$ precipitation with jute fiber (content).

Fiber content [(%) mm]	$CaCl_2$ (M)	Urea (M)	Bacterial OD_{600}	Incubation time (h)	Incubation temperature (° C)
0	0.5	0.5	2	48	30
[(0.5) 15]	0.5	0.5	2	48	30
[(1.5) 15]	0.5	0.5	2	48	30
[(3) 15]	0.5	0.5	2	48	30
[(5) 15]	0.5	0.5	2	48	30
[(10) 15]	0.5	0.5	2	48	30
[(20) 15]	0.5	0.5	2	48	30

Table 5. 3: Testing conditions $CaCO_3$ precipitation with jute fiber (length).

Fiber length [(mm) %]	$CaCl_2$ (M)	Urea (M)	Bacterial OD_{600}	Incubation time (h)	Incubation temperature (° C)
0	0.5	0.5	2	48	30
[(5) 3]	0.5	0.5	2	48	30
[(15) 3]	0.5	0.5	2	48	30
[(25) 3]	0.5	0.5	2	48	30

The precipitated $CaCO_3$ content of the MICP treated specimens were measured using a simplified digital manometer device (As described previous chapter) under constant volume and temperature followed by the ASTM standard method (ASTM D4373-14) (American Society for Testing and Materials, 2014) .

IV.   *Preparation of the samples*

The designed materials and test set up for MICP are shown in Figure 5.5. The dried "Mikawa" sand (75±5 g) was taken into a 50 mL standard syringe tube (diameter 3 cm, height 10 cm). In each cases, oven-dried samples (as described earlier), was compacted into 3 layers by applying a hammer shock on each layer of the sand. A lab-grade filter paper was used to cover the bottom portion of each column. Each sand column was filled with consistently mixed jute fiber using an automatic mixer (kitchen aid 9KSM160 series) considering different lengths and fiber contents. To neutralize the electrostatic charge of fiber and sand grains 10 mL of (DW) de-ionized water was added during the mixing process to ensure uniform distribution of fiber within the soil matrix.

Thereafter, a 12 mL of bacterial culture solution (ZoBEll2216E) was injected from the top of the syringe, and superfluous solutions were drained out at a controlled rate for bacterial stabilization (approximately 2 h) within the soil matrix. At the later injection phase, 16 mL of cementation solution (30.0 g/L of urea, 55.0 g/L of $CaCl_2$, and 3.0 g/L of nutrient bacto broth) was injected to the to the samples. The injected solution was kept approximately 2 mL above the surface of the sand maintained a fully saturated condition. The prepared samples were kept in an incubator at 30 °C for 14 days. The cementation solution was injected and drained every day for 14 days continuously. The pH values and Ca^{2+} concentrations from the outlet were measured frequently. The bacterial retention capacity (bacterial immobilization) during the MICP treatment was measured by difference between the primary injected bacterial solution (OD_{600}) to the effluent solution (OD_{600}). The improvement ratio (IR) was calculated using the following formula. All the measurements were conducted after the samples were removed from the syringes and in dried condition.

$$Improvement\ ratio\ (IR) = \frac{Qu\ of\ the\ treated\ samples}{Qu\ of\ the\ untreated\ samples}$$

The testing conditions were presented in Table 5. 4 and Table 5. 5 considering fiber content and length, respectively.

Table 5. 4: Testing conditions for sand solidification test (syringe) considering fiber content (%).

Cases	Fiber content [(%) mm]	Cementation solution injection	Bacterial Injection	Bacterial OD_{600}	Curing Temperature (° C)	Curing days
0	0	Everyday	Twice*	6	30	14
1	[(0.5) 15]	Everyday	Twice*	6	30	14
2	[(1.5) 15]	Everyday	Twice*	6	30	14
3	[(3) 15]	Everyday	Twice*	6	30	14
4	[(5) 15]	Everyday	Twice*	6	30	14
5	[(10) 15]	Everyday	Twice*	6	30	14
6	[(20) 15]	Everyday	Twice*	6	30	14

*Bacterial solution was injected at the beginning and after 7 days of the solidification test

Table 5. 5: Testing conditions for sand solidification test (syringe) considering

fiber length.

Cases	Fiber length [(mm) %]	Cementation solution injection	Bacterial Injection	Bacterial OD$_{600}$	Curing Temperature (° C)	Curing days
0	0	Everyday	Twice*	6	30	14
1	[(5) 3]	Everyday	Twice*	6	30	14
2	[(15) 3]	Everyday	Twice*	6	30	14
3	[(25) 3]	Everyday	Twice*	6	30	14

* Bacterial solution was injected at the beginning and after 7 days of the solidification test
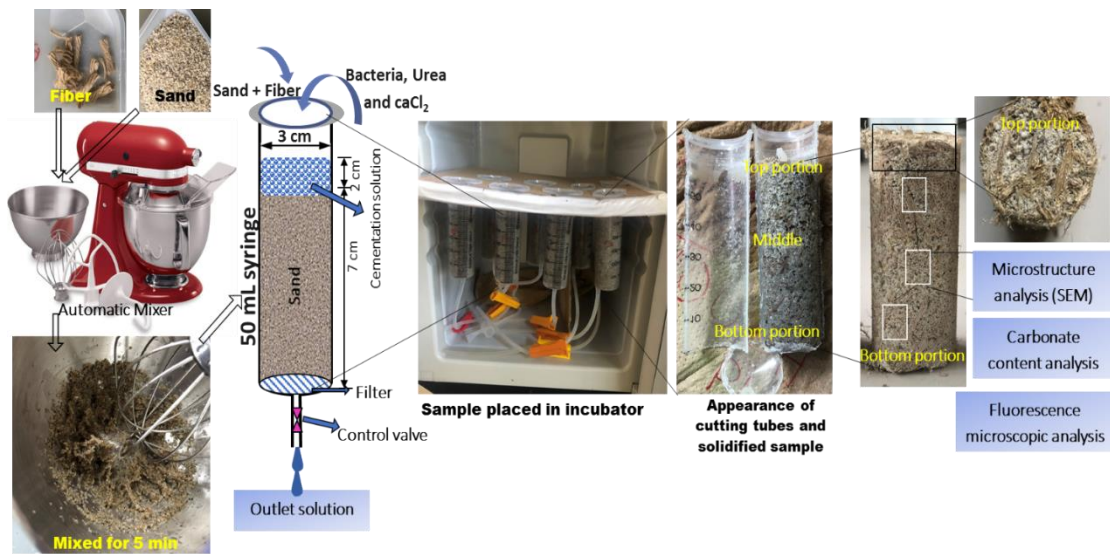
Figure 5. 5: Sample preparation and test up for MICP process in addition of jute fiber.

V. *UCS measurement of the treated samples*

To study the strength characteristics, the unconfined compressive strength (UCS) tests were performed after 14 days of curing using an automated INSTRON 2511-308 load cell (USA) (Figure 7), on a set of specimens (3 cm in diameter, 6 cm in height) cemented to various levels, in accordance with the ASTM D7012 (2014). The samples were compressed at the rate of 0.036 mm/min to reach a failure condition (critical stage).

Figure 5. 6: UCS machine (Instron-2511-308 load cell).

VI.   Shear wave velocity measurement of the treated samples

To understand the cementation behavior of the treated samples, a pair of 0.5 MHz transducers with oscilloscope were also used to measure the primary and secondary shear wave velocities (V_p, V_s) of the treated samples. The transmitted signal was a 200 kHz square wave across the length of the cylindrical specimen (~6 cm). The velocities (V_p, V_s) of the treated specimens were calculated using Sonic-Viewer-SX: 5251, Japan by measuring the time differences (Figure 5.7). Signals from the benders were captured using the two-channel digital oscilloscope at frequency bandwidth of 150 MHz. The elapsed time (digital oscilloscope, determined from the output waveforms) and the wave travel distance (sample height, measured by Vernier caliber) were used to compute the shear wave velocity, as shown in the following Equation (1).

$$V_s = \frac{L}{t - \delta t} \tag{1}$$

where L is the distance between the transmitter and receiver (i.e., specimen height), and t is the effective travel time of the signal from the transmitter to the receiver. δt is the delay of the wave when there is no specimen placed, measured by assembling only transmitter and receiver. The improvement ratio (IR) was calculated using difference between the comparative value of the treated samples to the comparative value of the untreated samples. All the measurements were conducted after the samples were removed from the syringes and in dried condition.

97

Figure 5. 7: Ultrasonic measurement of fiber treated MICP specimen.

VII.   *Microstructure analysis*

The morphology, microstructure, and interactions of the precipitated $CaCO_3$, sand particles, and jute fiber were investigated by using a scanning electron microscopy (SEM) (Miniscope TM 3000 Hitachi, Tokyo, Japan). The representative samples were carefully taken from the samples and observed through SEM after the oven dry at 60 °C. All the experiments were done in triplicate, and the mean value was plotted accordingly. Standard deviation was used to represent the error bars. The behavior of microorganisms and effect of adding fiber to the bacterial culture solution were also investigated using an automatic "Fluorescence Microscope" (BZ-X800, KEYENCE Corporation, Japan). The instruments used for microstructure analysis are presented in Figure 5.8. To observe the survivability of the bacteria cells, the fluorescence microscopy analysis was performed. First, the bacteria solution was centrifuged at 8000 rpm for 5 minutes, and the cell pellets were resuspended in 10 mmol/L concentrated HEPES buffer (pH 7.4), followed by the staining. 3 µL of the dye (combination of fluorescence dye A and B) was added to the bacteria suspension prepared, mixed thoroughly and incubated at room temperature in the dark for 15 minutes. Finally, 5 µL of the stained bacteria suspension was dropped in a 35 mm dish, subjected to fluorescence microscopy analysis.

Figure 5. 8: Instruments used for microstructure analysis.

5.3.2 Durability improvement

I.   Samples preparation for cyclic wet-dry test

The columns specimens (3 cm in diameter and 6 cm in height) were used in this work. The methods of culturing bacteria and treatment are similar to that reported in the previous chapter. The wet-dry (WD) cycles were performed in accordance with the method suggested in ASTM D559-03 (2003) using distilled water (DW) and artificial sea water (ASW). During the wetting process, specimens were submerged completely in distilled water at room temperature (25 ± 1 °C) for 6 hours. The saturated specimens were then placed in the oven at 60 ± 1 °C for at least 42 hours, and when the mass of the specimen became constant, their dry mass was recorded prior to the next WD cycle. Specimens were subjected to maximum of continuous 30 WD cycles, and the effect of WD cycles were evaluated using the following measurements (Figure 5.9). Mass loss and S-wave velocity of the specimens were determined with the number of cycles. Morphology of the precipitated $CaCO_3$ crystals before and after WD test was investigated by using scanning electron microscopy (SEM; Miniscope TM3000, Hitachi, Tokyo, Japan), and Xray diffraction (XRD; MiniFlex™, Rigaku Co., Ltd., Tokyo, Japan) analysis was conducted to identify the polymorphs of the precipitated $CaCO_3$.
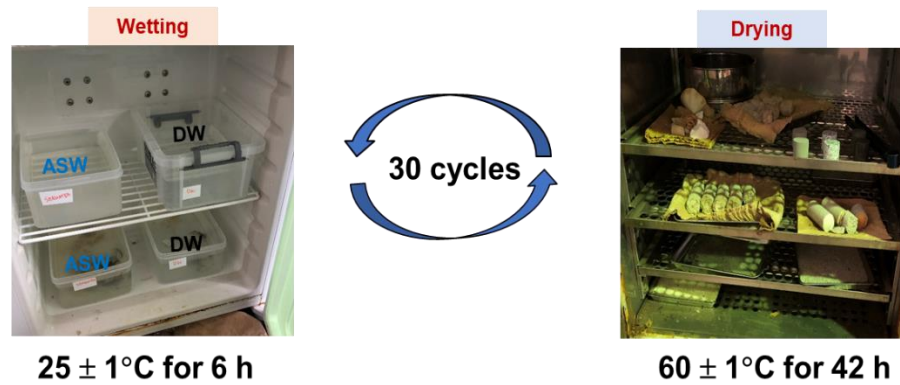
Figure 5. 9: Cyclic wet-dry test procedure.

5.4 Results and discussions

5.4.1 Results of strength improvemt

  I.   *Effects of fiber addition on ureolytic bacteria*

The fluorescence microscopic images of the cultured bacterial cell (with and without fiber) showed in Figure 5.10. From the images, it showed that the bacterial survival capacity persists longer days with the addition of jute fiber. After 10 days of cultivation, the no. of bacterial dead cell was also decreased in addition of fiber. The phenomenon behind this characteristic was, biopolymer (cellulose, hemicellulose, lignin, pectin and waxy substances) contained in the jute fiber (Munshi & Chattoo, 2008) . When jute fiber stepped into water, the water-soluble carbohydrate compounds (D-glucosidic bonds and hydroxyl groups) and biopolymers broken down into simple sugars (galactose) by a bio-chemical mechanism (Glöckner et al., 1999) and act as a source of nutrient for the bacteria, which is essential for the bacteria to survive for a long time than usual. However, further investigation could be conducted to quantify the mechanisms.
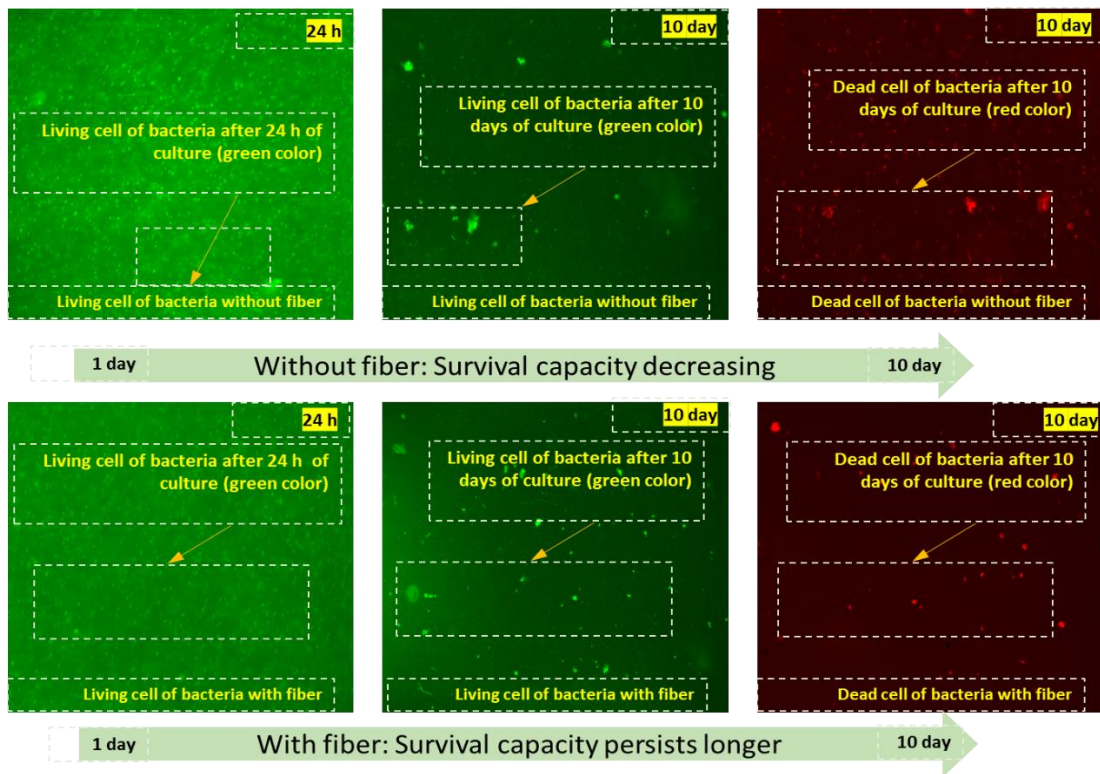
Figure 5. 10: Fluorescence microscopic images living and dead bacterial cell (with and without fiber).

II.   *Effects of adding fiber on CaCO₃ precipitation*

Studies reported that the trend in $CaCO_3$ precipitation during the MICP process was greatly influenced by fiber length and content (%) (Fang et al., 2020). Therefore, it is essential to investigate the trend in $CaCO_3$ precipitation for individual bacterial species because the $CaCO_3$ acts as the main binding materials in between the substrate particles for soil improvement during the MICP process. The effect of same fiber length and different fiber content on $CaCO_3$ precipitation was showed in Figure 5.11. As can be shown, the amount of the precipitated $CaCO_3$ crystals varied significantly depending on the fiber content. With the increasing of fiber content (0.5%) the amount of $CaCO_3$ precipitation was increased by approximately 29% and reached at 120% increment by the addition of 3% jute fiber compared without fiber addition (Figure 5.11 (a)). However, further addition of jute fiber decreased the amount of $CaCO_3$ (5% and 10% showed 84% and 23%, respectively). With the addition of 20% jute fiber the precipitation content dropped by 4%.

From this study, it was observed that, that the effect of $CaCO_3$ precipitation with 3% fiber is the best condition. From this study, it was also revealed that, higher fiber content intensely influenced the amount of $CaCO_3$ precipitation. This study suggested that the optimum calcium carbonate content obtained with an increase in fiber content up to 3% and further increased of fiber content leads to decrease $CaCO_3$ precipitation compared to the other fiber content condition. The reason for this phenomenon was natural jute fibers has non-regular cross sectional geometry and contains some chemical compound like pectin that played as an accelerator (pectin break down into sugar and used as the nutrient of bacteria) (Gupta et al., 2015) and inhibitor (excess amount of sugar and other chemical compound released from the jute fiber) for the microorganisms growth (depending on the fiber content) which also supported by previous studies (Choi et al., 2019).
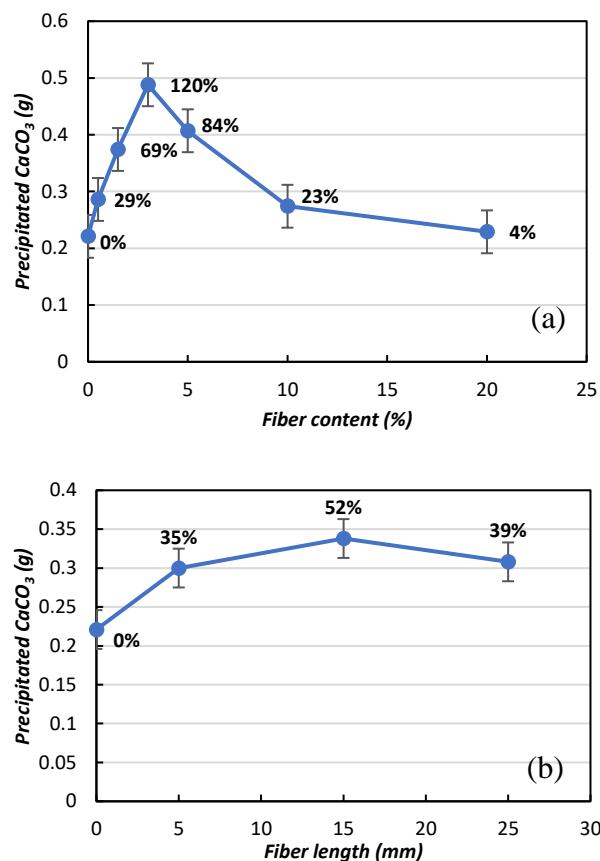
Figure 5. 11: Effect of fiber content on $CaCO_3$ precipitation by addition of jute fiber: (a) fiber content (b) fiber length.

Figure 5.11(b) shows the amount of $CaCO_3$ precipitation with the same fiber content but variations in length (5 mm, 15 mm and 25 mm, respectively). From the Fig. 8, it showed that, the $CaCO_3$ precipitation increased to 35% 52% and 39% compared to without addition (3% fiber content and the length was 5, 15, and 25 mm respectively). The variation in the values $CaCO_3$ precipitation amount within the same set of samples was relatively lower compared to fiber content. The findings of this study indicated that the content (weight %) of fiber addition considered more important for the MICP treatment to promote the precipitation of $CaCO_3$ rather than the fiber length, which are also in a good agreement with previous studies (Zhu et al., 2016).

III.   Effects of bacterial immobilization on calcium carbonate precipitation

Figure 5.12 summarized the variations in improvement ratio of bacterial immobilization (retention capacity) with respect to different fiber inclusions. Figure 5.12, shows that, in case of pure MICP sample (without fiber addition) approximately 50% bacteria were flushed out and bacterial retention capacity (immobilization) increased by fiber content (Figure 5.12 (a)) and yielded the improvement ratio an average of 1.2 to 1.6 (i.e., fiber content from 0.5-20%). Moreover, increasing fiber length (i.e., 5 mm-25 mm) the bacterial immobilization (retention capacity) decreased (Figure 5.12 (b)), and improvement ratio was marked at 1.2 in case of 15 mm fiber. This study showed, bacterial immobilization (retention capacity) was increased in the presence of fiber which is also reported by previous studies (Harkes et al., 2010).

Figure 5.13 shows, the effect of bacterial immobilization with calcium carbonate content by addition of jute fiber: (a) fiber content (b) fiber length. From the Figure 5.13 (a), it revealed that, the calcium carbonate content increased with increased fiber content up to a certain amount. In this study, 3% fiber content expressed the maximum calcium carbonate content (Figure 5.13 (a)). With further increasing the fiber content, the bacterial movement (M. Li et al., 2016) could be stuck (because of the fiber structure as described earlier) and resulted in decreased of calcium carbonate content within the soil matrix. Similar phenomena also observed with increasing the fiber length (Figure 5.13 (b)). From this study, it was clearly shown that, production of calcium carbonate was greatly influenced by the bacterial immobilization capacity (retention ability) and

an appropriate fiber content and length resulted of an increased amount of calcium carbonate content.

(a)

(b)
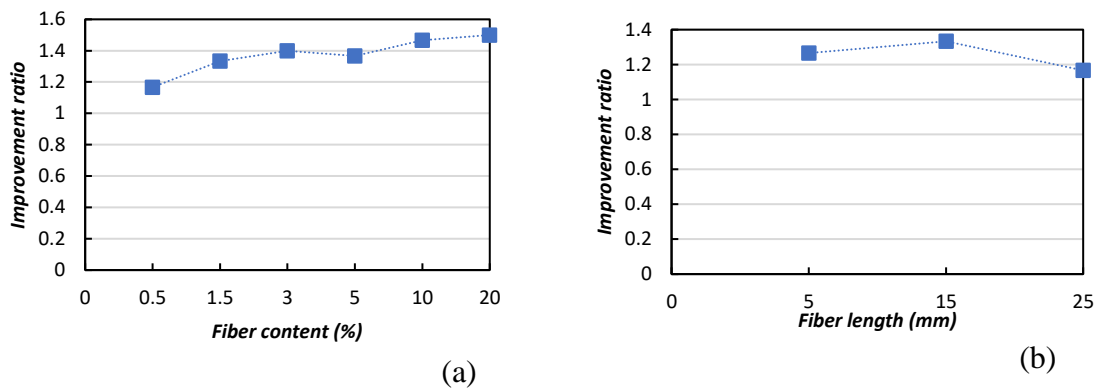
Figure 5. 12: Improvement ratio of bacterial immobilization by addition of jute fiber: (a) fiber content (b) fiber length
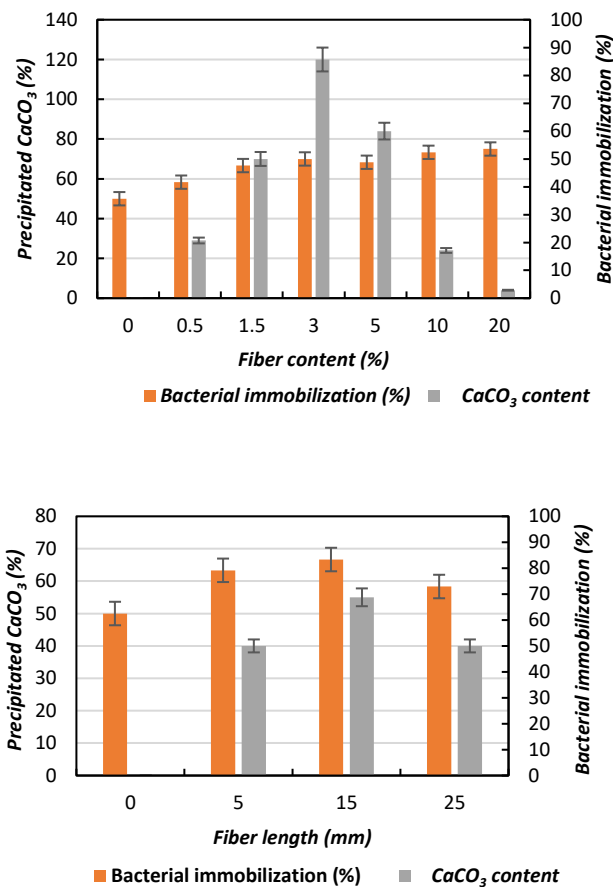
Figure 5. 13: Effect of bacterial immobilization with calcium carbonate content by addition of jute fiber: (a) fiber content (b) fiber length.

The stress-strain curves of the MICP treated samples with different fiber length, and fiber content are presented in Figure 5.14. From the Figure 5.14, it showed that, the MICP treated sample with fiber was significantly influenced by the addition of jute fiber (depending on the fiber content and length). The stress strain curve of the MICP treated biocemented sand without fiber was gradually compacted with increased strain, and stress and failure occur, which was considered as typical brittle failure. However, with increasing the fiber length (5 mm, 15 mm, and 25 mm), the stress of biocemented sand reached to the maximum strength, and then entered the residual deformation stage. Finally, failure occurred more slowly compared to without fiber Figure 5.14 (a). The slower rate of failure tendency indicated the improvement of ductility behavior of the samples. In addition, from the Figure 5.14 (a) it showed that, with increasing the fiber length, the strength (UCS) was declined. The results of this study indicated that, the addition of long fibers to the MICP treated samples could easily bent and eventually clustered within the sand, caused a negative impact to the MICP treatment and declined in UCS. This resulted indicated a significant findings compared to previous studies (C. Tang et al., 2007).

From Figure 5.14(b), it showed that the unconfined compressive strength (UCS) of the biocemented sample were increased initially (from 0.5% fiber content) and reached maximum strength (UCS) in a fiber content up to 3%. The unconfined compressive strength (UCS) interestingly decreased with further increasing the fiber content (up to a fiber content of 20%). The reason for this phenomenon was after adding fiber, the fiber was randomly distributed within the sand matrix by the interleaving mechanism, and cross sectional geometry (Dos Santos et al., 2010). This mechanism leads to form several interlacing points between fibers and formed a spatial distribution network and a spatial stress area that were capable to increase bacterial retention and survival capacity (as mentioned earlier) capable to hold more bacteria (resulted in increased $CaCO_3$ amount) than without fiber cases. The stress area and the network controlled the deformation of the sand and increased the ductile behavior of the MICP treated biocemented sand.
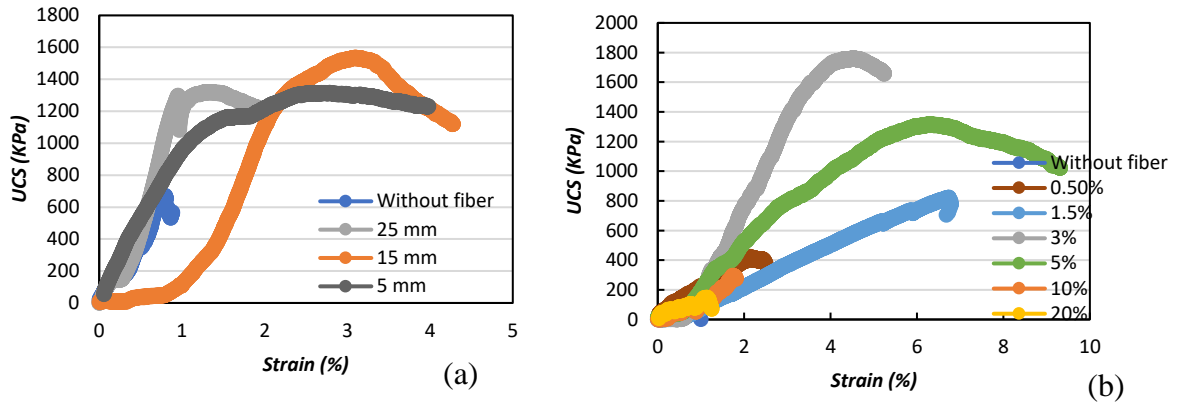
Figure 5. 14: Effects of fiber on unconfined compressive strength (UCS) of biocemented sand by addition of jute fiber: (a) fiber length (b) fiber content.

The relationship between estimated UCS and the $CaCO_3$ (%) obtained from this study (considering fiber length and content) showed in Figure 5.15. With increasing the fiber length (5 mm-15 mm), the $CaCO_3$ (%) increased, and the UCS also increased and reached to a maximum UCS with 15 mm fiber length (Figure 5.15 (a)). With further increasing the fiber length (25 mm) the $CaCO_3$ (%) decreased and resulted UCS dropped. Figure 5.15 (b) showed that, fiber content played a considerable role in both $CaCO_3$ (%) and UCS. With the increasing of fiber content (0.5-3%) the amount of calcium carbonate content increased and resulted UCS increased and reached to the maximum point (approximately 1.6 MPa). Further increasing of fiber content (5-20%) caused the decreased of $CaCO_3$ (%) and UCS (Teng et al., 2020a; Y. Zhao et al., 2020) The findings of this study clearly revealed that, fiber content (% weight) played an significant role compared to fiber length for precipitating $CaCO_3$ content.
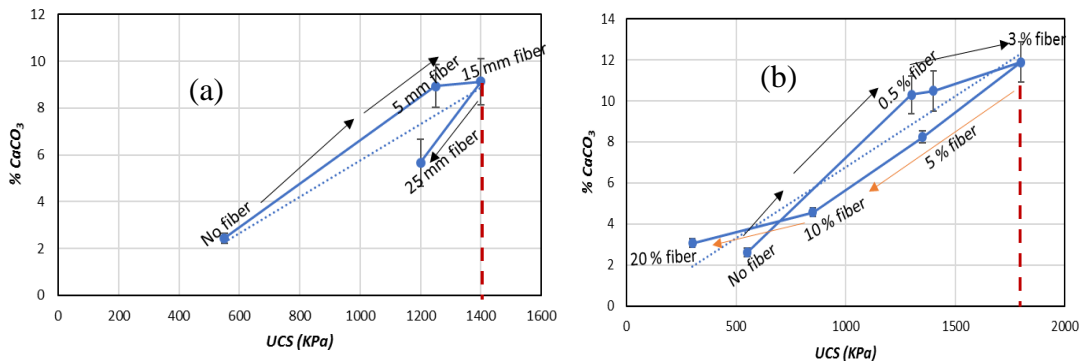
Figure 5. 15: Average (%) $CaCO_3$ of the biocemented sand after MICP treatment by addition of jute fiber: (a) fiber length (b) fiber content.

106
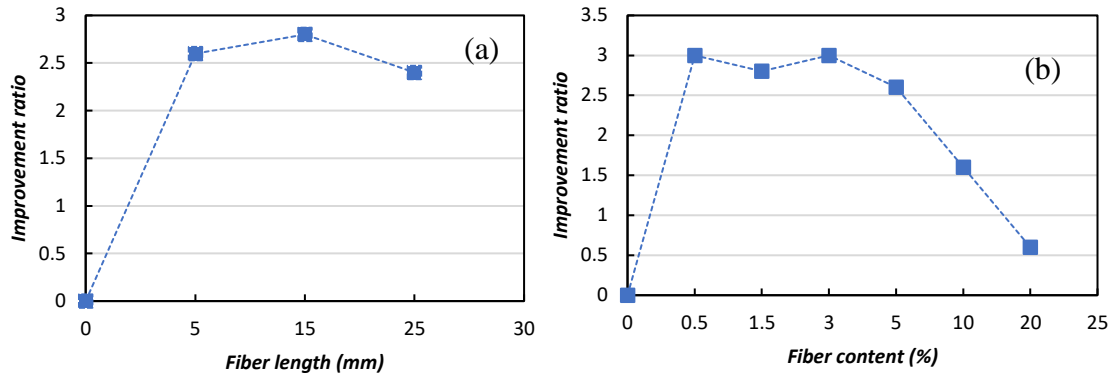
Figure 5. 16: Improvement ratio (IR) of the MICP treated biocemented sample strength (UCS) by addition of jute fiber: (a) fiber length (b) fiber content.

Figure 5.16 shows the effect of fiber length on soil strength improvement (UCS). From the Figure 5.16 (a), the improvement ratio (IR) indicated that, the IR increased (from 2.5-3) with increased appropriate fiber length (5-15 mm), but with further instead, the fiber length IR drooped, and negative influence was evident. From Figure 5.16 (b), IR value indicated significant influence of fiber content for soil strength improvement. A relatively higher improvement was achieved with the addition of 0.5-3% natural jute fiber, and the improvement ratio was 2.5 and 3.1, respectively.

In general, the results of this study suggested that, mixing of natural jute fiber could play a significant method for improving biocemented sand by MICP method depending on appropriate length i.e., 15 mm and content i.e., 3% (by weight of sand). The reason was, when jute fiber mixed with sand, the cohesion, friction and interface between the jute fibers and sand particles increased (depending on fiber length/content) resulted bacterial frequent movement and enhanced immobilization of the bacteria within the soil matrix (Figure 5.17 (a)) and uniform distribution of calcium carbonate within the sand matrix and consequently increase effectiveness of soil properties (UCS, ductility etc.). However, if the fiber content was too high i.e., 20% the bacterial movement hindered, resulted uneven distribution of bacteria in soil and calcium carbonate precipitation non-uniformly. In addition, increasing fiber length (i.e., 25 mm) reduced the efficiency of bacterial immobilization (Figure 5.17 (b)) because of uneven distribution of fiber and decreased retention capacity of bacteria resulted the reduction of the effectiveness of soil properties.
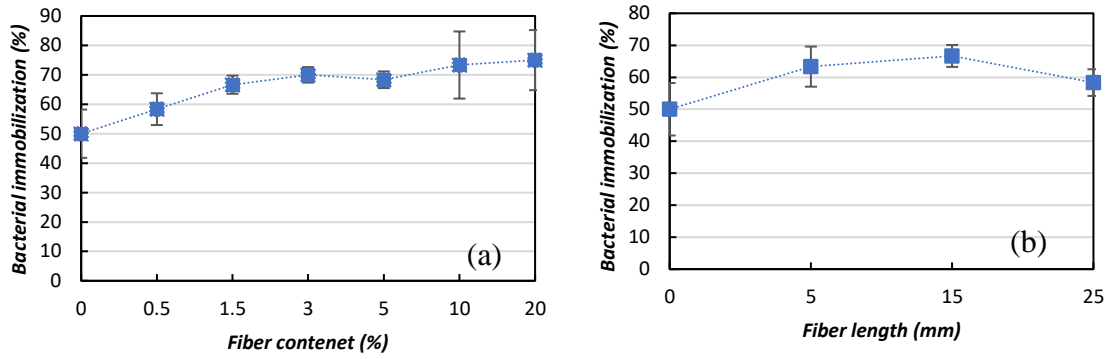
Figure 5. 17: Influence of bacterial retention capacity by the addition of jute fiber: (a) fiber content (b) fiber length.
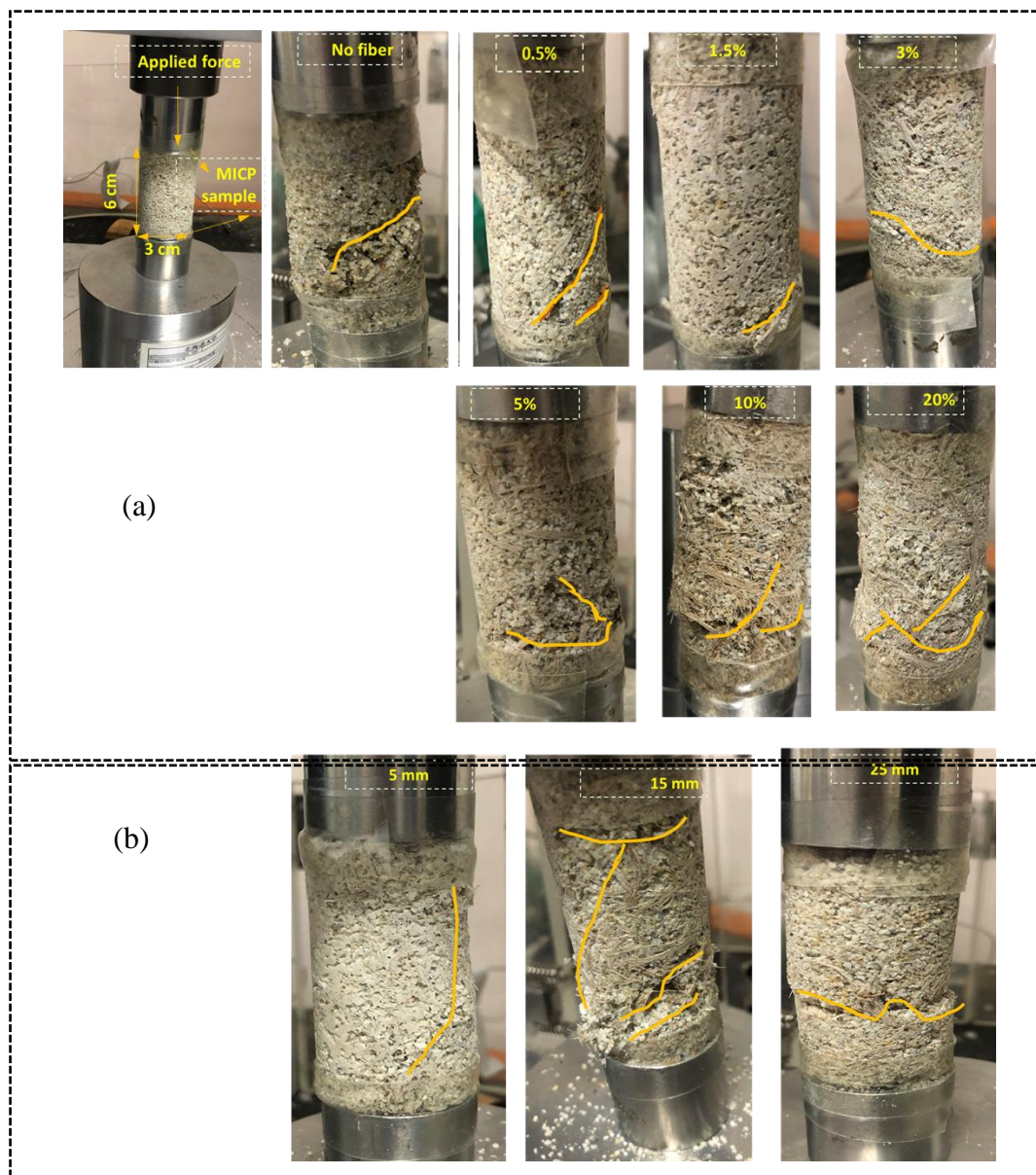
Figure 5. 18: Effect Failure behavior of the MICP treated sample by addition of jute fiber: (a) fiber content (b) fiber length.

The fracture morphologies of the biocemented samples with different fiber content (0, 0.5, 1.5, 3, 5, 10, and 20%) and length (5 mm, 15 mm, and 25 mm) were also compared in Figure 5.18 (a) and (b) during the unconfined compressive strength test. From the Figure 5.18 (considering both of fiber content and length), it can be seen that, the addition of jute fiber with the MICP treated sample significantly improved the unconfined compressive strength, and because of the lower biocementation level, the fracture generally started from the lower end Figure 5.18 (a)). Without the fibers, fractures appeared throughout the whole sample from the bottom upward, suggested a brittle failure of the samples. The results also showed that, the fracture morphologies of the biocemented samples were closely interlinked with different fiber content, Figure 5.18 (a) and length, Figure 5.18 (b) because of the interaction and friction within the sand-fiber matrix. With increasing the fiber content (i.e., 0.5-5%), the fiber formed a three-dimensional (3D) grid within the soil matrix which restricted the development of the failure pattern and effectively improved the strength of the soil and enhances the brittleness resulted delayed the overall damages of the MICP treated samples. However, further increasing of fiber content (i.e., 10-20%) developed ''bulging'' behavior of the sample. For the case of fiber length, short fiber length (i.e, 5 mm-15 mm) showed the significant improvement of the biocemeneted specimen. Long fiber (i.e., 25 mm) occurred the sudden fracture of the sample due to uneven distribution and entangled into bundles during the sample preparations. Therefore, for the actual engineering application, it is suggested to determine the optimum fiber content and length to be added to the soil, for obtaining a maximum effect.

V.   *Results of shear wave velocity measurement*

The results also validated by primary and secondary shear wave velocities (Vp, Vs) showed in Table 5.6. Previous studies also showed that accelerated carbonation system enhanced the interface between the fiber and the cementitious matrix which improved the strong mechanical anchorage and interlocking (M. Chen et al., 2015; Qiu et al., 2019) by filling the pores with calcite and fiber of the system. However, the findings of this study could play a significant role for improving the engineering properties of the soil by fiber matrix MICP treatment.

Table 5. 6: Summary of test results for the biocemented sand after MICP treatment with jute fiber.

Fiber content (%)	Unit weight (g)	V_s (km/s)	V_p (km/s)	UCS (MPa)	Average $CaCO_3$ (%)
0	65.6	0.92	1.12	0.5	2.4
0.5	64.2	0.87	1.22	1.5	9.3
1.5	63.5	0.95	1.24	1.4	11.88
3	60.1	0.92	1.25	1.6	13.29
5	61.5	0.9	1.23	1.3	7.9
10	60.2	0.99	1.22	0.8	4.6
20	59.9	0.93	1.24	0.3	3.29
Fiber length (mm)					
5	62.4	0.92	1.28	0.5	2.4
15	61.9	0.87	1.12	1.3	8.4
25	63.6	0.95	1.27	1.4	9.7

VI.   Microstructure analysis

i.   Effects of fiber addition on $CaCO_3$ precipitation

The microstructure analysis and interaction of precipitated $CaCO_3$ to jute fiber are shown in Figure 5.19 (with fiber and without fiber). Test results indicated that, the precipitated crystals irregular bulk and coated around the jute fiber and formed a $CaCO_3$ bridge, which could be very effective for binding filling the void space and increase the binding capability in between the sand particles. Similar observations were also reported in previous studies (Al Qabany et al., 2012; Hejazi et al., 2012; Shao et al., 2014) The adsorption capacity of the microorganisms and $CaCO_3$ precipitation to the fiber was greatly influenced by the surface micro-structures of the fiber. Different fiber and surface micro-structures leads to differ the $CaCO_3$ precipitation pattern (Lei et al., 2020). In addition, the reduction in void space due to the $CaCO_3$ precipitation could be considered to be a primary strengthening factor (DeJong et al., 2010) and reduced brittleness behavior of the MICP treated sand.
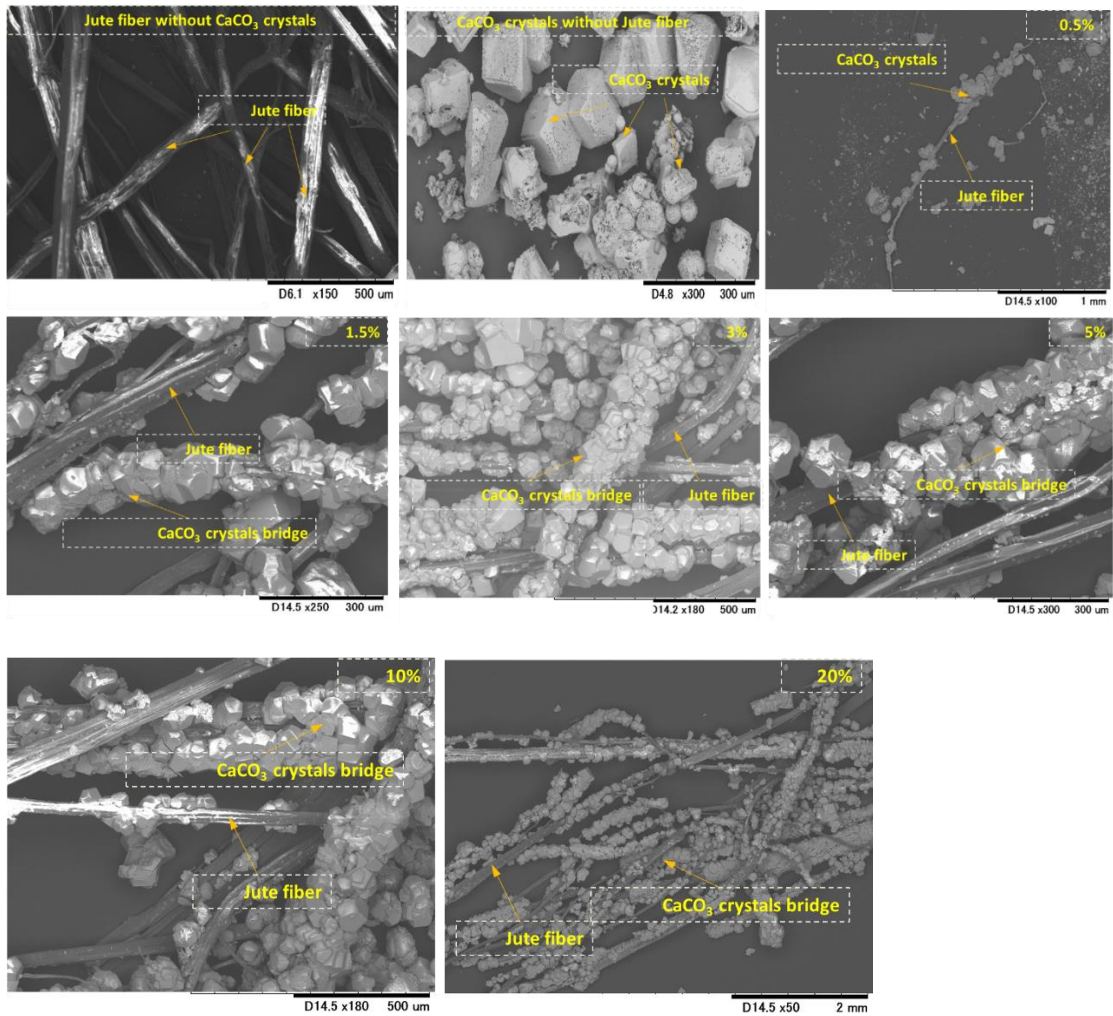
Figure 5. 19: SEM images of precipitated $CaCO_3$ with/without jute fiber after MICP process (without sand materials).

ii. Effects of fiber addition on strength improvement

The SEM images of MICP treated biocemented samples by addition of jute fiber (length and content) and distribution of $CaCO_3$ within the sand matrix are shown in Figure 5.19. The images also represented sand particles without MICP treatment, sand particles with fiber without MICP treatment, biocemented sand particles with different fiber content and length, respectively. From the microscopic images, the void spaces were dominant in both cases of sand-fiber matrix without MICP treatment. After the MICP treatment, the fibers were covered by calcium carbonate crystals (like a bridge) which provided the strong bonding capacity in between the sand particles and also filled the void space and yielded an enhanced cementation level (Figure 5.20), which is presented more clearly by a schematic diagram in Figure 5.21. With increased amount

of the fiber content (up to a certain amount) and fiber length (up to a certain length) more calcium carbonate precipitation occurred in between the soil pore space and contact point and resulted enhanced engineering properties of the soil.
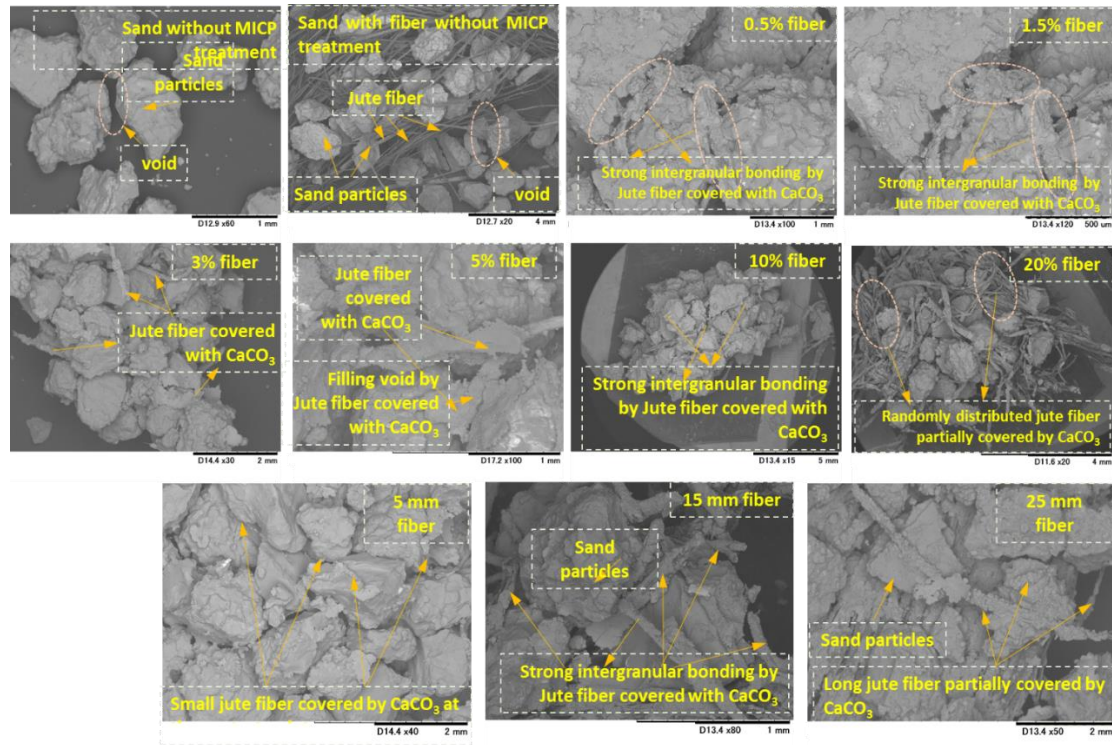
Figure 5. 20: SEM images of MICP treated biocemented samples by addition of jute fiber (length and content) and distribution of $CaCO_3$ within the sand matrix.
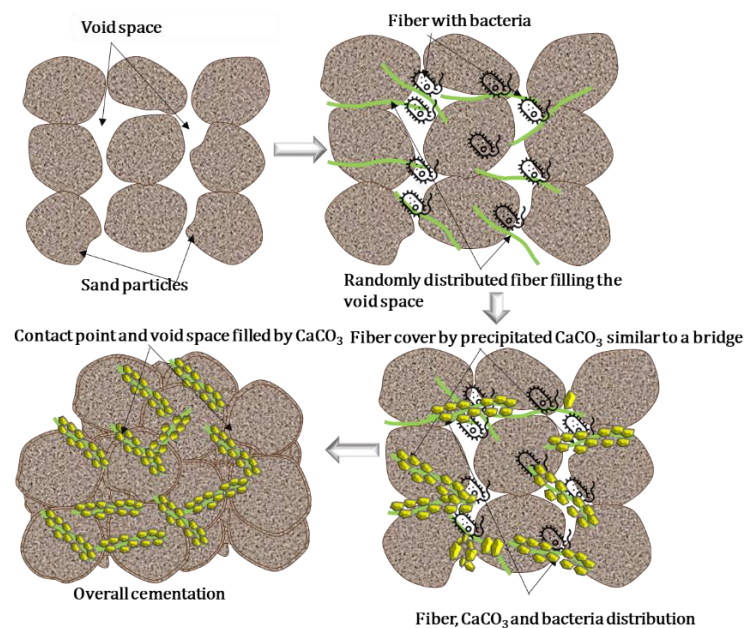
Figure 5. 21: Schematic diagram of biocement sample by addition of jute fiber.

5.4.2 Results of durability improvemt

I.   Physical changes and mass loss

The physical damage during cyclic tests was evaluated by the mass loss of the specimens. The mass loss was carefully measured after every cycle with constant temperature using distilled water (DW) and artificial sea water (ASW). Figure 1 shows the mass loss of the specimens subjected to 30 cyclic WD actions. In the case of 0 percent fiber treated MICP specimens, mass loss was found to be greater than 50% after 30 WD cycles. The mass loss propensity decreased as the fiber addition was increased, and in 3 percent fiber treated MICP specimens, the mass loss was just 20% (DW) and 30% (DW) (ASW).

In case of DW, mass loss severely occurred at early stage. After 20 cycle the specimen becomes a stable position and mass loss didn't occur severely. Without addition of fiber the mass loss occurred rapidly (around 40% after 20 cycle), but addition of fiber mass loss occurred gradually (around 20% after 20 cycle). Within another few more WD cycles (Figure 5.22 (a)), the rate of mass loss decreases gradually and tends to become to the equilibrium state. In case of ASW (Figure 5.22 (b)), mass loss severely occurred continuously. Without addition of fiber the mass loss occurred around 60% after 20 cycles, but addition of fiber mass loss occurred gradually (around 25-30% after 20 cycle). Treated specimens were more vulnerable in ASW compared to DW. Similar observations was reported by (Gowthaman et al., 2021; Klerk et al., 2020).
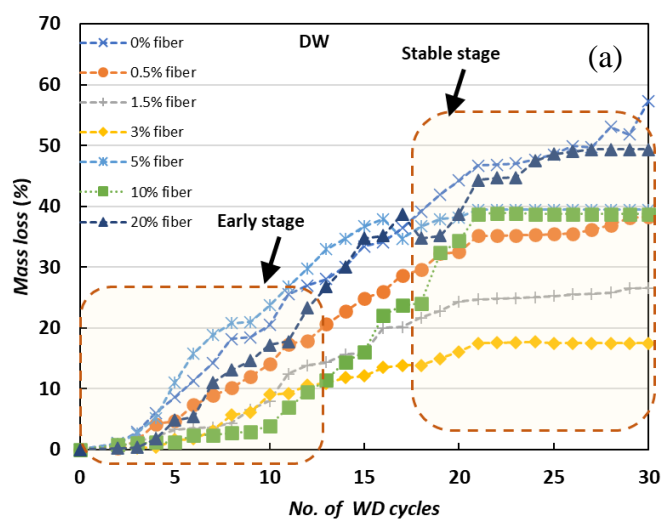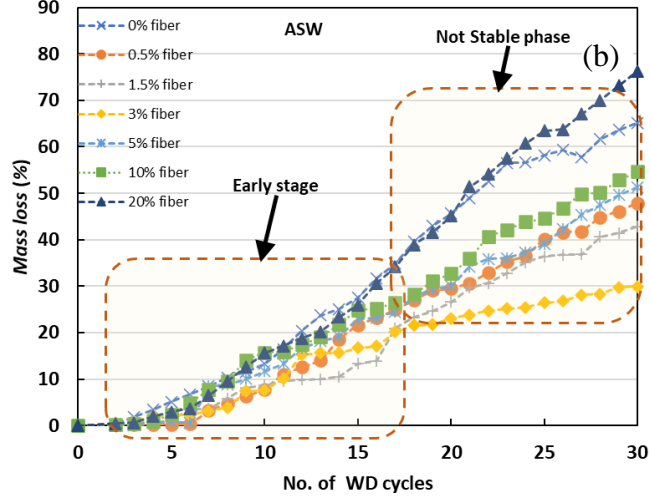
Figure 5. 22: Average mass loss of the specimens subjected to WD cyclic treatments based on (a) DW and (b) ASW.

II.   Strength deterioration ratio

It is clearly perceived that the physical and mechanical behaviors are significantly influenced by the WD cycles. To understand the effect of fiber addition on mechanical damage, strength deterioration ratios (SDR) were calculated using the following equations (2).

$$SDR = 1 - \frac{UCS_{(f)}}{UCS_{(i)}} \tag{2}$$

The $UCS_{(f)}$ represents the compressive strength at the end of the cyclic treatment and $UCS_{(i)}$ represents the compressive strength of primary MICP specimens.

Based on the observations (Figures 5.23 (a)), the average $CaCO_3$ decreasing gradually and in the first stage (up to 10 WD cycles), severe degradation was witnessed in all cases. In case of DW, the SDR value was not significant at the eagerly stage (up to 10 WD cycles) but with more cyclic treatment (up to 30 WD cycles) SDR value was considerably decreased (Figures 5.23 (b)). The SDR values considerably decrease with the decreasing in calcium carbonate content ((Figures 5.23 (c))), in case of ASW. The tendency demonstrates that the high deposition of carbonates likely to be preserving the MICP responses against WD actions in ASW. Fiber treated MICP Specimens achieve high precipitation content in a stable from, which could strengthen the primary connections, providing high resistive forces during the development of fatigue stresses.

114

Also, these strong connections could withstand against suspension and corrosion induced by WD process and resulted improvement of SDR value ((Figures 5.23 (d)).

However, from the WD cyclic test using the DW and ASW values, it can be precisely concluded that the MICP specimens underwent severe mechanical degradation under ASW (over 60%), and fiber addition significantly improve the strength deterioration ratio (over 40%-50%). This overall observation suggests that the mechanical degradation conspicuously occurs at the early stage of the WD process (ASW), compared to that occurred at the later stage (DW) and fiber addition could significantly improve durability of the MICP treated samples.
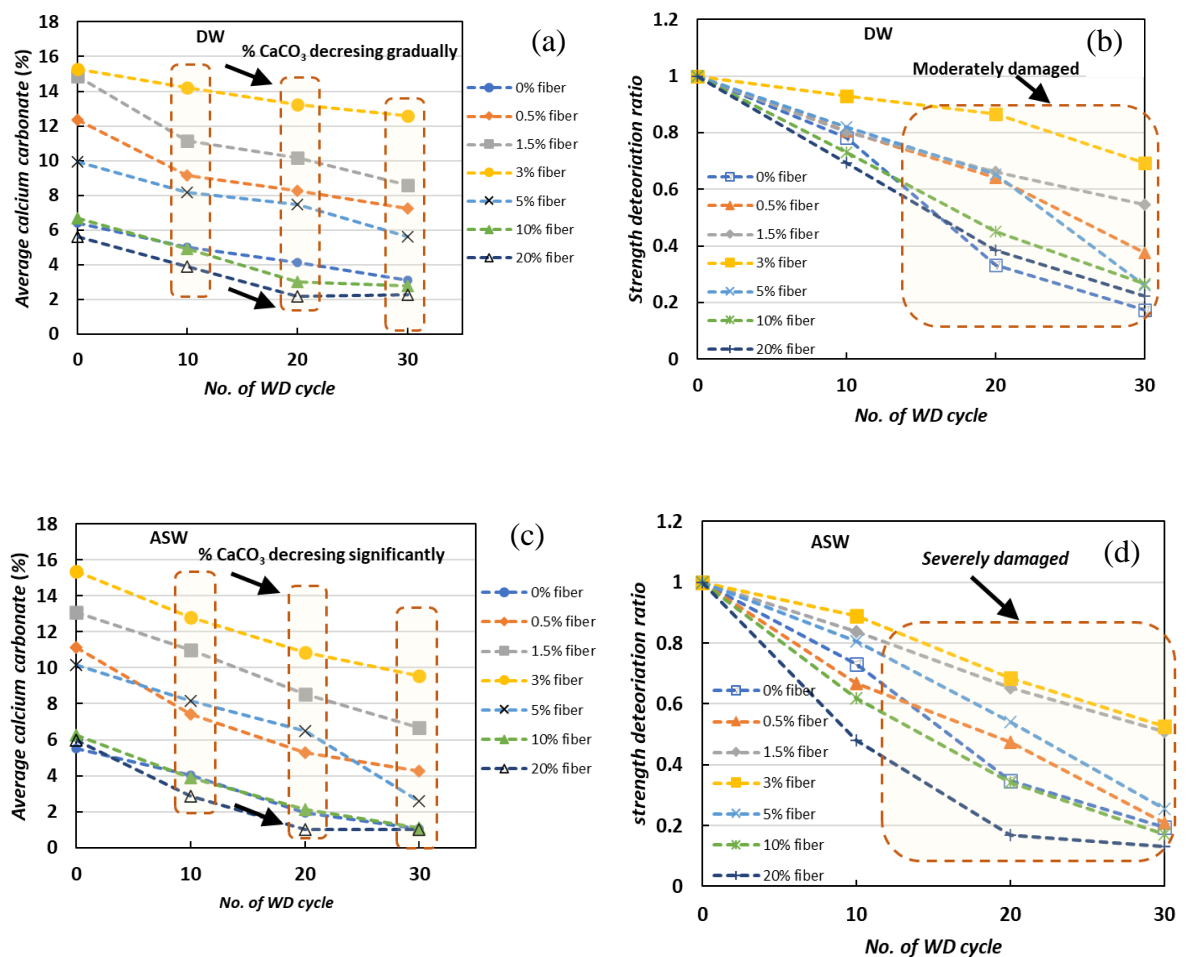
Figure 5. 23: The average calcium carbonate (%) of the samples treated with (a) DW; (c) ASW and the strength deterioration ratio in (b) DW; (d) ASW after the exposure of cyclic WD tests.

III.   Shear wave velocity measurements

For better understanding the changes in the mechanical behavior, the specimens were monitored using S-wave and P-wave velocity, and the results are provided in Figure 5.24. The precipitated calcium carbonate at particle contact has the utmost effect of P-wave velocity (Figure 5.24 (a)) and S-save velocity (Figure 5.24 (b)), because the P-wave and S-waves can only be transmitted through solids (not through soil pores) (Al Qabany et al., 2011). The results reveal that irrespective of the cementation levels, variation in velocity measurements follows relatively a similar pattern with increasing WD cycles in both DW (Figure 5.24 (a-b)) and ASW (Figure 5.24 (c-d)).

Consequently, a rapid drop was observed within first few cycles (up to 10 WD cycles), followed by a smooth and gradual reduction. These rapid reductions in P-wave and S-wave velocity are consistent with those of observed in mass loss (Figure 5.22), and this could possibly be attributed to the weakening of particle connections due to the corrosion induced during WD process. On the other hand, the average velocity reduction occurred between 5 – 15 WD cycles ranges only between 0.08 km/s-0.12 km/s, suggesting the minor damage in the later stage while sever damage occurred in ASW. This observation is in a very good agreement with that observed in %$CaCO_3$ and strength deterioration ratio in Figure 5.23.
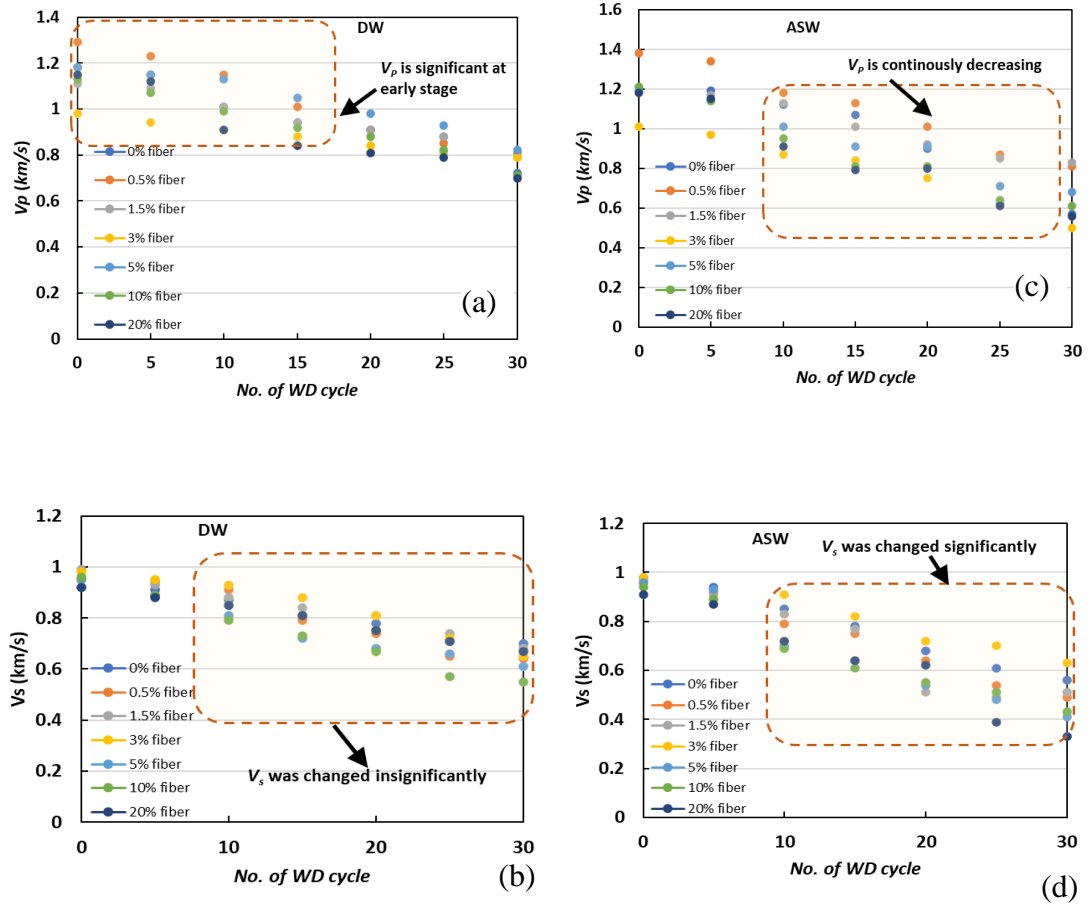
Figure 5. 24: Variations of shear wave velocities of specimens under exposure of cyclic WD tests (a) p-wave velocities in DW (b) s-wave velocities in DW and (c) p-wave velocities in ASW (d) s-wave velocities in ASW.

IV.   *Microstructure analysis (SEM and XRD) of the treated samples*

Figure 5.26 presents the microstructures of fiber treated specimens in DW (after 30 WD cycles). From the SEM images, it is clear that the soil structure has been significantly affected within first few WD cycles, and then tended to be relatively stable. Higher degradation is evidenced on the surface compared to that observed at core of the specimens. The surface carbonate deposits were found to be shrunken and degraded. Microcracks were also observable at and around the intact bonds and become very severe with ASW treated samples (Figure 5.26).

When specimens are subjected to drying, the interior relative humidity does not drop immediately but decreases in a gradual manner (Zhang et al., 2012), whereas the surface undergoes rapid evaporations, experiencing high negative stresses. Also, the core zone of the sample is confined stiffly, the developed fatigue stresses therefore

caused more damages at outer surface of the column, attributing to the progression of macropores. Similar initial surface degradations due to WD stresses were also often reported to concrete specimens (Gao et al., 2014; Zhang et al., 2012).

Furthermore, the difference in thermal expansion coefficient of calcium carbonate and soil material could be another possible factor that could result the development of internal fatigue stresses under temperature change, inducing the degradation process. The above mechanism has also been reported to magnesium potassium phosphate cement, in which the internal fatigue stresses resulted pores and microcracks (Li et al., 2019). When the calcites are flooded by water for a long time, a minor portion would possibly undergo chemical dissolution (Ciantia et al., 2014; Khanlari and Abdilor, 2015). Ciantia et al. (2015) have confirmed that the long-term weathering of carbonatic rocks is due to the dissolution of diagenetic calcite bonds. In this study, the effect of dissolution is assumed to be negligible under the standard conditions. For a similar instance, Ciantia et al. (2015) studied the deterioration of carbonate rocks and observed the occurrence of instantaneous debonding of depositional bonds (menisci shaped calcite ensembles) when subjected to saturation. The researchers also found that single wetting process caused a considerable loss in compressive strength, and the loss was more pronounced for high porosity calcarenites (Ciantia et al., 2014).
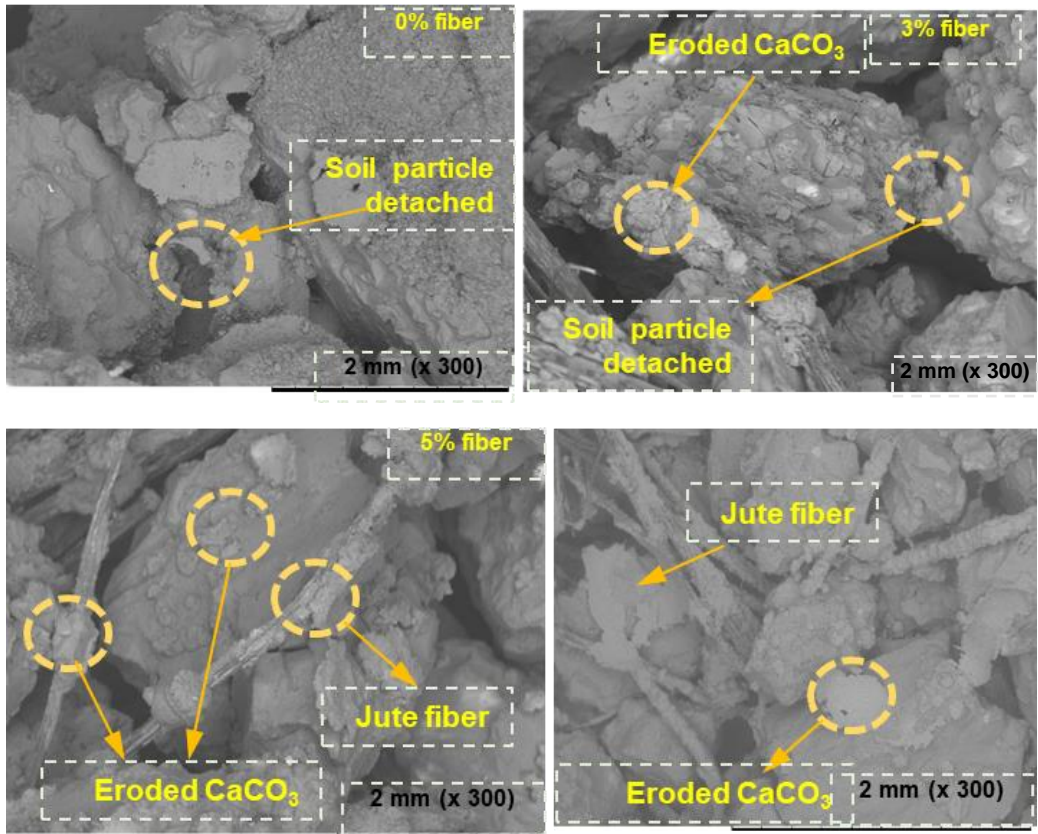
Figure 5. 25: SEM images (DW) of the specimens after subjected to WD cycles.
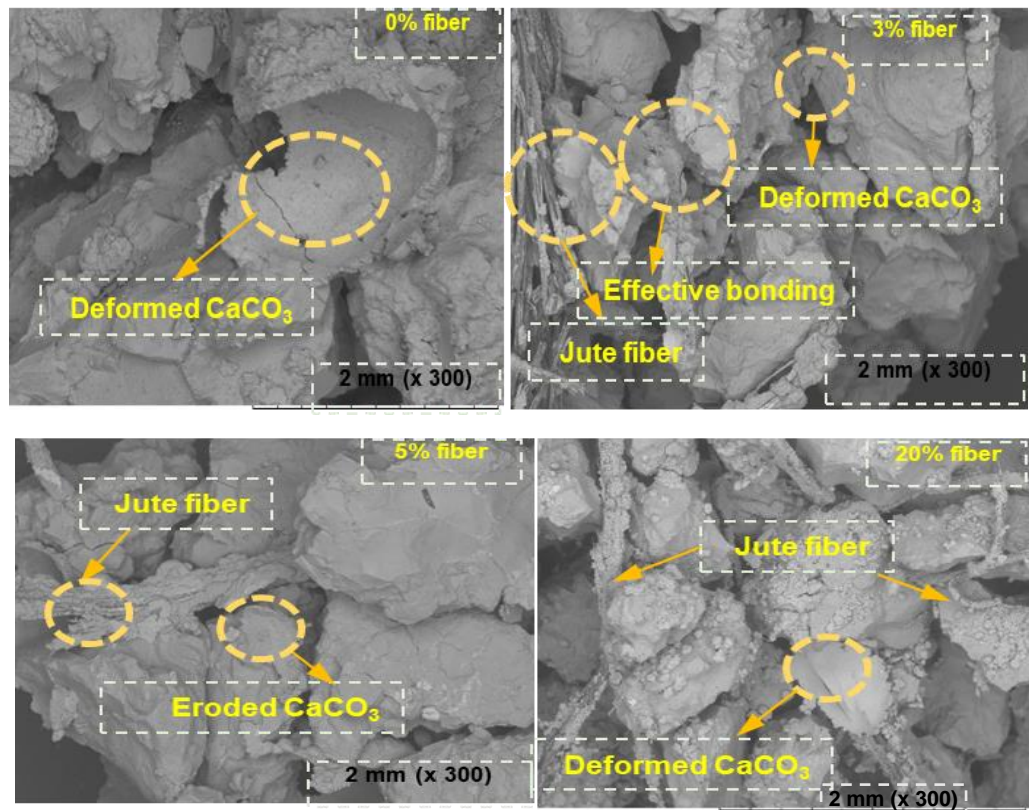
Figure 5. 26: SEM images (ASW) of the specimens after subjected to WD cycles.

V.   Durability characteristics and mechanisms

MICP treatment, the calcium carbonate is precipitated in various forms such as primary bonds (strongly forms at particle contacts), individual crystals and accumulation (on the grain surface), amorphous and powdery deposits (Lin et al., 2016; Wang et al., 2019). In fact, these powdery bonds are often formed when the carbonates are deposited at its early stage of the crystallization. When the specimens are submerged during the wetting, the water penetrates the specimen and drives the powdery deposits to fall into suspension (Figure 5.27). This corrosion mechanism is similar to that reported to the calcarenite rocks (Ciantia, et al., 2015). The MICP treated soils have porous structure. In fact, the resultant stress acting on soil particles are distributed to the connections around them i.e. to the calcium carbonate bonds. When the acting tensile stresses exceed the maximum tensile strength of carbonate bonds, the bonds would start cracking. When the soil samples were treated by MICP, a part of $CaCO_3$ precipitation was only attached to the surface of sand particles that may not bond the sand particles and thus can easily be eroded during WD cycles. During the initial wetting. Water penetrates through porous system and inundates the material, resulting the powdery deposits fall into suspension and disintegration occurred which leads to loss particles contacts and mass loss.

The fiber acted as bridge and tension members between soil particles and calcium carbonate that improve the bonding between soil particles. In MICP-treated samples with fiber, fibers across the samples took the tension within the soil due to the fiber soil friction, which effectively improve the durability of the samples (Figure 5.28). However, the WD induced erosion could be controlled by treating the soil with appropriate quantity of fiber and calcium carbonate content.
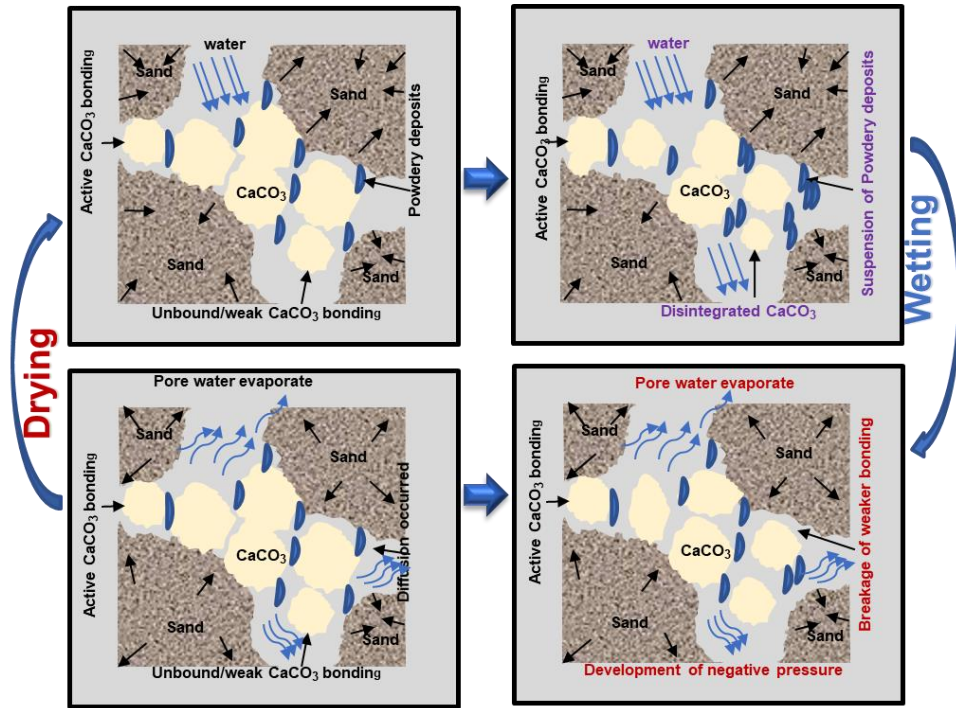
Figure 5. 27: Schematic illustration of deformation of MICP treed specimens after subjected to WD cycles.
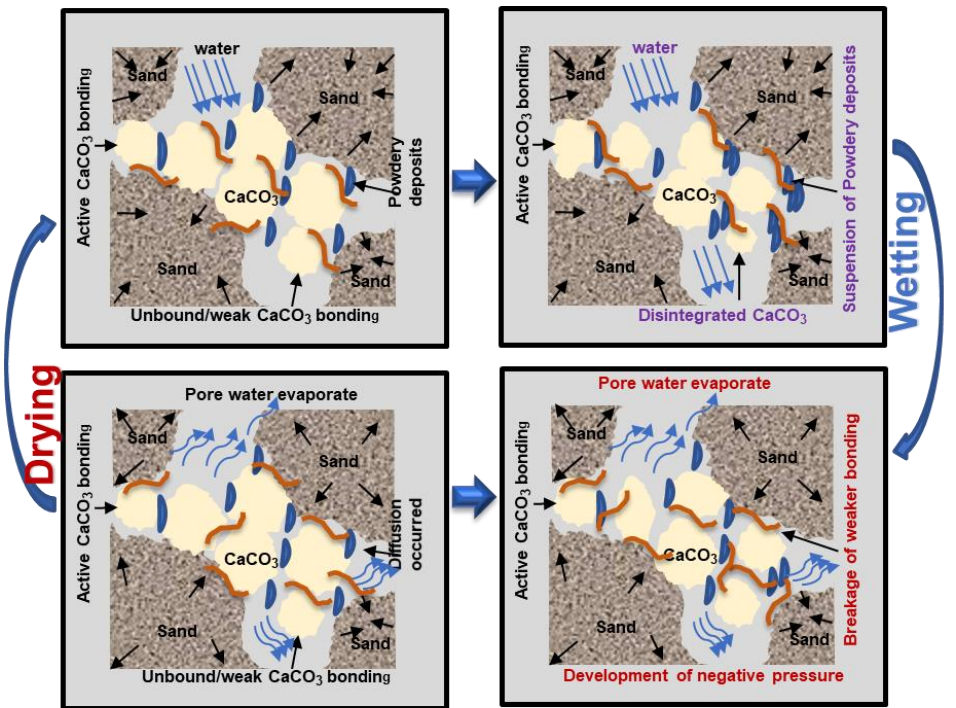
Figure 5. 28: Schematic illustration of deformation of fiber reinforce MICP treed specimens after subjected to WD cycles.

Figure 5.29 shows the results obtained from the XRD analysis. The analysis was performed to verify the occurrence of phase transformation of carbonate deposits, precipitation of new minerals and dissolving of existing minerals. The XRD results confirm that there are no observable changes in the morphology of minerals throughout the WD process in DW and ASW. The observed peaks are identical with the increase in number of cycles, suggesting neither formation of new minerals nor phase changes were induced.
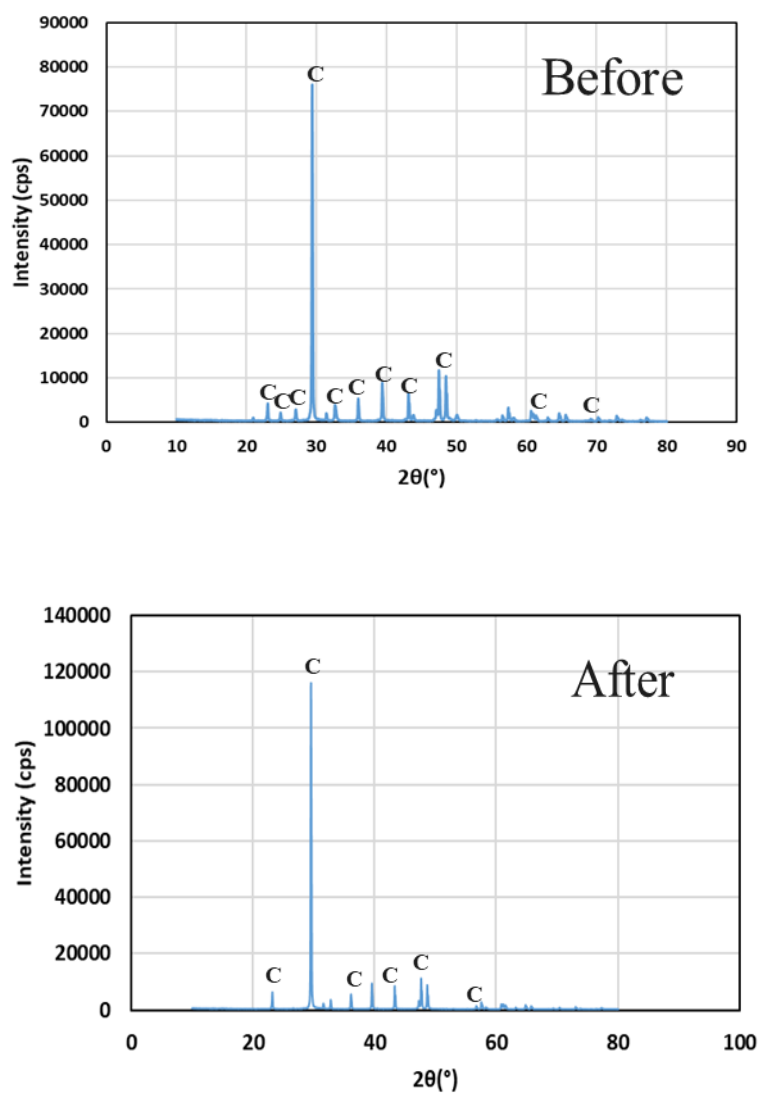
Figure 5. 29: XRD results of specimens subjected to WD cycles.

5.5 Conclusions

This study was conducted to investigate the effect of adding jute fiber to the biocmented sand by MICP method. Throughout the study, jute fiber was at six contents i.e., 0, 0.5, 1.5, 3, 5, 10 and 20% (by sand weight) and three lengths i.e., (5, 15 and 25 mm) were used for the sand treatment by MICP method. Based on the results of this study, the following conclusions could be outlined:

   i.   Jute fiber has significant effects on the microbial performance, calcium carbonate precipitation pattern and solidification of sand. Using the fluorescence microscopy, the survival capacity of the microorganisms was well demonstrated to be increasing due to the addition of jute fiber. The addition could effectively improve not only the bacterial performance, but also the mechanical characteristics UCS and ductility of sand. The UCS of the sample increased with the increasing in fiber content; however, higher fiber addition was found to be decreasing the UCS. From the results obtained in this study, the optimum content of jute fiber for the enhancement could be 3%, with 15 mm in length.

   ii. The calcium carbonate precipitation was positively correlated with the added jute fiber which yielded the significant improvement of engineering properties of the soil. The SEM analysis suggested that the added jute fiber well coupled with calcium carbonate (i.e., calcium carbonate was attached on and along the surface of fibers), forming reliable bridges within the soil matrix, which tended to limit the development of failure planes within specimens. This could eventually result more increase in both the strength and the toughness of the specimens compared to those of control biocemented specimens (without jute fiber).

   iii. As the amount and length of jute fiber increased beyond the optimum level, the fibers tend to be entangled with each other during preparation of a samples, which hindered the entry of bacteria and reduced the space for the survival of bacteria and calcium carbonate formation.

   iv. In this study, natural jute fiber was used; however, the effect of chemically treated jute fiber, effect of roughness of jute fiber (surface) have not been

investigated in detail. In order to better understand the effects of fiber on soil stabilization (considering chemical pretreatment of the fiber, fiber roughness, etc.) by MICP process, further studies are therefore highly recommended.

v. Cyclic wet-dry (WD) effects appear to have adverse effects on the physical and mechanical characteristics of fiber reinforce MICP treated soils in both DW and ASW. The deterioration mechanism of MICP soils due to WD cycles is related to the degradation of calcium carbonates and bonding effects in between the sand particles, and that is found to be occurring at two stages: short-term and long-term. The short-term deterioration rapidly occurs within the first few WD cycles in DW due to the suspension and corrosion of powdery carbonate deposits. The long-term deterioration could be observable after 15 WD cycles in ASW. The fatigue stresses developed during WD process could deform the primary bonds, and particularly impairing the surface of the specimens. However, addition of jute fiber the improved in bonding effect and increased the aggregate stability and mechanical durability. The results also suggested that the MICP specimens are less susceptible to WD actions, compared to that observed under ASW effects.

CHAPTER 6 : STRENGTH AND DURABILITY IMPROVEMENT OF THE BIO-CEMENTED SAND BY EICP METHOD

6.1 Introduction

Enzyme Induced carbonate precipitation (EICP) is a bio-inspired ground improvement technique. In EICP, free urease enzyme is used to catalyze hydrolysis of urea, the reaction between calcium chloride and urea that induces calcium carbonate precipitation in soil (Hamdan et al., 2016). EICP has the potential to eliminate some of the limitations of soil improvement using microbially induced carbonate precipitation (MICP) in which ureolytic bacteria are employed to produce urease enzyme (Khodadadi et al., 2017). The induced carbonate precipitation changes the mechanical properties of the treated soil through binding particles together, roughening particles surfaces, and filling pores (Kavazanjian and Hamdan 2015).

EICP solution (crude urease) can be sprayed on the soil surface for erosion control, injected or percolated into soil as in permeation grouting, or mechanically mixed with soil for compaction during fill placement or deep mixing. Previous studies on EICP have employed injection and percolation methods for soil treatment to allow for applying multiple cycles of treatment (Yasuhara et al., 2012; Neupane et al., 2015). While multiple cycles of treatment can be applied via injection or permeation, mixing EICP solution with soil does not allow for more than a single treatment cycle due to the disturbance induced by multiple treatment cycles to the soil, limiting the precipitation yield and the strength gain of the improved soil. Therefore, approaches that can increase the strength and durability of soil treated by mechanical mixing of the EICP solution with the soil is of interest to engineers studying this treatment method.

Adding fiber reinforcement is one potential means of increasing the strength of soil treated by mechanical mixing soil with an EICP solution (crude urease). Stabilized soils with fiber reinforcement have several applications in geotechnical engineering including coastal erosion protection and in ground improvement projects. For economic development use of locally available materials, the waste material should be encouraged in order to save the natural resources for future generation (Sudhakaran et al., 2018).

The use of fibers for improvement of soil strength and ductility is well established (Gray and Al-Refeai 1986; Consoli et al., 2009). The type and amount of fiber and fiber properties such as length and modulus influence the degree of improvement (Dos Santos et al., 2010). Hejazi et al., (2012) compared the influence of the amounts of synthetic and natural fibers (as a percentage of dry weight of fibers and soil) on soil strength enhancement. They reported that the optimum content for synthetic fibers they used varied between 0.1 and 0.4%, whereas it changed to between 0.5 and 1% for natural fibers they used. Hejazi et al., (2012) found an optimum fiber content of 0.75% and an optimum length of 20 mm for use of natural sisal fibers in soil enhancement. The optimum fiber content obtained by Li et al., (2015), who used synthetic fibers in MICP-treated soil, is in agreement with the range reported by Hejazi et al., (2012). In addition, limited study has been reported to use natural fiber reinforcement in EICP method.

6.2 Objectives

The primary objectives of this work were to improve the strength of the fiber reinforced EICP treated samples by investigating the effects of natural fiber (jute) on the EICP treated soil considering fiber length, and content (ratio) to improve the engineering properties (ductility, toughness and brittleness behavior) of the biocemented sand specimen. The mechanical properties of the EICP treated sand, microstructure of the specimen, interaction between the fiber and sand were investigated and analyzed using unconfined compressive strength (UCS), scanning electron microscopy (SEM), and X-ray diffraction (XRD) method. Subsequently, the durability performance of the treated samples was investigated using distilled water and artificial sea water.

6.3 Materials and methods

6.3.1 Strength improvement

I.   Fiber used in this study

The jute fiber was cut into several percentages (content) by weight (0.5%, 1.5%, 3%, 5%, 10% and 20%) and following the results from chapter 5, the fiber length was

decided 15 mm (in length) were used for mixture with mikawa sand particles. The physical appearance of the prepared jute fiber samples, and methodology was followed as previous chapter (Chapter 5). As previous described, before mixing with the sand and EICP treatment, all of the jute fibers used in this study were dried for 24 hours at 60 °C.

II.   *Used urease enzyme and soil properties*

The EICP solution (crude urease) used throughout this study was composed of 0.5 M urea and optimum ratio of Mg-calcium chloride, (as described to Chapter 4). In order to prevent premature carbonate precipitation as described to previous chapter (Chapter 4), a substrate solution (i.e., the calcium and magnesium chloride and urea solution) and the crude urease enzyme solution were prepared in separate containers and mixed together right before applying to soil. The soil used in this study was commercially available "Mikawa" sand as described to chapter 5.

III.   *Preparation of the samples*

The designed materials and test set up for EICP are shown in Table 6.1. The dried "Mikawa" sand (75±5 g) was taken into a 50 mL standard syringe tube (diameter 3 cm, height 10 cm). In each cases, oven-dried samples (as described earlier), was compacted into 3 layers by applying a hammer shock on each layer of the sand. A lab-grade filter paper was used to cover the bottom portion of each column. Each sand column was filled with consistently mixed jute fiber using an automatic mixer (kitchen aid 9KSM160 series) considering different lengths and fiber contents. To neutralize the electrostatic charge of fiber and sand grains 10 mL of (DW) de-ionized water was added during the mixing process to ensure uniform distribution of fiber within the soil matrix. The samples were then put in a 30°C incubator. Following that, 26 mL of the prepared urea-CaCl$_2$-urease solution (cementation solution) was injected into the syringe, with the final amount of the solution remaining above the top surface of the sand sample. A new solidification solution of the same amount and concentration was injected into the samples at 48-hour intervals, steadily draining the previously injected solution. The crude urease injection period was chosen to prevent clogging and to account for the quick reaction rate (48 h). The injected solution was held about 2 mL above the sand's surface to maintain a completely saturated state. The prepared samples were kept in an

incubator at 30 °C for 14 days. The cementation solution was injected and drained every day for 14 days continuously. The pH values and Ca^{2+} concentrations from the outlet were measured frequently.

Table 6. 1: Testing conditions for sand solidification tests.

Cases	Fiber content [(%) mm]	Cementation solution injection	EICP Solution Injection	Curing Temperature (° C)	Curing days
0	0	48 h	48 h	30	14
1	[(0.5) 15]	48 h	48 h	30	14
2	[(1.5) 15]	48 h	48 h	30	14
3	[(3) 15]	48 h	48 h	30	14
4	[(5) 15]	48 h	48 h	30	14
5	[(10) 15]	48 h	48 h	30	14
6	[(20) 15]	48 h	48 h	30	14

IV.   UCS measurement of the treated samples

UCS measurement of the treated samples were conducted as described to previous chapter (5.3.1-e)

V.   Shear wave velocity measurement of the treated samples

Shear wave velocity measurement of the treated samples were conducted as described to previous chapter (5.3.1-f)

VI.   Microstructure analysis

Microstructure analysis of the treated samples were conducted as described to previous chapter (5.3.1-g).

6.3.2 Durability Improvement

I.   Samples preparation for cyclic wet-dry test

The columns specimens (3 cm in diameter and 6 cm in height) were used in this work. The wet-dry (WD) cycles were performed in accordance with the method suggested in ASTM D559-03 (2003) using distilled water (DW) and artificial sea water (ASW). During the wetting process, specimens were submerged completely in distilled water at room temperature (25 ± 1 °C) for 6 hours. The saturated specimens were then placed in the oven at 60 ± 1 °C for at least 42 hours, and when the mass of the specimen

became constant, their dry mass was recorded prior to the next WD cycle. Specimens were subjected to maximum of continuous 30 WD cycles, and the effect of WD cycles were evaluated using the following measurements. Mass loss and S-wave velocity of the specimens were determined with the number of cycles as described to Chapter 5.3.2.

6.4 Results and discussions

6.4.1 Results of strength improvemt

I.   Effects of adding fiber on $CaCO_3$ precipitation

It's well established that, the $CaCO_3$ acts as the main binding materials in between the sand particles for soil improvement during the EICP process. Therefore, it was impotant to investigate the effect of adding jute fiber on $CaCO_3$ precipitation. The effect of same fiber length and different fiber content on CaCO3 precipitation was showed in Figure 6.1. From the results, it showed that, the amount of the precipitated $CaCO_3$ crystals was not varied significantly and remains almost constant and the precipitated crystals was loosely attached to the jute fiber (SEM image, Figure 6.2). Another noticeable observation was, the precipitated crystals was much smaller in size and formed like a powdery deposits compare to MICP process.
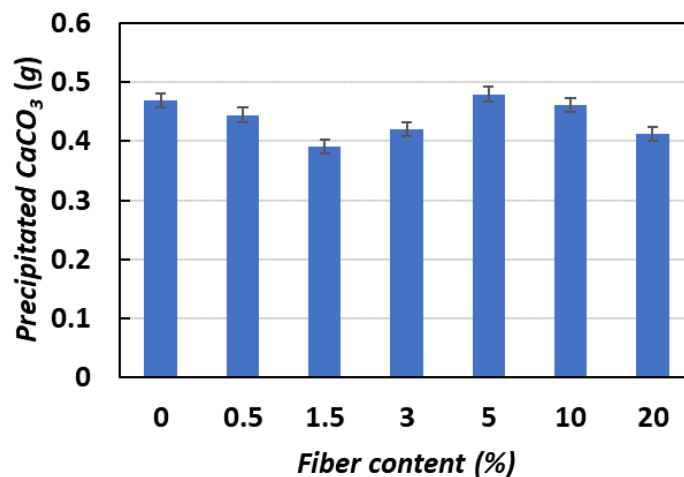
Figure 6. 1: Effect of fiber content on CaCO3 precipitation by addition of jute fiber.
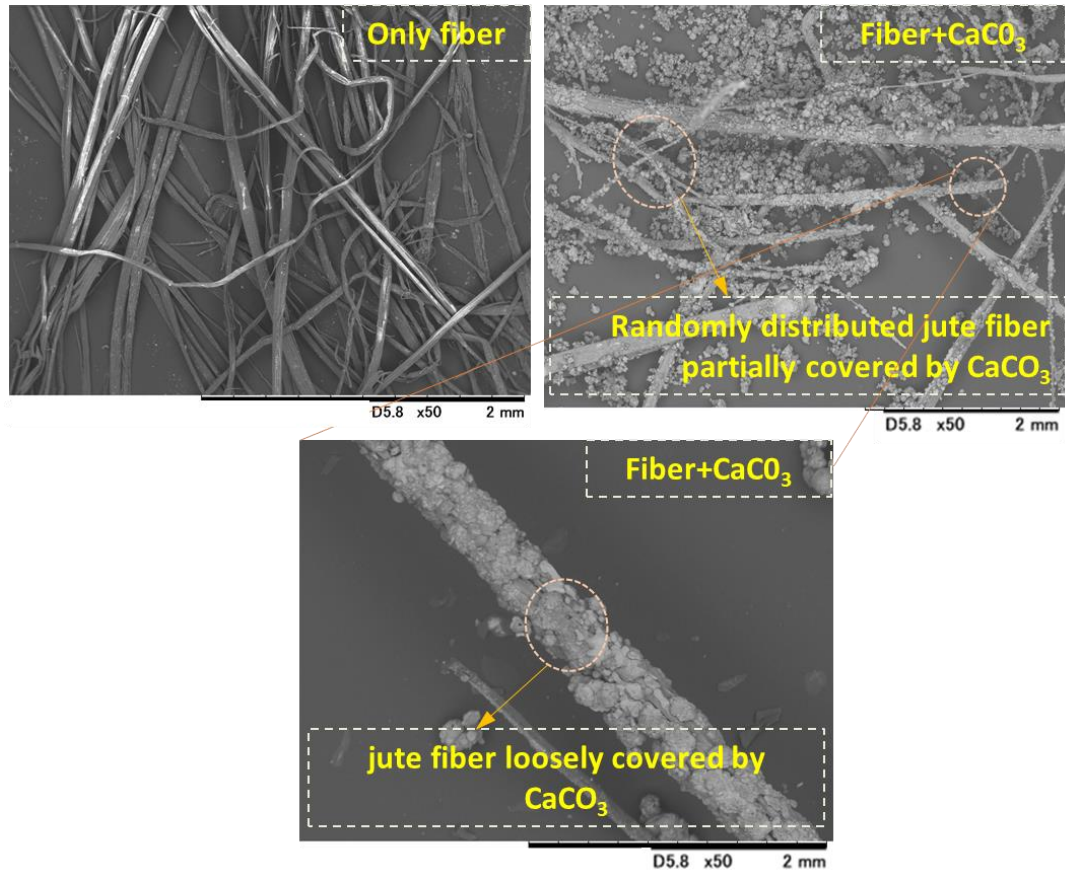
Figure 6. 2: SEM images of the precipitated CaCO$_3$ crystals to the jute fiber.

II.   *Results of UCS measurement*

The stress-strain curves of the EICP treated samples with different are presented in Figure 6.3. Results showed that (Figure 6.3) the strength of the EICP treated samples with fiber was moderately influenced by the addition of jute fiber (depending on the fiber content). The stress strain curve of the EICP treated biocemented sand without fiber was gradually compacted with increased strain, and stress and failure occurs, which was considered as typical brittle failure. Similar observation was noticed during MICP treated sample in previous studies. However, with increasing the fiber content, the stress of biocemented sand reached to the maximum strength, and then entered the residual deformation stage. Finally, failure occurred more slowly compared to without fiber at 20% fiber cases. Maximum strength was observed at 0.5% fiber cases. The slower rate of failure tendency indicated the improvement of ductility behavior of the samples. Li et al., (2015) and Almajed et al., (2018) obtained a similar pattern for strength versus fiber content for EICP-treated soil.
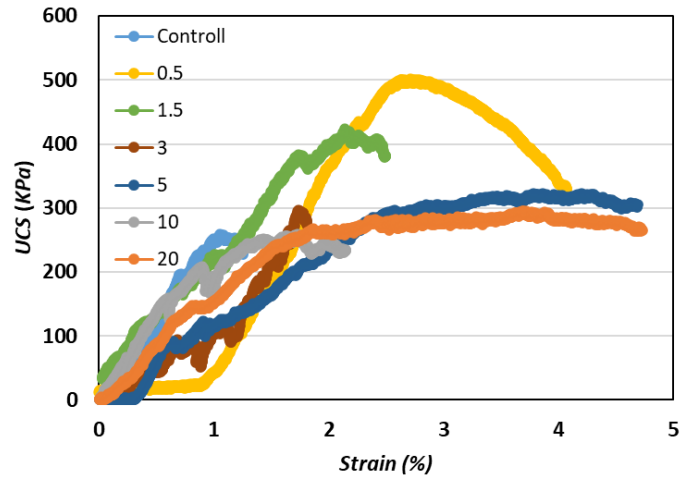
Figure 6. 3: Effects of fiber on unconfined compressive strength (UCS) of biocemented sand by addition of jute fiber.

The relationship between the estimated UCS and the $CaCO_3$ (%) obtained from this study showed in Figure 6.4. Results showed moderately strength improvement of the fiber treated EICP samples. The strength slightly improved by adding jute fiber and the precipitated carbonate didn't contribute much for strength improvement as expected (Figure 6.5). The possible reason was the deposition of powdery crystals as described to the Microstructure analysis sections below.
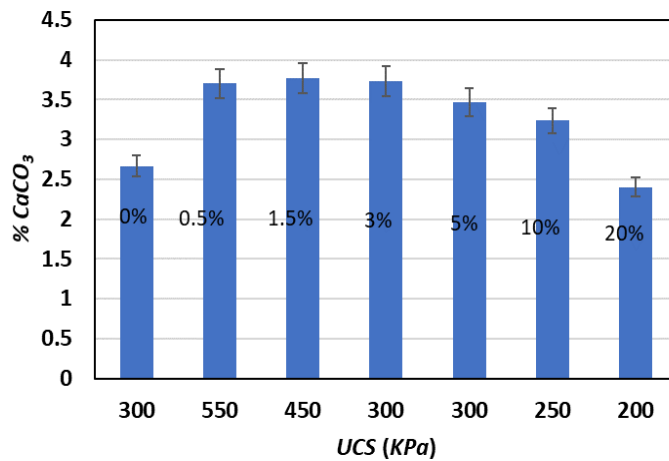
Figure 6. 4: Average (%) $CaCO_3$ of the biocemented sand after EICP treatment by addition of jute fiber.
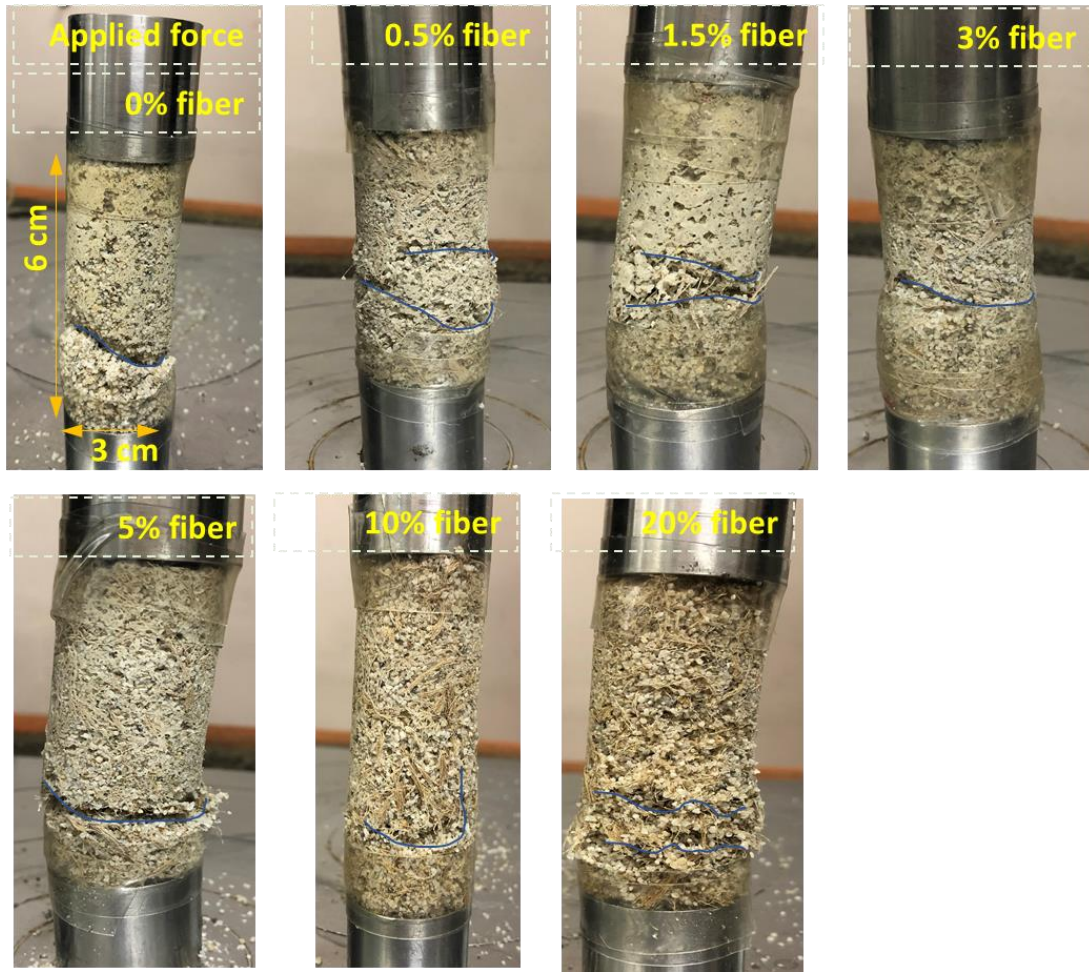
Figure 6. 5: Effect of failure behavior of the EICP treated sample by addition of jute fiber.

III.   *Microstructure analysis*

The SEM images of EICP treated biocemented samples by addition of jute fiber and distribution of $CaCO_3$ within the sand matrix are shown in Figure 6.6. The images also represented sand particles without fiber treatment, and biocemented sand particles with different fiber content, respectively. From the microscopic images, the void spaces were dominant in both cases of sand-fiber matrix without EICP treatment. After the EICP treatment, the fibers were covered by calcium carbonate crystals (like a bridge) which provided the moderate bonding capacity in between the sand particles and also filled the void space and yielded an enhanced cementation level, which is presented more clearly by a schematic diagram in previous chapter. Microscopic images also shows that the $CaCO_3$ deposited on the fiber surface enhances the binding force

between the fiber and sand particles and forms a "fiber–CaCO₃–sand" structure system through the bridging action of the fiber. The fibers overlap each other to form a three-dimensional mesh, which constrains the displacement and deformation of sand. The significant differences between the MICP treated fiber and EICP treated fiber reinforcement was, in case of EICP treated the precipitated crystals are much smaller and formed a powdery deposit onto the san grains instead of in between sand particles and couldn't contribute for strength improvement. Further study in recommended to improve this methodology.
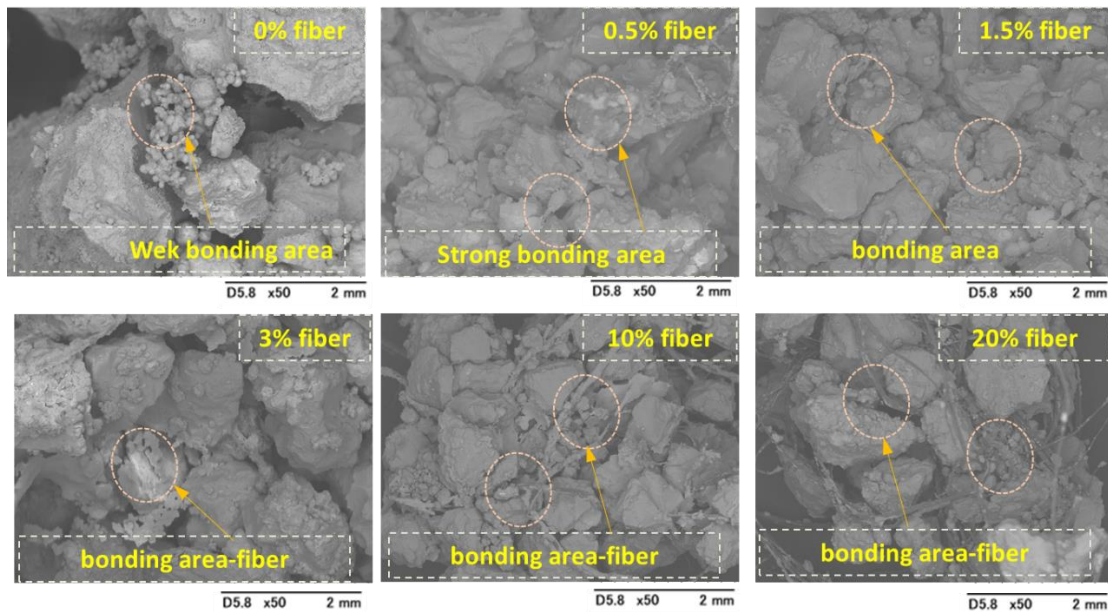
Figure 6. 6: SEM images of EICP treated biocemented samples by addition of jute fiber and distribution of CaCO₃ within the sand matrix.

6.4.2 Results of durability improvemt

I.   *Physical changes and mass loss*

The mass loss of the specimens was used to assess physical damage during cyclic experiments. After each cycle, the mass loss was carefully measured using distilled water (DW) and artificial sea water (ASW) at a constant temperature. The mass loss of the specimens subjected to 30 cyclic WD behavior as shown in Figure 6.7. After 30 WD cycles, mass loss in 0 percent fiber treated EICP specimens was found to be greater than 70 percent. The mass loss tendency slight decreased as the fiber addition was increased, and mass loss was only 50% (DW) and 40% (DW) in 0.5 percent fiber treated EICP specimens (ASW).

In case of DW, mass loss severely occurred at early stage. After 20 cycle the specimen becomes a stable position and mass loss didn't occur severely. Without addition of fiber the mass loss occurred rapidly (around 50% after 20 cycle), but addition of fiber mass loss occurred gradually (around 40% after 20 cycle) unlike MICP. Within another few more WD cycles (Figure 23(a)), the rate of mass loss slightly decreases gradually and tends to become to the equilibrium state. In case of ASW (Figure 23(b)), mass loss severely occurred continuously. Without addition of fiber the mass loss occurred around 80% after 20 cycles, but addition of fiber mass loss occurred gradually (around 30-40% after 20 cycle). Treated specimens were more vulnerable in ASW compared to DW. In EICP case, the precipitated crystals weakly attached in between the sand particles and with the fiber, which is the main reason to losse the strength quickly.
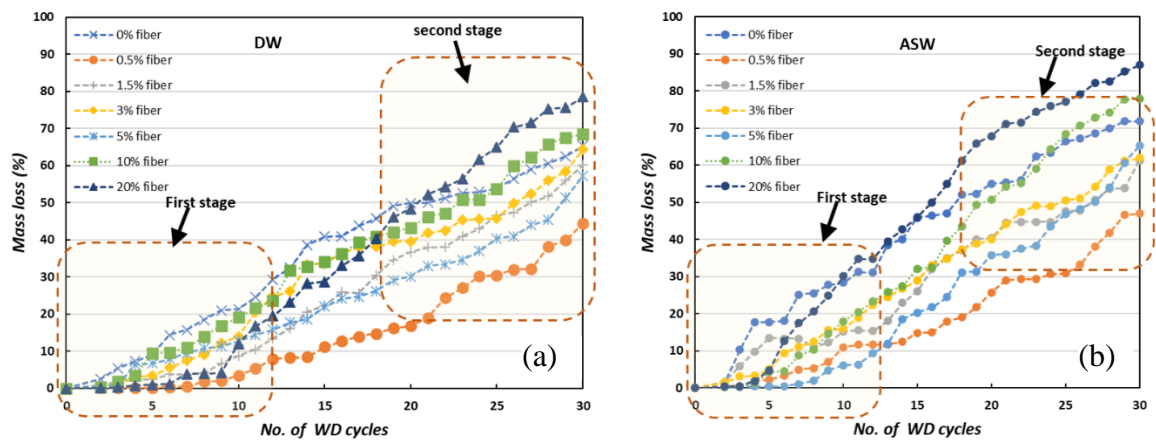
Figure 6. 7: Average mass loss of the specimens subjected to WD cyclic treatments based on (a) DW and (b) ASW.

II. Strength deterioration ratio

The strength deterioration ration was calculated as unlike MICP procedure as described to previous chapter. From the results, it is shown that, (Figures 6.8 (a)), the average $CaCO_3$ decreasing gradually and in the first stage (up to 10 WD cycles), severe degradation was witnessed in all cases. In case of DW, the SDR value was not significant at the eagerly stage (up to 10 WD cycles) but with more cyclic treatment (up to 30 WD cycles) SDR value was considerably decreased (Figures 6.8 (b)). The SDR values considerably decreased with the decreasing in calcium carbonate content

((Figures 6.8 (c))), in case of ASW. The tendency demonstrates that the high deposition of carbonates likely to be preserving the EICP responses against WD actions in ASW. Fiber treated EICP specimens unable to achieve a stable from, and due to the weak primary connections, and high resistive forces during the development of fatigue stresses leads to weaking the bonding connections and thus mass loss occurred. Also, the powdery deposits lead to weak connections against suspension and corrosion induced by during WD process and resulted less improvement of SDR value ((Figures 6.8 (d)).

However, from the WD cyclic test using the DW and ASW values, it can be precisely concluded that the EICP specimens was more susceptible than MICP treated samples. The overall observation suggests that the mechanical degradation conspicuously occurs at the early stage of the WD process (ASW), compared to that occurred at the later stage (DW) and fiber addition could moderately improve durability of the EICP treated samples.
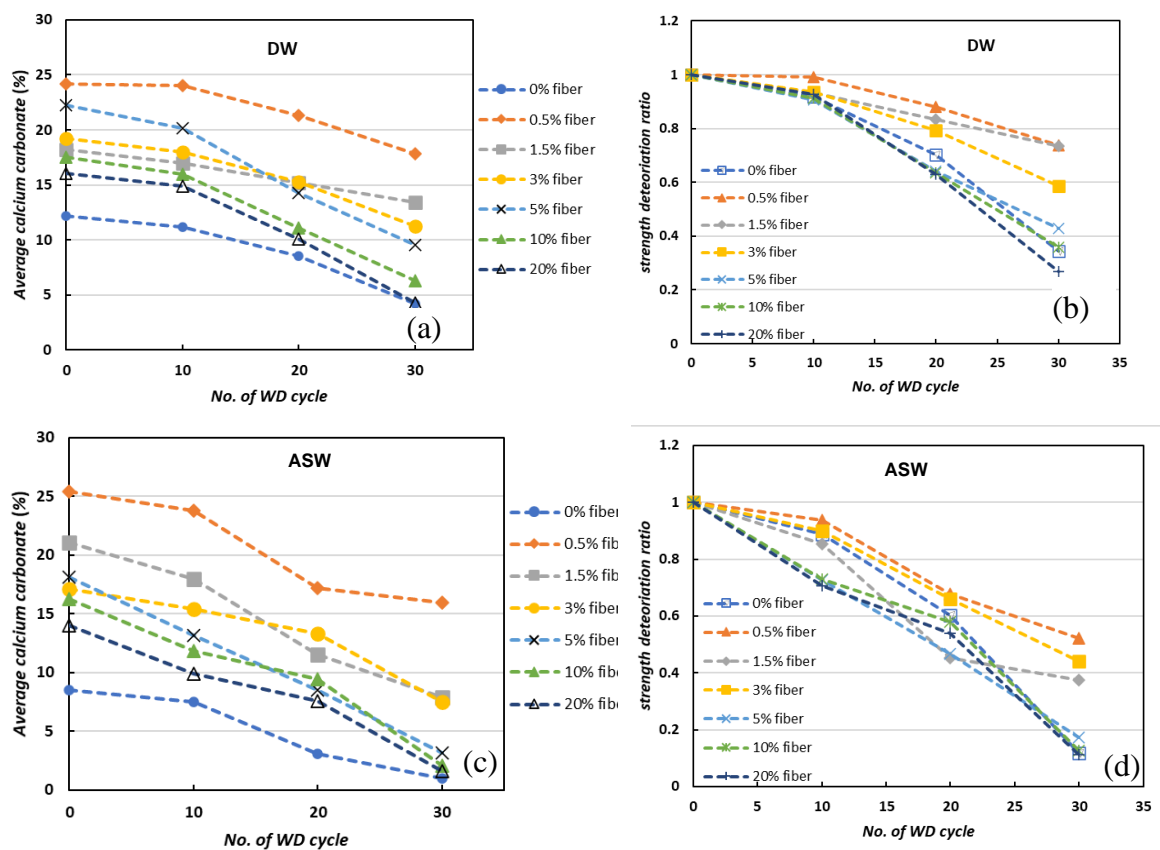
Figure 6. 8: The average calcium carbonate (%) of the samples treated with (a) DW; (c) ASW and the strength deterioration ratio in (b) DW; (d) ASW after the exposure of cyclic WD tests.

Figure 6.9 presents the microstructures of fiber treated EICP specimens in DW (after 30 WD cycles). From the SEM images, it is clear that the soil structure has been significantly affected within first few WD cycles unlike MICP, and higher degradation is evidenced on the surface compared to that observed at core of the specimens. The surface carbonate deposits were found to be shrunken and degraded. Microcracks were also observable at and around the intact bonds and become very severe with ASW treated samples (Figure 6.10).

When the specimens are subjected to drying, the interior relative humidity does not drop immediately but decreases in a gradual manner (Zhang et al., 2012), whereas the surface undergoes rapid evaporations, experiencing high negative stresses. Also, the core zone of the sample is confined stiffly, the developed fatigue stresses therefore caused more damages at outer surface of the column, attributing to the progression of macropores. Similar initial surface degradations due to WD stresses were also often reported to concrete specimens (Gao et al., 2014; Zhang et al., 2012). Furthermore, the difference in thermal expansion coefficient of calcium carbonate and soil material could be another possible factor that could result the development of internal fatigue stresses under temperature change, inducing the degradation process. The above mechanism has also been reported to magnesium potassium phosphate cement, in which the internal fatigue stresses resulted pores and microcracks (Li et al., 2019). When the calcites are flooded by water for a long time, a minor portion would possibly undergo chemical dissolution (Ciantia et al., 2014; Khanlari and Abdilor, 2015). Ciantia et al., (2015) have confirmed that the long-term weathering of carbonatic rocks is due to the dissolution of diagenetic calcite bonds. In this study, the effect of dissolution is assumed to be negligible under the standard conditions. For a similar instance, Ciantia et al., (2015) studied the deterioration of carbonatic rocks and observed the occurrence of instantaneous debonding of depositional bonds (menisci shaped calcite ensembles) when subjected to saturation. The researchers also found that single wetting process caused a considerable loss in compressive strength, and the loss was more pronounced for high porosity calcarenites (Ciantia et al., 2014).
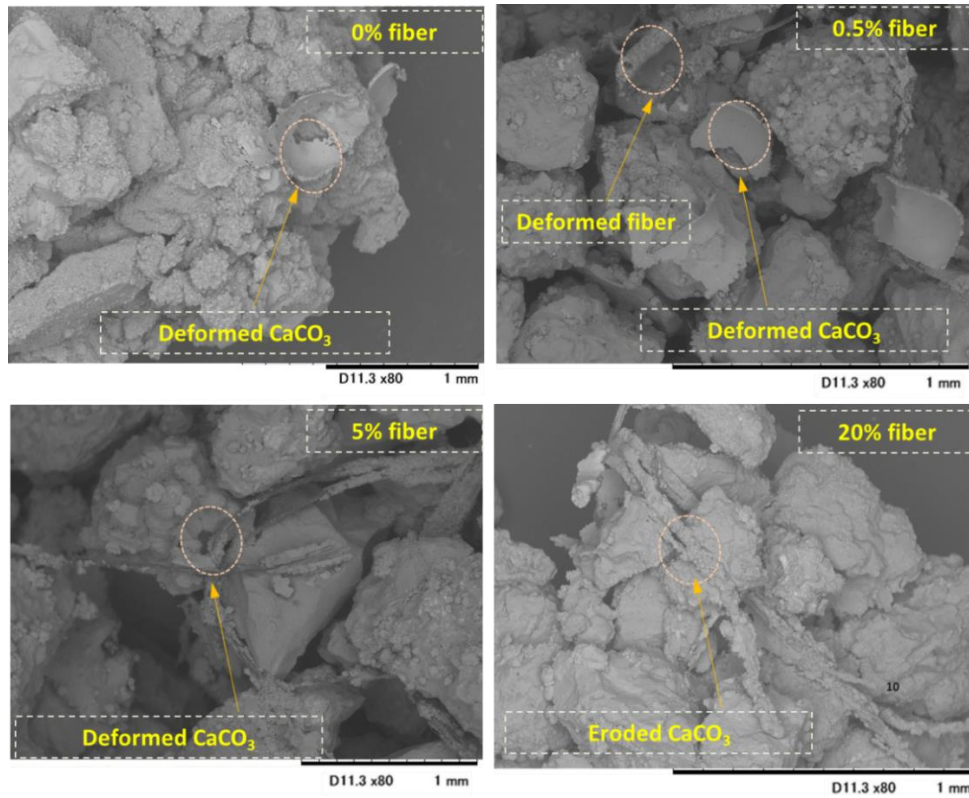
Figure 6. 9: SEM images (DW) of the specimens after subjected to WD cycles.
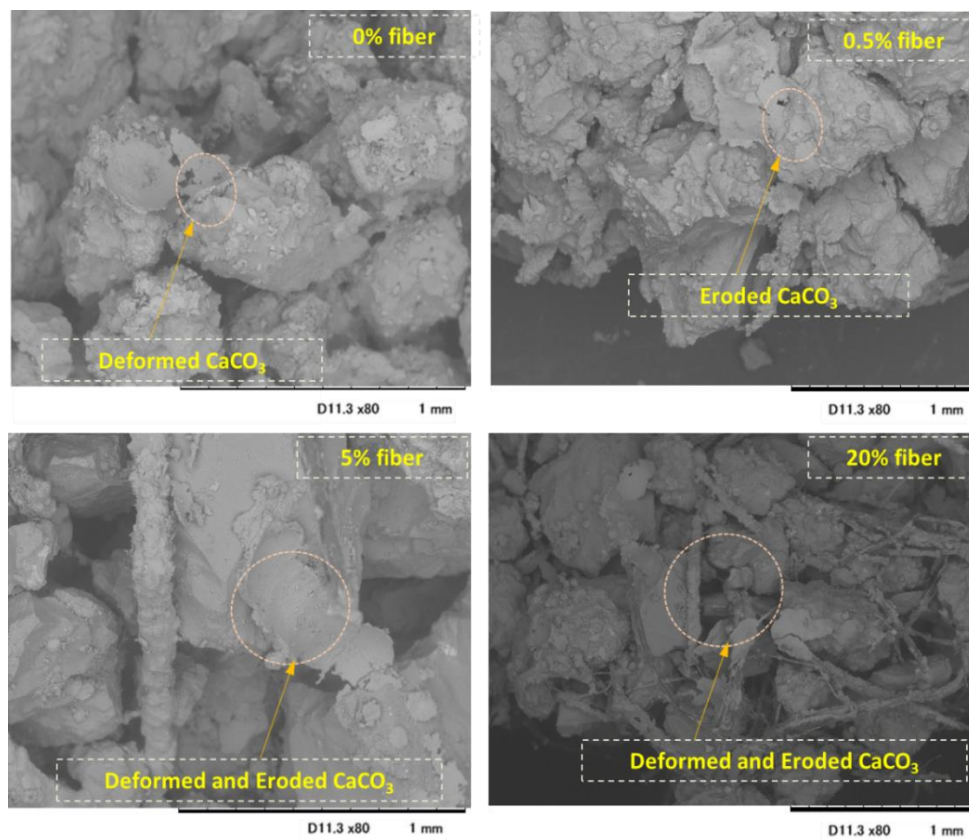
Figure 6. 10: SEM images (ASW) of the specimens after subjected to WD cycles.

IV.   Durability characteristics and mechanisms

During EICP treatment, the calcium carbonate is precipitated in various forms such as primary bonds (strongly forms at particle contacts), individual crystals and accumulation (on the grain surface), amorphous and powdery deposits (Lin et al., 2016; Wang et al., 2019). In fact, these powdery bonds are often formed when the carbonates are deposited at its early stage of the crystallization-and recrystallization process. When the specimens are submerged during the wetting, the water penetrates the specimen and drives the powdery deposits to fall into suspension. This corrosion mechanism is similar to the MICP process as described to previous chapter.

V.   XRD results

The results of the XRD study are shown in Figure 6.11. The investigation was carried out to confirm the presence of phase transformations in carbonate deposits, as well as the precipitation of new minerals and the dissolution of existing minerals. The XRD results show that there are no visible changes in mineral morphology during the WD phase in both DW and ASW. The observed peaks are similar to the increase in cycle number, implying that neither new mineral formation nor phase changes were caused.
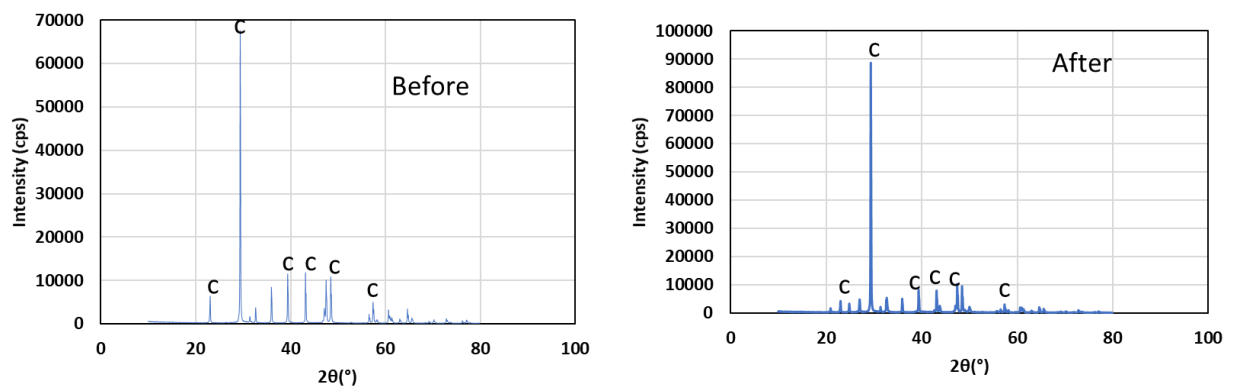
Figure 6. 11: XRD results of specimens subjected to WD cycles.

6.5 Conclusions

This study was conducted to investigate the effect of adding jute fiber to the biocmented sand by EICP method. This study demonstrates that addition of natural jute fiber can moderately increase the strength of EICP-treated sand prepared specimens using the mix-and-compact method of preparation. In agreement with other studies, it was observed that there is an optimum fiber content at which the strength reaches a maximum value. At the optimum fiber content, the EICP-treated sand reinforced with 15 mm jute fibers showed 3 times higher strength than EICP treated sand without fiber reinforcement. Based on the results of this study, the following conclusions could be outlined:

   i.   Jute fiber has significant effects on the EICP treated samples. The addition could effectively improve the mechanical characteristics, UCS and ductility of sand.

  ii.   The calcium carbonate precipitation was positively directly correlated with the added fiber. The SEM analysis suggested that the added jute fiber well coupled with calcium carbonate (i.e., calcium carbonate was attached on and along the surface of fibers), forming reliable bridges within the soil matrix, which tended to limit the development of failure planes within specimens. This could eventually result more increase in both the strength and the toughness of the specimens compared to those of control biocemented specimens (without jute fiber).

 iii.   Overall, the exhaustion stresses created during the WD process have the ability to interfere with the primary bonds, impacting the specimens' surface in particular. In contrast, the addition of jute fiber increased bonding as well as aggregate stability and mechanical durability. According to the findings, EICP treated specimens are less susceptible to WD behavior than those identified when ASW effects are present,

CHAPTER 7 : PROPOSAL FOR COASTAL EROSION PROTECTION METHOD

7.1 Potential advantages of EICP and disadvantages of MICP

It is well-established that urease can occur as both an intra- and extra-cellular enzyme (Ciurli et al., 1996; Marzadori et al., 1998). Free soil urease (i.e., urease not bound to a living organism) readily occurs apart from the host microorganism and is generally derived from dead and decaying microorganisms and from plant sources. A major consequence of absorptive association of free-soil urease with soil particles is that the absorbed urease can persist for very long periods of time without proteolytic degradation or loss function (Pettit et al., 1976). In fact, the longevity of urease-soil colloids is of significant agricultural importance in nitrogen regulation to plants provided via urea fertilization (Pettit et al., 1976; Krogmeier et al., 1989; Ciurli et al. 1996). By contrast, exogenously added urease, as a free enzyme, has a limited lifespan as its activity and function decrease with time (Pettit et al., 1976; Marzadori et al., 1998). A potential advantage to short-lived urease activity may be in engineering applications where a desired goal may be achieved over a limited time, after which the enzyme naturally degrades thereby eliminating long term impacts to the ecosystem.

The small size of a solubilized urease enzyme affords it a distinct advantage over microbial urease for engineering applications that require penetration into very small pore spaces, e.g., in finer-grained soils. Nearly all known bacteria are greater than 300 nm in diameter, with the majority in the range of 500-5000 nm, limiting their ability to penetrate soils finer than fine sand and facilitating bioclogging. The free urease enzyme is water soluble and, therefore, is expected to reach any space that water-based solutions can penetrate. Another potential advantage of using urease enzyme for $CaCO_3$ precipitation, in contrast to slower microbial methods, is that carbonate precipitation induced by the free enzyme is rapid (since ureolysis begins immediately upon contact of the enzyme with urea), which makes it well-suited for applications where rapid desiccation of the cementation solution is a concern. Furthermore, unlike MICP, the free enzyme method does not consume or compete for the organic substrate (urea) and therefore is more efficient with respect to utilization of the urea than similar processes that rely on microbial urease. In addition, although ureolytic microbes are common in

many natural soils, most current MICP studies have relied on bio-augmentation (i.e., introduction of microbes grown ex-situ) to achieve soil stabilization goals, and the effectiveness of bio-augmentation in highly processed mined soils (i.e, mine tailings) is uncertain.

7.2 Potential disadvantages to EICP and advantages of MICP

Disadvantages of using free enzyme rather than microbial urease include that the use of the free enzyme does not provide nucleation points on the soil surface for $CaCO_3$ precipitation. In the microbially-mediated approach, the microbes typically attached themselves to the soil particle surface and may provide nucleation points for mineral precipitation. Furthermore, the rapid precipitation of carbonate minerals induced by free urease enzyme may be a disadvantage in that it leads to smaller and less-structured (more amorphous) crystals and may hinder penetration into the soil in some cases. Other disadvantages of using the free enzyme include the higher cost of procuring the free enzyme and solubility limitations in high ionic strength mediums.

With increasing population and civil infrastructure demands worldwide, the availability of suitable soil sites for construction continues to decrease and ground improvement is now an integral part of modern development. The most common methods to strengthen soils use either one or a combination of several mechanisms such as compaction, preloading, vibration and chemical grouting. These techniques have been proven to have different degrees of effectiveness in improving soil strength and other properties. However, they come at a cost of consumption of a substantial amount of energy either in their application or production of the grouting materials or both. Microbial-induced calcite precipitation (MICP) uses naturally occurring bacteria to bind soil particles together through calcium carbonate ($CaCO_3$) precipitation as shown in Figure 1, thereby increasing the strength. The expected life of MICP-treated soil is more than 50 years, which is compatible with the expected service life of many geotechnical structures. Therefore, biogeochemical processes in MICP offer the potential for solving many engineering issues related to ground improvement. MICP also offers advantages over other common approaches as it uses natural processes and it has the potential of being a comparatively inexpensive technique.

7.3 Proposed methodology for a new coastal preservation method: Geo-textile Tube Technology

The recent trend in the mitigation of coastal erosion and costal protection has been shifted now-a-days towards soft novel cheaper, sustainable, and eco-friendly methods. Pro-active methods and solutions are being developed and employed, which are not only eco-friendly, construction-friendly, and cheaper but also address the root cause of the problem without much adverse effects. Such kind of modern tool is geotextile tube which is one of the geosynthetics structures that are increasingly used in coastal protection. They are made from polypropylene (PP), polyester (PET), polyethylene (PE), polyamide (nylon), polyvinylidene chloride (PVC), and fiberglass. Sewing thread for geotextiles is made from Kevlar or any of the above polymers. Different fabric composition and construction are suitable for different applications. Traditional Geotextile tubes widely used for dewatering, flood control, and coastal protection. Geotextiles are either woven or non-woven permeable fabric or synthetic material which can be used in combination with geotechnical engineering material. But our proposed method is coastal protection along with MICP method and these "Geotube®" (Figure 7.1). In case of traditional methods, different rays from sun can damage the "Geotube®" after a certain time and soil protection may not be sustainable and the cost of re-constructing "Geotube®" is much. But, in our proposed method, sand cementation using MICP method can be applied over the "Geotube®". As a result, the surface of the coast and "Geotube®" will be strengthened and will remain longer, and soil will be protected. In this method, cost is low comparatively and local ureolytic bacteria is used, so this is eco-friendly and sustainable. This method can be applied in a broad range of civil engineering applications including construction, paving, drainage, and other applications.

In addition, plants exude 10–30% of the carbon captured from the atmosphere, by photosynthesis, through their roots and associated mycorrhizal fungal associations and included references). Any compound in the root tissue may be released into the soil in the form of an exudate; thus, root exudates are a complex material composed of polysaccharides, proteins, phospholipids, cells that detach from the external layers of the root and many other compounds. Respired CO_2 and organic acid anions that naturally decompose and can react with calcium-rich carbonates within soils are of particular interest and protect the soil (Figure 7.2).

Finally, the coastal area will be protected (Figure 7.3). The treatment strategy of the proposed methods are presented in Table 7.1 and Table 7.2.
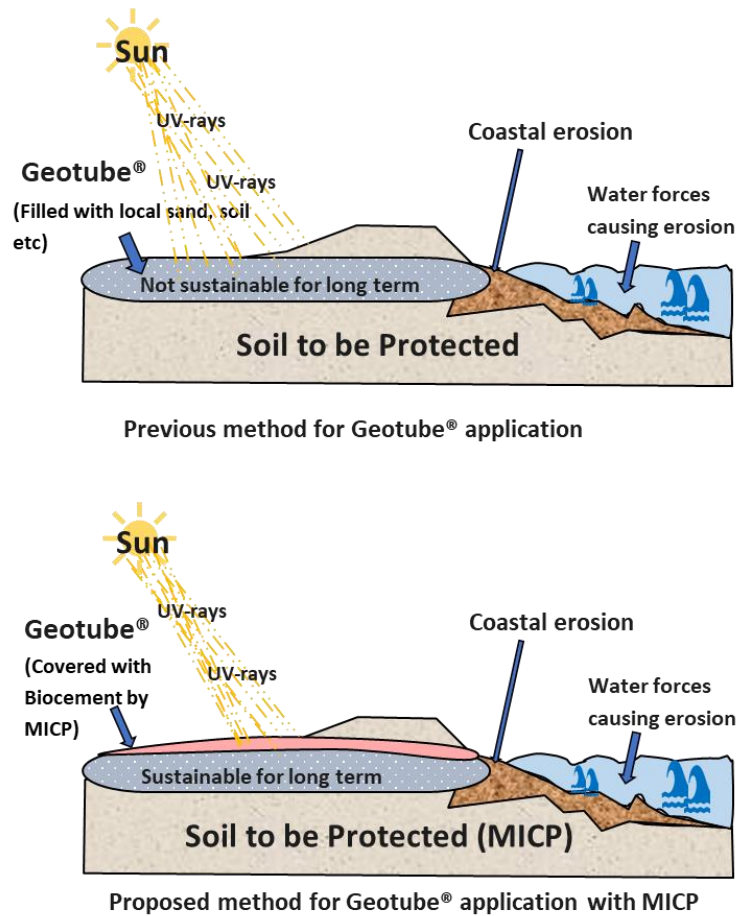
Figure 7. 1: Proposed methodology for coastal erosion protection (Proposal 1).
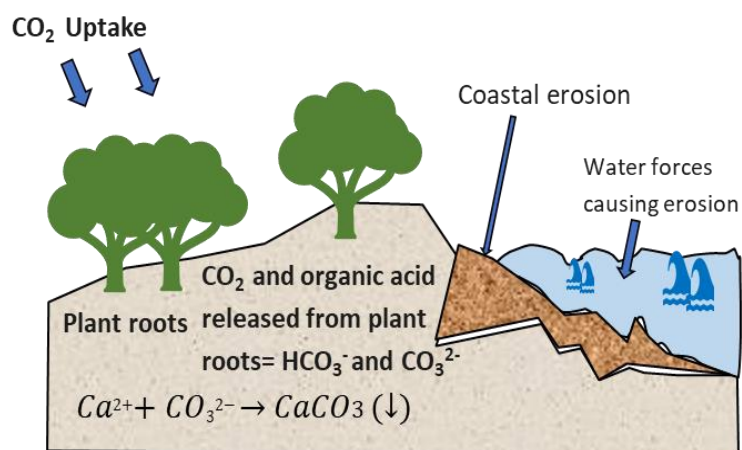
Figure 7. 2: Proposed methodology for coastal erosion protection (Proposal 2).
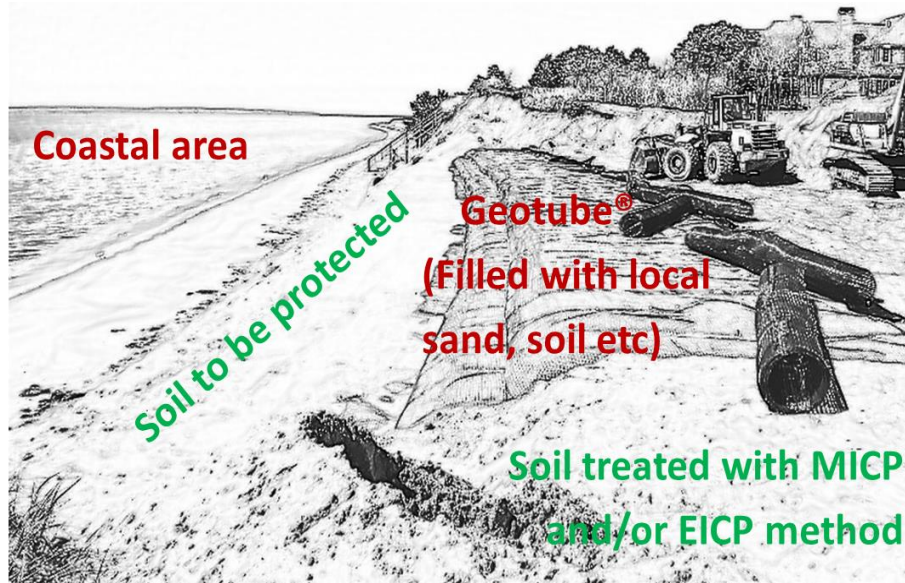
Figure 7. 3: Final view of the protected coastal area.

Table 7. 1: Treatment strategy in field scale (MICP).

Treatment type	Treatment procedure
MICP (injection method) ☐ *More than two injection intervals are recommended.* *Consideration* *Possible to obtain higher strength (depending on the location)-needs longer time to occur the reaction.*	***Site-specific investigation*** - Compatibility of grain size distribution and intrinsic characteristics - *In-situ* ground water characteristics ***Preliminary field-works*** - Clearance of obstacles from the surface of the area to be treated, and surface smoothening (if required) ***Treatment*** - Spraying or pumping bacteria culture (*phase 1*) - 2-3 hours of retention time - Spraying or pumping cementation solution (*phase-2*) - Cementation solution spraying or pumping: Every 24 hours basis *(until desirable level is achieved)* - Bacteria spraying or pumping: Once in a week (i.e., once in seven cementation sprayings) basis - Treatment monitoring: *groundwater-ammonium ions monitoring, ultrasonic waves, pH, atmosphere* ***Post-treatment*** - Performance-monitoring/ assessment: ultrasonic waves and visual monitoring *(once in a while, after prolonged rainfalls, after seasonal winters)* - Occasional retreatments *(if required)*
Desirable conditions	
Atmospheric temperature: 20 – 30 °C ☐ *July, August and September are recommended for field implementation in Greece.* ***Limitations*** ☐ *Required 2-3 weeks to achieve the desirable results. Might need to supply nutrient. Suitable for aerobic conditions. Storage required. Costly compared to EICP. Homogenous solidification is a challenge.* ***Limitations*** ☐ *Required to control the bacterial growth, population, cementation solution and nutrient supply.* ☐ *This method is applicable for sandy materials based on these results. Other applications could be possible with a proven investigation.*	

Table 7. 2: Treatment strategy in field scale (EICP).

Treatment type	Treatment procedure
EICP (injection method) ☐ *Several injection intervals are recommended.* *Consideration* *Possible to obtain higher strength within a very short period of time (depending on the location)-needs to control reaction rate.*	*Site-specific investigation* - Compatibility of grain size distribution and intrinsic characteristics - Need to make sure the filtration process to extract the crude enzyme *Preliminary field-works* - Clearance of obstacles from the surface of the area to be treated, and surface smoothening (if required) *Treatment* - Spraying or pumping EICP solution (*phase 1*) - Retention time doesn't require. - Spraying or pumping cementation solution (*phase-2*) - Cementation solution spraying or pumping: Every 24 hours basis *(until desirable level is achieved)* - Treatment monitoring: *groundwater-ammonium ions monitoring, ultrasonic waves, pH and reaction rate* *Post-treatment* - Performance-monitoring/ assessment: ultrasonic waves and visual monitoring *(once in a while, after prolonged rainfalls, after seasonal winters)* - Occasional retreatments *(if required)*
Desirable conditions	
Atmospheric temperature: 20 – 30 °C ☐ *July, August and September are recommended for field implementation in Greece.* *Limitations* ☐ *Required to control the hydrolysis rate.* ☐ *This method is applicable for sandy materials based on these results. Other applications could be possible with a proven investigation.*	

CHAPTER 8 : CONCLUSIONS AND FUTURE WORK

8.1 Summary of the current study and main findings

The objectives of this Ph.D. study were to investigate the viability of using MICP and EICP method as a novel alternative for coastal erosion protection method. This study discussed about the characteristics of ureolytic bacterial species isolated from the coastal area of Greece. The findings in this thesis suggested that the isolated ureolytic bacteria (G1, G2, and G3 species) have the potential to be used as alternative microbial MICP agents for biocement applications, especially in coastal areas. The results of our experiment provide insight into the factors that affect urease activity of the local ureolytic bacteria species with a prospect for successful sand solidification. This research showed a positive result leading to the enhanced possibility of application in coastal erosion protection by assimilation of knowledge from microbial mechanism and design applications considering the engineering viewpoint. This study also presents the effects of various cultural conditions to optimize the urease activity for the isolated bacterial species that could be applied to solve problems relating to environmental biotechnology, civil engineering, and geotechnical engineering. Moreover, the isolated ureolytic bacteria described in this study may hold additional potential in the field of MICP and can serve as an advantageous reference resource for researchers in microbial biotechnology and construction microbial biotechnology. The results of this study can also be applied to the creation of artificial beachrock using the MICP method for coastal erosion protection in Mediterranean countries, and other coastal areas as well for bio-mediated soil improvement, establishing an economical and environmentally friendly countermeasure for coastal erosion protection and bio-stabilization.

Soil improvement using EICP (Enzyme-Induced Carbonate Precipitation) methods in the geotechnical and geo-environmental field has become a prominent interest worldwide. The objective of this study was to develop an improved extraction technique of crude urease from watermelon seeds in both dry and germinated conditions. Subsequently, this study also analyzed the improvement methodology of crystal polymorphs and soil bonding incorporation of various Mg^{2+}/Ca^{2+} ratios. The optimization of enzyme-mediated carbonate precipitation was also investigated by Scanning Electron Microscope (SEM) and X-ray Diffraction (XRD) analysis. Results

confirmed that the precipitated crystals are mainly calcite, vaterite and aragonite primarily (depending on the Mg^{2+}/Ca^{2+} ratios). Therefore, to improve the bonding capacity in between the sand particles a novel improvement methodology was investigated by adding various Mg^{2+}/Ca^{2+} ratios. The mechanical properties of the treated soil (Mikawa Sand, D_{50} = 0.870 mm) specimens were tested by unconfined compressive strength (UCS) and this confirmed the effectiveness of adding various Mg^{2+}/Ca^{2+} ratios. The results of the UCS tests showed that, the lower molar ratios of Mg^{2+}/Ca^{2+} can significantly improve the UCS of the specimen (up to 50%) which could be considered a significant outcome for different bio-geotechnical applications.

Jute fiber has significant effects on the microbial performance, calcium carbonate precipitation pattern and solidification of sand. Using the fluorescence microscopy, the survival capacity of the microorganisms was well demonstrated to be increasing due to the addition of jute fiber. The addition could effectively improve not only the bacterial performance, but also the mechanical characteristics UCS and ductility of sand. The UCS of the sample increased with the increasing in fiber content; however, higher fiber addition was found to be decreasing the UCS. From the results obtained in this study, the optimum content of jute fiber for the enhancement could be 3%, with 15 mm in length.

Cyclic wet-dry (WD) effects appear to have adverse effects on the physical and mechanical characteristics of fiber reinforce EICP treated soils in both DW and ASW. The deterioration mechanism of EICP soils due to WD cycles is related to the degradation of calcium carbonates and bonding effects in between the sand particles, and that is found to be occurring at two stages: short-term and long-term. The short-term deterioration rapidly occurs within the first few WD cycles in DW due to the suspension and corrosion of powdery carbonate deposits. The long-term deterioration could be observable after 15 WD cycles in ASW. The fatigue stresses developed during WD process could deform the primary bonds, and particularly impairing the surface of the specimens. However, addition of jute fiber the improved in bonding effect and increased the aggregate stability and mechanical durability. The results also suggested that the EICP specimens are less susceptible to WD actions, compared to that observed under ASW effects. Incorporating fibers reduces the uniformity of EICP-solidified sand. In severe cases, the failure will develop along the path of minimum structural resistance (the least CaCO3 distribution), thus weakening the mechanical properties of

the treated sand. Therefore, future studies can investigate the engineering properties of EICP-solidified sand with different mixing conditions. The adoption of better grouting technologies can lead to further improvement of the uniformity, strength, and toughness of fiber-stabilized sand.

Overall, in both DW and ASW, cyclic wet-dry (WD) effects tend to have a negative impact on the physical and mechanical characteristics of fiber reinforce MICP treated soils. The degradation of calcium carbonates and bonding effects between sand particles was found to be involved in the deterioration of MICP soils caused by WD cycles, and this occurs in two stages: short-term and long-term. Due to the suspension and degradation of powdery carbonate deposits, short-term decay occurs rapidly during the first few WD cycles in DW. After 15 WD cycles in ASW, long-term degradation could be seen. The fatigue stresses generated during the WD process have the potential to deform the primary bonds, affecting the surface of the specimens in particular. The addition of jute fiber, on the other hand, improved bonding and improved aggregate stability and mechanical durability. The findings have indicated that MICP specimens are less vulnerable to WD behavior than those found when ASW effects are present.

8.2 Limitations of this study

Miftah et al. reviewed the effectiveness of the MICP and EICP techniques in soil improvement and expressed that these methods could be effective in many geotechnical applications. However, certain concerns limit the effectiveness of these techniques. In the MICP method, concerns such as the type of soil, environmental issues, and the uniform treatment of soil mass are factors that create problems for its application. In the EICP method, the cost of enzymes happens to be too high since 57–98% of the cost of enzyme solutions is incurred on the urease enzyme. The soil type also plays an important role in governing the effectiveness of the biotreatment. The MICP method is restricted to the subsoil, and other regions of the soil may not provide a feasible environment to the bacterial growth. MICP does not show good results when used on very fine soils because comparatively larger sizes of bacteria cannot be accommodated in the pores of fine soils.

On the other hand, EICP does not pose any hindrance in its application due to its size. Miftah et al. also discussed the environmental concerns related to the use of MICP.

This technique leaves microbes in soils after treatment, which means that it may require the permission of the concerned authorities and regular inspection to ensure that the energy of microbes is not hazardous to the surroundings. Furthermore, the release of ammonia through MICP is dangerous to people and the ecology of the area where it is applied, especially to the air and water. Additionally, the increase in pH may develop potential corrosion, and further contamination of groundwater due to chloride may be possible after the precipitation of CaCO3. On the other hand, urease used in the EICP technique may not have a long-term impact on the environment because it becomes degraded after a certain time period. The use of microbes for soil treatment needs a specific environment in the soil mass for their cultivation, and the storage of bacterial strains is an expensive process. With these limitations in the use of alternate means for calcite precipitation, EICP seems to be better than MICP. It has also been observed that high concentrations of calcium chloride and urea hinder the bacterial activity, reducing the amount of calcite precipitation. Conversely, using enzymes can very well be possible with high concentrations of calcium chloride and urea, which paves the way for a greater amount of calcite precipitation. Therefore, the EICP technique is preferable over MICP. Yasuhara et al. mentioned that maintaining bacteria for their cultivation requires technical expertise. Controlling bacterial activity also poses a challenge in the MICP method; the EICP technique is free of this constraint.

8.3 Future research works

8.3.1 Suggestions for future research works for MICP/EICP method

The overall feasibility of MICP treatment in real field applications have been evaluated in very few scenarios. These studies provide important findings beneficial for upscaling of MICP such as distribution of $CaCO_3$ content and its influence on strength enhancement. Treatment homogeneity has become the most crucial factors that requires the most attention. Harkes et al., (2010) demonstrated that fixation and even distribution of bacteria through an effective injection method is a key step towards achieving homogeneous $CaCO_3$ precipitation in the treatment body. van Passen in his MICP experiments in 1 m^3 and 100 m^3 sand volumes showed that there is a significant heterogeneity in the calcium carbonate precipitation which may be a negative impact on the improvement in engineering properties. Gomez et al. also performed in-situ MICP treatment using surface percolation in California desert, USA to mitigate fugitive

dust. Two-centimeter-deep crust was successfully formed in the study showing the avenues for upscaling the process. However, the control and predictability of the in-situ distribution of bacterial activity and reactant solutions and the subsequent distribution of $CaCO_3$ and related engineering properties in the subsurface are not yet adequate and has become the greatest challenge for upscaling and application of MICP in real field.

Another main challenge in implementing MICP is that it can be effectively utilized for sands belonging to a specific particle size range. Its efficiency is generally minimum in fine grained soils such as silt and clay as well as in sands with a significant proportion of coarser materials. As per the literature, MICP treatment is most efficient for sands of particle sizes in the range 0.5-3 mm. In finer soils, subsequent bioclogging limits the applicability whereas in coarser materials, high amount of cementitious materials is required to gain sufficient strength thus making the treatment less cost-effective.

Further, apart from the technical aspects, MICP application in field also depends on economical and legislative issues. The release of ammonium chloride in the subsurface may pose undesired ecological effects and hence need to be treated. There are two proposed strategies so far: (i) treating ammonia rich effluent before discharge or (ii) back feeding the ammonia as a fertilizer to the surrounding plants. As in any other treatment process, the feasibility of MICP is highly dependent on the economic aspects. Among them, material cost of the substances and expenses for bacteria culturing makes the major proportion of the total treatment cost. Most of the MICP studies have utilized the conventional culture media like yeast extract, ammonium sulphate, tris-buffer, tryptic soy broth, nutrient broth, luria broth for culturing of bacteria whereas cementation solutions are mostly incorporated with laboratory-grade reagents ($CaCl_2$, urea, $NaHCO_3$ and nutrients) which make up huge cost components. Therefore, nowadays research are moving more towards inexpensive media for bacteria cultivation and low grade chemicals as cementation media which can reduce the cost by significant proportions.

Urea hydrolysis results the undesirable byproducts of free ammonia and ammonium ions depending on the pH level, and the removal of ammonium byproducts from the system is one of the major concerns for the future work. If the MICP reactions could be controlled at low pH levels (below 7.5), around 98% of ammonia could be formed as ions, inhibiting the release of ammonia gas, and future work should focus on low pH MICP. The ammonium ions can be possibly eliminated by collecting and

treated the drained solutions, that could help to avoid the contamination with ground water. Immobilization of ammonium ions within the target treatment zones can also be a feasible pathway to avoid ground water contaminations.

Therefore, future works are highly recommended to couple the MICP technique with possible ion exchange methods, adsorption methods and precipitation methods and to propose new environmental-friendly ammonium-free MICP methods; on the environmental perspective, this research area appears to be the future of MICP research field. There are also possible bio-mediated geotechnical methods (less investigated) such as denitrification, sulfate reduction, iron reduction and hydroxyapatite mineralization, which can also induce the bio-cement similar to the MICP. These pathways should also be studied as possible alternatives, as those processes can eliminate the formation of ammonium by products. Overall, the full assessment of the feasibility of the process should include cost of required substrates, large scale culturing of bacteria and removal of by-products. Therefore, it is clear that to successfully implement MICP in real field problems a series of uncertainties need to be overcome.

8.3.2 Suggestions for future research works for in plant-derived urease method

In this study, we followed very simple method to extract the urease enzyme from watermelon seeds. Finally, a centrifuged extract was used for the study. However, it was not a fully transparent solution and it consisted with some suspended particles. Although the urease activity in these suspended particles contributes to the urea hydrolysis and finally to the CC precipitation, these suspended particles may clog between sand particles. This may be a disadvantage for penetrating cementation solution into deeper areas. Therefore, it is important to investigate a new, low-cost extraction method to extract almost all urease into the solution. In addition to that, a well-controlled distribution of CC should be achieved to use this method from laboratory to large scale applications. We could not achieve it from our current study. The control of the rate of CC precipitation is one solution. Then, the amount of PPCC can be reduced. Therefore, it is necessary to consider those matters more clearly from future research works.

The major challenges in this novel area for field applications include assessment of subsurface soil condition including soil type, pH, mineralogy and their interaction

with the available fluids and minerals, ground water flow characteristics and available minerals in the ground water. The control and predictability of the in-situ distribution of CC and related engineering properties in the subsurface are also not yet sufficient. Furthermore, there is a possibility to release NH_3 during urea hydrolysis process. The ratio of urea/$CaCl_2$ can be maintained as low as possible to diminish the production of NH_3. However, this is not a permanent solution to overcome the problem with NH_3. Therefore, these form the greatest challenge for further optimization. It is also necessary to investigate the durability, longevity and reversibility of the carbonate precipitation process under economical point of view.

The potential of the use of artificial bio minerals has brought a new revolution in various engineering applications. However, it is needed to explore deeply about this novel area in order to bring it environmentally safe, cost effective and to develop this technology from lab to field scales. The work conveyed in this dissertation presents systematic studies of the factors affecting enzyme induced carbonate precipitation (EICP) as a potential technique for soil improvement. While the work presented herein provides substantial insight into EICP, additional investigations focusing on significant parameters of interest would be helpful in gaining further understanding of the EICP technique, ultimately leading to application of this technology on a field scale. These parameters include the mechanism by which the addition of powdered milk enhances the precipitation process, grain size effects, and the effects of soil mineralogy, soil and pore water chemistry, and soil surface texture.

Furthermore, there may be a benefit to slowing down the rate of precipitation by finding an agent that inhibits the EICP reaction in order to get more uniform cementation and a high percentage of calcite precipitate. In addition to understanding these effects on EICP, substantial work will be needed on the best method(s) with which to employ EICP in the field. Therefore, more testing under many different conditions is highly desired to determine the feasibility of EICP soil improvement technology for field applications.

8.3.3 Suggestions for future works using plant fiber materials

The addition of fiber in the MICP process has the potential to in- crease the ductility of the MICP-treated sand and to prevent the loss of postpeak strength. Fiber content had positive effects on improving the shear strength parameters (angle of internal friction and cohesion) of the mixtures. The cohesion and angle of internal friction of fiber-reinforced sand prepared at different ratios of fiber increased by 29–45 kPa and 7.6–11°, respectively. The inclusion of fibers improves the ductility of the soil by preventing the loss of postpeak strength. The strengthening effect of fiber is mainly achieved by the cohesions and frictions between fibers and sand particles, while the improvement in ductility is mainly achieved by the tension and large failure strain of fiber in the cracks. These results are valid only for the materials used in this study. Bacteria concentration, concentration of cementation media, length, and aspect ratio of fibers were kept constant in this study. During the preparation of samples, the fibers easily formed into clumps, resulting in decreased uniformity of distribution of the fibers in the soil sample. Achieving a more even fiber distribution in the sand column was thus shown to greatly improve calcium carbonate distribution and soil sample strength improvement. These findings merit further investigation, analysis, and discussion in future research. In addition, the orientation of the fibers was not considered. Further investigations are needed using different types of concentrations, different fiber lengths, different aspect ratios, and different orientations of the fibers to fully evaluate the effect of fiber inclusion on the MICP-treated soils. The economically feasible alternative to the current soil improvement methods is not considered in this study.

REFERENCES

Abas Wani, A.; Sogi, D.S.; Grover, L.; Saxena, D.C. Effect of Temperature, Alkali Concentration, Mixing Time and Meal/Solvent Ratio on the Extraction of Watermelon Seed Proteins—A Response Surface Approach. *Biosyst. Eng.* 2006, 94, 67–73, doi:10.1016/j.biosystemseng.2006.02.004.

Abdul L et al (2012) Shoreline response to three submerged offshore breakwaters along Kerteh Bay Coast of Terengganu. Res *J Appl Sci Eng Technol* 4(16):2604–2615

Achal, V.; Mukherjee, A.; Basu, P.C.; Reddy, M.S. Strain improvement of Sporosarcina pasteurii for enhanced urease and calcite production. *J. Ind. Microbiol. Biotechnol.* 2009, 36, 981–988.

Adams, G.O.; Fufeyin,P.T.; Okoro, S.E.; Ehinomen, I. Bioremediation, Biostimulation and Bioaugmentation: A Review. *Int. J. Environ. Bioremediat. Biodegrad.* 2015, 3, 28–39.

Ahenkorah, I.; Rahman, M.M.; Karim, M.R.; Beecham, S.; Saint, C. A Review of Enzyme Induced Carbonate Precipitation (EICP): The Role of Enzyme Kinetics. *Sustain. Chem.* 2021, 2, 92–114, doi:10.3390/suschem2010007.

Ahenkorah, I.; Rahman, M.M.; Karim, M.R.; Teasdale, P.R. A comparison of mechanical responses for microbial and enzyme-induced cemented sand. *Géotechnique Lett.* 2020, 10, 1–26.

Airoldi L et al (2005) An ecological perspective on the deployment and design of low-crested and other hard coastal defence structures. *Coast Eng.* 52(10–11):1073–1087

Akiyama M and Kawasaki S (2012a) Novel grout material using calcium phosphate compounds: in vitro evaluation of crystal precipitation and strength reinforcement. *Enginering Geology* Vol. 125: 119–128.

Imran, M.; Shinmura, M.; Nakashima, K.; Kawasaki, S.Effects of Various Factors on Carbonate Particle Growth Using Ureolytic Bacteria. 2018.

Al Qabany, A.; Soga, K.; Santamarina, C. Factors affecting efficiency of microbially induced calcite precipitation. *J. Geotech. Geoenvironmental Eng.* 2012, *138*, 992–1001.

Al-Salloum, Y.; Hadi, S.; Abbas, H.; Almusallam, T.; Moslem, M.A. Bio-induction and bioremediation of cementitious composites using microbial mineral precipitation–A review. *Constr. Build. Mater.* 2017, 154, 857–876, doi:10.1016/j.conbuildmat.2017.07.203.

Amarakoon, G.G.N.N.; Kawasaki, S. Factors Affecting Sand Solidification Using MICP with Pararhodobacter sp. *Mater. Trans.* 2017, *59*, 72–81.

American Society for Testing and Materials Standard Test Method for Rapid Determination of Carbonate Content of Soils. *Astm D4373-14* 2014.

Arab, M.G.; Rohy, H.; Zeiada, W.; Almajed, A.; Omar, M. One-Phase EICP Biotreatment of Sand Exposed to Various Environmental Conditions. *J. Mater. Civ. Eng.* 2021, 33, 04020489, doi:10.1061/(asce)mt.1943-5533.0003596.

Arias, D.; Cisternas, L.; Rivas, M. Biomineralization Mediated by Ureolytic Bacteria Applied to Water Treatment: A Review. *Crystals* 2017, 7, 345, doi:10.3390/cryst7110345.

Ashis, M. Application of geotextiles in Coastal Protection and Coastal Engineering Works: An overview. *Int. Res. J. Environ. Sci.* 2015, 4, 96–103.

ASTM D2487-17, 2017. Standard Practice for Classification of Soils for Engineering

Purposes (Unified Soil Classification System). *ASTM International*, West Conshohocken, PA.

ASTM D559-03, 2003. In: Standard Test Methods for Wetting and Drying Compacted Soil-Cement Mixtures. *ASTM International*, West Conshohocken, PA, West Conshohocken PA 19428-2959, United States, pp. 1–7.

Bagnold RA (1940) Beach formation by waves: some model experiments in a wave tank. *J ICE* 15(1):27–52

Batisha A (2012) Adaptation of sea level rise in Nile Delta due to climate change. *J Earth Sci Clim Chang* 03(02):114

Blakeley, R.L.; Zerner, B. Jack bean urease: The first nickel enzyme. *J. Mol. Catal.* 1984, 23, 263–292, doi:10.1016/0304-5102(84)80014-0.

Blakely, R.L. and Zerner, B. (1984). "Jack Bean Urease: The First Nickel Enzyme."

Borsje BW et al (2011) How ecological engineering can serve in coastal protection. *Ecol Eng* 37(2):113–122

Cai F et al (2009) Coastal erosion in China under the condition of global climate change and measures for its prevention. *Prog Nat Sci* 19(4):415–426

Carmona, J.P.; Oliveira, P.J.V.; Lemos, L.J. Biostabilization of a sandy soil using enzymatic calcium carbonate precipitation. *Procedia Eng*. 2016, 143, 1301–1308.

Chandra, A.; Ravi, K. Effect of Magnesium Incorporation in Enzyme-Induced Carbonate Precipitation (EICP) to Improve Shear Strength of Soil. In Lecture Notes in Civil Engineering; Springer, Singapore 2020; Volume 56, pp. 333–346.

Chapman MG, Underwood AJ (2011) Evaluation of ecological engineering of "armoured" shorelines to improve their value as habitat. *J Exp Mar Biol Ecol* 400(1–2):302–313

Chen, H.J.; Peng, C.F.; Tang, C.W.; Chen, Y.T. Self-healing concrete by biological substrate. *Materials (Basel)*. 2019, *12*, 1–16.

Cheng, L.; Shahin, M.A.; Asce, M.; Mujah, D. Influence of Key Environmental Conditions on Microbially Induced Cementation for Soil Stabilization. *J. Geotech. Geoenviron. Eng* 2017, 143, 1–11, doi:10.1061/(ASCE).

Choi, S.-G.; Hoang, T.; Alleman, E.J.; Chu, J. Splitting Tensile Strength of Fiber-Reinforced and Biocemented Sand. *J. Mater. Civ. Eng*. 2019, *31*, 06019007.

Choi, S.-G.; Wang, K.; Chu, J. Properties of biocemented, fiber reinforced sand. *Constr. Build. Mater*. 2016, *120*, 623–629.

Ciantia MO, Castellanza R, Crosta GB, Hueckel T (2015) Efects of mineral suspension and dissolution on strength and compressibility of soft carbonate rocks. *Eng Geol* 184:1–18. https:// doi. org/ 10. 1016/j. enggeo. 2014. 10. 024

Ciantia MO, Castellanza R, di Prisco C (2014) Experimental study on the water-induced weakening of calcarenites. *Rock Mech Rock Eng* 48:441–461. https:// doi. org/ 10. 1007/ s00603- 014- 0603-z

Clemens, D.L.; Lee, B.Y.; Horwitz, M.A. Purification, characterization, and genetic analysis of Mycobacterium tuberculosis urease, a potentially critical determinant of host-pathogen interaction. *J. Bacteriol*. 1995, 177, 5644–5652.

Cochrane, B.H.W., Reichert, J.M., Eltz, F.L.F., Norton, L.D., 2005. Controlling soil erosion and runoff with polyacrylamide and phosphogypsum on subtropical soil. *Trans. Am. Soc. Agric. Eng*. 48, 149–154.

Consoli, N.C.; Vendruscolo, M.A.; Fonini, A.; Rosa, F.D. Fiber reinforcement effects on sand considering a wide cementation range. *Geotext. Geomembranes* 2009.

Craig, R.F., 1983. Soil Mechanics, Dictionary Geotechnical Engineering/Wörterbuch

GeoTechnik. Springer US, Boston, MA.

Crone, T., 2004. The Basic Sedement Transport Equations Made Ridiculously Simple. In OCEAN/ESS 410 *Marine Geology and Geophysics*.

Crowley, R., Davies, M., Ellis, T.N., Hudyma, N., Ammons, P., Matemu, C., 2019. Microbial induced calcite precipitation of dune sand using a surface spray technique, in: Geotechnical Special Publication. *American Society of Civil Engineers*, Reston, VA, pp. 213–222.

Cuccurullo, A.; Gallipoli, D.; Bruno, A.W.; Augarde, C.; Hughes, P.; La Borderie, C. Earth stabilisation via carbonate precipitation by plant-derived urease for building applications. *Geomech. Energy Environ*. 2020, 100230, doi:10.1016/j.gete.2020.100230.

Cui, M.-J.; Lai, H.-J.; Hoang, T.; Chu, J. One-phase-low-pH enzyme induced carbonate precipitation (EICP) method for soil improvement. Acta Geotech. 2021, 16, 481–489, doi:10.1007/s11440-020-01043-2.

Danjo, T.; Kawasaki, S. Formation mechanisms of beachrocks in Okinawa and Ishikawa, Japan, with a Focus on Cements. Mater. Trans. 2014, 55, 493–500.

Danjo, T.; Kawasaki, S. Microbially Induced Sand Cementation Method Using Pararhodobacter sp. Strain SO1, Inspired by Beachrock Formation Mechanism. Mater. Trans. 2016, 57, 428–437.

Daryono LR, Nakashima K, Kawasaki S et al (2020) Sediment characteristics of beachrock: a baseline investigation based on microbial induced carbonate precipitation at krakal-sadranan beach, yogyakarta. Indones Appl Sci 10:520. https:// doi. org/ 10. 3390/ app10 020520

Das, N., Kayastha, A. M., & Srivastava, P. K. (2002). Purification and characterization of urease from dehuskedpigeonpea (Cajanuscajan L.) seeds. Phytochemistry, 61(5), 513-521.

Davis, K.J. The Role of Mg2+ as an Impurity in Calcite Growth. Science 2000, 290, 1134–1137, doi:10.1126/science.290.5494.1134.

De Muynck, W.; De Belie, N.; Verstraete, W. Microbial carbonate precipitation in construction materials: A review. Ecol. Eng. 2010, 36, 118–136, doi:10.1016/j.ecoleng.2009.02.006.

DeJong, J.T.; Mortensen, B.M.; Martinez, B.C.; Nelson, D.C. Bio-mediated soil improvement. *Ecol. Eng.* 2010, *36*, 197–210.

Deng, W.; Wang, Y. Investigating the Factors Affecting the Properties of Coral Sand Treated with Microbially Induced Calcite Precipitation. Adv. Civ. Eng. 2018, 2018, 9590653.

Dhami, N.K., Reddy, M.S., Mukherjee, A., 2016. Significant indicators for biomineralisation in sand of varying grain sizes. Constr. Build. Mater. 104, 198–207.

Diel, J., Vogel, H.J., Schlüter, S., 2019. Impact of wetting and drying cycles on soil structure dynamics. Geoderma 345, 63–71.

Dilrukshi, R.A.N.; Nakashima, K.; Kawasaki, S. Soil improvement using plant-derived urease-induced calcium carbonate precipitation. Soils Found. 2018, 58, 894–910, doi:10.1016/j.sandf.2018.04.003.

Dixon, N., Crosby, C.J., Stirling, R., Hughes, P.N., Smethurst, J., Briggs, K., Hughes, D., Gunn, D., Hobbs, P., Loveridge, F., Glendinning, S., Dijkstra, T., Hudson, A., 2019. In situ measurements of near-surface hydraulic conductivity in engineered clay slopes. Q. J. Eng. Geol. Hydrogeol. 52, 123–135.

Dixon, N.E.; Gazzola, C.; Blakeley, R.L.; Zerner, B. Jack bean urease (EC 3.5.1.5).

Metalloenzyme. Simple biological role for nickel. J. Am. Chem. Soc. 1975, 97, 4131–4133, doi:10.1021/ja00847a045.

Do, J., Montoya, B., Gabr, M., 2017. Mechanical behavior of sands treated by microbial induced calcite precipitation at low confining stress, in: ICSMGE 2017 - 19th International Conference on Soil Mechanics and Geotechnical Engineering. pp. 353–356.

Doner, H.E.; Pratt, P.F. Solubility of Calcium Carbonate Precipitated in Aqueous Solutions of Magnesium and Sulfate Salts. Soil Sci. Soc. Am. J. 1969, 33, 690–693, doi:10.2136/sssaj1969.03615995003300050021x.

DOS SANTOS, A.P.S.; CONSOLI, N.C.; BAUDET, B.A. The mechanics of fibre-reinforced sand. *Géotechnique* 2010, *60*, 791–799.

Duraisamy, Y., 2016. Strength and Stiffness Improvement of Bio-cemented Sydney Sand. Doctoral dissertation, University of Sydney, Sydney, Australia.

Einstein, H.A., 1950. The bed-load function for sediment transport in open channel flows. US Department of Agriculture, Washington, DC.

EL-Hefnawy, M.E.; Sakran, M.; Ismail, A.I.; Aboelfetoh, E. Extraction, purification, kinetic and thermodynamic properties of urease from germinating Pisum Sativum L. seeds. BMC Biochem. 2014, 15, 15, doi:10.1186/1471-2091-15-15.

Evelpidou, N.; Vassilopoulos, A.; Leonidopoulou, D.; Poulos, S. AN INVESTIGATION OF THE COASTAL EROSION CAUSES IN SAMOS ISLAND, EASTERN AEGEAN SEA. Tájökológiai Lapok 2008, 6, 295–310.

Fang, X.; Yang, Y.; Chen, Z.; Liu, H.; Xiao, Y.; Shen, C. Influence of Fiber Content and Length on Engineering Properties of MICP-Treated Coral Sand. *Geomicrobiol. J.* 2020, *37*, 582–594.

Farukh, M.A., Yamada, T.J., 2018. Synoptic climatology of winter daily temperature extremes in Sapporo, northern Japan. Int. J. Climatol. 38, 2230–2238.

Fattet, M., Fu, Y., Ghestem, M., Ma, W., Foulonneau, M., Nespoulous, J., Le Bissonnais, Y., Stokes, A., 2011. Effects of vegetation type on soil resistance to erosion: Relationship between aggregate stability and shear strength. Catena 87, 60–69.

Feder, M.J.; Akyel, A.; Morasko, V.J.; Gerlach, R.; Phillips, A.J. Temperature-dependent inactivation and catalysis rates of plant-based ureases for engineered biomineralization. Eng. Rep. 2021, 3, doi:10.1002/eng2.12299.

Feng, K., Montoya, B.M., 2017. Quantifying Level of Microbial-Induced Cementation for Cyclically Loaded Sand. J. Geotech. Geoenvironmental Eng. 143, 06017005.

Ferris, F.G.; Phoenix, V.; Fujita, Y.; Smith, R.W. Kinetics of calcite precipitation induced by ureolytic bacteria at 10 to 20°C in artificial groundwater. Geochim. Cosmochim. Acta 2004, 68, 1701–1710.

Follmer, C. Insights into the role and structure of plant ureases. Phytochemistry 2008, 69, 18–28.

Fujita, M.; Nakashima, K.; Achal, V.; Kawasaki, S. Whole-cell evaluation of urease activity of Pararhodobacter sp. isolated from peripheral beachrock. Biochem. Eng. J. 2017, 124, 1–5.

Ge, P.; Nayanthara, N.; Buddhika, A.; Dassanayake, N.; Nakashima, K.; Kawasaki, S.; Lanka, S.; Author, C. Biocementation of Sri Lankan Beach Sand Using Locally Isolated Bacteria: A Baseline Study on The. Int. J. GEOMATE 2019, 17, 55–62.

Glöckner, F.O.; Fuchs, B.M.; Amann, R. Bacterioplankton compositions of lakes and oceans: A first comparison based on fluorescence in situ hybridization. *Appl. Environ. Microbiol.* 1999.

Gowthaman, S.; Mitsuyama, S.; Nakashima, K.; Komatsu, M.; Kawasaki, S. Biogeotechnical approach for slope soil stabilization using locally isolated bacteria and inexpensive low-grade chemicals: A feasibility study on Hokkaido expressway soil, Japan. *Soils Found.* 2019, *59*, 484–499.

Gowthaman, S.; Nakashima, K.; Kawasaki, S. A state-of-the-art review on soil reinforcement technology using natural plant fiber materials: Past findings, present trends and future directions. *Materials (Basel).* 2018, *11*, 1–23.

Gupta, M.K.; Srivastava, R.K.; Bisaria, H. Potential of Jute Fibre Reinforced Polymer Composites : A review ISSN 2277-7156 Review Article Potential of Jute Fibre Reinforced Polymer Composites : A Review. *Int. J. Fiber Text. Res.* 2015, *5*, 30–38.

Hamdan, N., Kavazanjian, E., 2016. Enzyme-induced carbonate mineral precipitation for fugitive dust control. Geotechnique 66, 546–555.

Hamdan, N.M. Applications of Enzyme Induced Carbonate Precipitation (Eicp) for Soil Improvement. Ph.D. Thesis, Arizona State University, Tempe, AZ, USA, 2015.

Hamed Khodadadi, T.; Kavazanjian, E.; van Paassen, L.; DeJong, J. Bio-Grout Materials: A Review. In Proceedings of the Grouting 2017; American Society of Civil Engineers: Reston, VA, USA, 2017; pp. 1–12.

Han, Z., Cheng, X., Ma, Q., 2016. An experimental study on dynamic response for MICP strengthening liquefiable sands. Earthq. Eng. Eng. Vib. 15, 673–679.

Harkes, M.P.; van Paassen, L.A.; Booster, J.L.; Whiffin, V.S.; van Loosdrecht, M.C.M. Fixation and distribution of bacterial activity in sand to induce carbonate precipitation for ground reinforcement. *Ecol. Eng.* 2010, *36*, 112–117.

Hejazi, S.M.; Sheikhzadeh, M.; Abtahi, S.M.; Zadhoush, A. A simple review of soil reinforcement by using natural and synthetic fibers. *Constr. Build. Mater.* 2012, *30*, 100–116.

Imran, M.; Kimura, S.; Nakashima, K.; Evelpidou, N.; Kawasaki, S. Feasibility Study of Native Ureolytic Bacteria for Biocementation Towards Coastal Erosion Protection by MICP Method. *Appl. Sci.* 2019, *9*, 4462.

Islam, M.S.; Ahmed, S.J. Influence of jute fiber on concrete properties. *Constr. Build. Mater.* 2018, *189*, 768–776.

Jahns, T. Urea uptake by the marine bacterium Deleya venusta HG1. J. Gen. Microbiol. 2009, 138, 1815–1820.

Javadi, N.; Khodadadi, H.; Hamdan, N.; Kavazanjian, E. EICP Treatment of Soil by Using Urease Enzyme Extracted from Watermelon Seeds. In Proceedings of the IFCEE 2018; American Society of Civil Engineers: Reston, VA, USA, 2018; pp. 115–124.

Jonkers, H.M.; Thijssen, A.; Muyzer, G.; Copuroglu, O.; Schlangen, E. Application of bacteria as self-healing agent for the development of sustainable concrete. Ecol. Eng. 2010, 36, 230–235.
Journal of Molecular Catalysis, Vol. 23, pp. 263 – 292.

Kadhim, F.J.; Zheng, J.J. Review of the Factors That Influence on the Microbial Induced Calcite Precipitation. Civ. Environ. Res. 2016, 8, 69–76.

Kafarski, P.; Talma, M. Recent advances in design of new urease inhibitors: A review. J. Adv. Res. 2018, 13, 101–112.

Kappaun K., Piovesan A.R., Carlini C.R. and Ligabue-Braun R., Ureases: Historical aspects, catalytic, and non-catalytic properties-A review, J. Adv. Res., Vol. 3, Issue 13, pp. 3-17.

Katz, A. The interaction of magnesium with calcite during crystal growth at 25–90°C

and one atmosphere. Geochim. et Cosmochim. Acta 1973, 37, 1563–1586, doi:10.1016/0016-7037(73)90091-4.

Kavazanjian, E.; Hamdan, N. Enzyme Induced Carbonate Precipitation (EICP) Columns for Ground Improvement. In Proceedings of the IFCEE 2015; American Society of Civil Engineers: Reston, VA, USA, 2015; Volume GSP 256, pp. 2252–2261.

Kayastha, A. M., & Das, N. (1999). A simple laboratory experiment for teaching enzyme immobilization with urease and its application in blood urea estimation. Biochemical Education, 27(2), 114-117.

Keykha, H.A.; Asadi, A.; Zareian, M. Environmental Factors Affecting the Compressive Strength of Microbiologically Induced Calcite Precipitation-Treated Soil. Geomicrobiol. J. 2017, 34, 889–894.

Khanlari G, Abdilor Y (2015) Influence of wet–dry, freeze–thaw, and heat–cool cycles on the physical and mechanical properties of upper red sandstones in central Iran. Bull Eng Geol Environ 74:1287–1300. https:// doi. org/ 10. 1007/ s10064- 014- 0691-8

Khodadadi Tirkolaei, H.; Javadi, N.; Krishnan, V.; Hamdan, N.; Kavazanjian, E. Crude Urease Extract for Biocementation. J. Mater. Civ. Eng. 2020, 32, 04020374, doi:10.1061/(asce)mt.1943-5533.0003466.

Krajewska, B. Urease-aided calcium carbonate mineralization for engineering applications: A review. J. Adv. Res. 2017, 13, 59–67.

Kubo, R.; Kawasaki, S.; Suzuki, K.; Yamaguchi, S.; Hata, T. Geological Exploration of Beachrock through Geophysical Surveying on Yagaji Island, Okinawa, Japan. Mater. Trans. 2013, 55, 342–350.

Labana, S.; Singh, O.V.; Basu, A.; Pandey, G.; Jain, R.K. A microcosm study on bioremediation of p-nitrophenol-contaminated soil using Arthrobacter protophormiae RKJ100. Appl. Microbiol. Biotechnol. 2005, 68, 417–424, doi:10.1007/s00253-005-1926-1.

Lee, C.; Lee, H.; Kim, O.B. Biocement fabrication and design application for a sustainable urban area. Sustainability 2018, 10, 4079–4096.

Lee, S.C.; Hashim, R.; Motamedi, S.; Song, K.-I. Utilization of geotextile tube for sandy and muddy coastal management: A review. Sci. World J. 2014, 2014, 494020.

Lee, Y.S.; Park, W. Current challenges and future directions for bacterial self-healing concrete. Appl. Microbiol. Biotechnol. 2018, 102, 3059–3070.

Lei, X.; Lin, S.; Meng, Q.; Liao, X.; Xu, J. Influence of different fiber types on properties of biocemented calcareous sand. *Arab. J. Geosci.* 2020, *13*.

Li, L.; Zhao, Q.; Zhang, H.; Amini, F.; Li, C. A Full Contact Flexible Mold for Preparing Samples Based on Microbial-Induced Calcite Precipitation Technology. Geotech. Test. J. 2014, 37, 917–921.

Li, L.; Zhao, Q.; Zhang, H.; Amini, F.; Li, C. A Full Contact Flexible Mold for Preparing Samples Based on Microbial-Induced Calcite Precipitation Technology. *Geotech. Test. J.* 2014, *37*, 20130090.

Li, M.; Li, L.; Ogbonnaya, U.; Wen, K.; Tian, A.; Amini, F. Influence of fiber addition on mechanical properties of MICP-treated sand. *J. Mater. Civ. Eng.* 2016, *28*, 1–10.

Li, M.; Li, L.; Ogbonnaya, U.; Wen, K.; Tian, A.; Amini, F. Influence of Fiber Addition on Mechanical Properties of MICP-Treated Sand. *J. Mater. Civ. Eng.* 2015, *28*, 1–10.

Li, M.; Li, L.; Ogbonnaya, U.; Wen, K.; Tian, A.; Amini, F. Influence of fiber addition on mechanical properties of MICP-treated sand. *J. Mater. Civ. Eng.* 2016, *28*.

Martinez, B.C.; DeJong, J.T.; Ginn, T.R.; Montoya, B.M.; Barkouki, T.H.; Hunt, C.; Tanyu, B.; Major, D. Experimental Optimization of Microbial-Induced Carbonate Precipitation for Soil Improvement. *J. Geotech. Geoenvironmental Eng.* 2013.

Mazzei, L.; Musiani, F.; Ciurli, S. The structure-based reaction mechanism of urease, a nickel dependent enzyme: Tale of a long debate. J. Biol. Inorg. Chem. 2020, 25, 829–845.

Miftah, A.; Khodadadi Tirkolaei, H.; Bilsel, H. Bio-precipitation of CaCO 3 for soil improvement: A Review. IOP Conf. Ser.: Mater. Sci. Eng. 2020, 800, 012037, doi:10.1088/1757-899X/800/1/012037.

Mobley H.L.T., Hausinger R.P., Microbial ureases: Significance, regulation, and molecular characterization. Microbiol. Rev. Vol. 53, Issue 1, 1989, pp. 85-108.

Mobley, H.; Island, M.D.; Hausinger, R.P. Molecular biology of microbial ureases. Microbiol. Rev. 1995, 59, 451–480.

Mortensen, B.M.; Haber, M.J.; Dejong, J.T.; Caslake, L.F.; Nelson, D.C. Effects of environmental factors on microbial induced calcium carbonate precipitation. J. Appl. Microbiol. 2011, 111, 338–349.

Mortensen, B.M.; Haber, M.J.; Dejong, J.T.; Caslake, L.F.; Nelson, D.C. Effects of environmental factors on microbial induced calcium carbonate precipitation. *J. Appl. Microbiol.* 2011, *111*, 338–349.

Mujah, D.; Shahin, M.A.; Cheng, L. State-of-the-Art Review of Biocementation by Microbially Induced Calcite Precipitation (MICP) for Soil Stabilization. Geomicrobiol. J. 2017, 34, 524–537.

Mujah, D.; Shahin, M.A.; Cheng, L. State-of-the-Art Review of Biocementation by Microbially Induced Calcite Precipitation (MICP) for Soil Stabilization. Geomicrobiol. J. 2017, 34, 524–537, doi:10.1080/01490451.2016.1225866.

Munshi, T.K.; Chattoo, B.B. Bacterial population structure of the jute-retting environment. *Microb. Ecol.* 2008.

Mwandira, W.; Nakashima, K.; Kawasaki, S. Bioremediation of lead-contaminated mine waste by Pararhodobacter sp. based on the microbially induced calcium carbonate precipitation technique and its effects on strength of coarse and fine grained sand. *Ecol. Eng.* 2017, *109*, 57–64.

Nafisi, A.; Montoya, B.M.; Evans, T.M. Shear Strength Envelopes of Biocemented Sands with Varying Particle Size and Cementation Level. *J. Geotech. Geoenvironmental Eng.* 2020, *146*, 1–14.

Nam, I.H.; Chon, C.M.; Jung, K.Y.; Choi, S.G.; Choi, H.; Park, S.S. Calcite precipitation by ureolytic plant (Canavalia ensiformis) extracts as effective biomaterials. KSCE J. Civ. Eng. 2015, 19, 1620–1625, doi:10.1007/s12205-014-0558-3.

Natarajan, K.R. Kinetic Study of the Enzyme Urease from Dolichos biflorus. *J. Chem. Educ.* 1995, *72*, 556.

Nayanthara, P.G.N.; Dassanayake, A.B.N.; Nakashima, K.; Kawasaki, S. Microbial Induced Carbonate Precipitation Using a Native Inland Bacterium for Beach Sand Stabilization in Nearshore Areas. Appl. Sci. 2019, 9, 3201, doi:10.3390/app9153201.

Neumeier, U. Experimental modelling of beachrock cementation under microbial influence. Sediment. Geol. 1999, 126, 35–46.

Neupane, D.; Yasuhara, H.; Kinoshita, N.; Ando, Y. Distribution of mineralized carbonate and its quantification method in enzyme mediated calcite precipitation technique. Soils Found. 2015, 55, 447–457.

Neupane, D.; Yasuhara, H.; Kinoshita, N.; Unno, T. Applicability of Enzymatic Calcium Carbonate Precipitation as a Soil-Strengthening Technique. J. Geotech. Geoenviron. Eng. 2013, 139, 2201–2211, doi:10.1061/(ASCE)GT.1943-5606.0000959.

Novitsky, J.A. Calcium carbonate precipitation by marine bacteria. Geomicrobiol. J. 1981, 2, 375–388.

Omoregie, A.I.; Ngu, L.H.; Ong, D.E.L.; Nissom, P.M. Low-cost cultivation of Sporosarcina pasteurii strain in food-grade yeast extract medium for microbially induced carbonate precipitation (MICP) application. Biocatal. Agric. Biotechnol. 2019, 17, 247–255.

Omoregie, A.I.; Ngu, L.H.; Ong, D.E.L.; Nissom, P.M. Low-cost cultivation of Sporosarcina pasteurii strain in food-grade yeast extract medium for microbially induced carbonate precipitation (MICP) application. *Biocatal. Agric. Biotechnol.* 2019, *17*, 247–255.

Osinubi, K.J.; Eberemu, A.O.; Ijimdiya, T.S.; Yakubu, S.E.; Gadzama, E.W.; Sani, J.E.; Yohanna, P. Review of the use of microorganisms in geotechnical engineering applications. SN Appl. Sci. 2020, 2, 207, doi:10.1007/s42452-020-1974-2.

Putra, H.; Yasuhara, H.; Erizal; Sutoyo; Fauzan, M. Review of Enzyme-Induced Calcite Precipitation as a Ground-Improvement Technique. Infrastructures 2020, 5, 66, doi:10.3390/infrastructures5080066.

Putra, H.; Yasuhara, H.; Kinoshita, N. Applicability of natural zeolite for nh-forms removal in enzyme-mediated calcite precipitation technique. Geosciences 2017, 7, 61.

Putra, H.; Yasuhara, H.; Kinoshita, N.; Hirata, A. Optimization of Enzyme-Mediated Calcite Precipitation as a Soil-Improvement Technique: The Effect of Aragonite and Gypsum on the Mechanical Properties of Treated Sand. Crystals 2017, 7, 59, doi:10.3390/cryst7020059.

Putri, P.Y.; Ujike, I.; Sandra, N.; Rifwan, F.; Andayono, T. Calcium Carbonate in Bio-Based Material and Factor Affecting Its Precipitation Rate for Repairing Concrete. Crystals 2020, 10, 883, doi:10.3390/cryst10100883.

Qiu, R.; Tong, H.; Fang, X.; Liao, Y.; Li, Y. Analysis of strength characteristics of carbon fiber–reinforced microbial solidified sand. *Adv. Mech. Eng.* 2019, *11*, 1–7.

Rahman, M.M.; Hora, R.N.; Ahenkorah, I.; Beecham, S.; Karim, M.R.; Iqbal, A. State-of-the-Art Review of Microbial-Induced Calcite Precipitation and Its Sustainability in Engineering Applications. Sustainability 2020, 12, 6281, doi:10.3390/su12156281.

Rohy, H.; Arab, M.; Zeiada, W.; Omar, M.; Almajed, A.; Tahmaz, A. One Phase Soil Bio-Cementation with EICP-Soil Mixing. In Proceedings of the World Congress on Civil, Structural, and Environmental Engineering, Rome, Italy, April 2019.

Salifu, E.; MacLachlan, E.; Iyer, K.R.; Knapp, C.W.; Tarantino, A. Application of microbially induced calcite precipitation in erosion mitigation and stabilisation of sandy soil foreshore slopes: A preliminary investigation. Eng. Geol. 2016, 201, 96–105.

Sarayu, K.; Iyer, N.R.; Murthy, A.R. Exploration on the biotechnological aspect of the ureolytic bacteria for the production of the cementitious materials—A review.

Appl. Biochem. Biotechnol. 2014, 172, 2308–2323.

Shao, W.; Cetin, B.; Li, Y.; Li, J.; Li, L. Experimental Investigation of Mechanical Properties of Sands Reinforced with Discrete Randomly Distributed Fiber. *Geotech. Geol. Eng.* 2014, *32*, 901–910.

Sheehan, C.; Harrington, J. An environmental and economic analysis for geotube coastal structures retaining dredge material. Resour. Conserv. Recycl. 2012, 61, 91–102.

Silva-Castro, G.A.; Uad, I.; Rivadeneyra, A.; Vilchez, J.I.; Martin-Ramos, D.; González-López, J.; Rivadeneyra, M.A. Carbonate Precipitation of Bacterial Strains Isolated from Sediments and Seawater: Formation Mechanisms. Geomicrobiol. J. 2013, 30, 840–850.

Sirko, A.; Brodzik, R. Plant ureases: Roles and regulation. Acta Biochim. Pol. 2000, 47, 1189–1195.

Sulistiawati Baiq, H. Examination Of Calcite Precipitation Using Plant-Derived Urease Enzyme For Soil Improvement. Int. J. GEOMATE 2020, 19, doi:10.21660/2020.72.9481.

Sumner, J.B. The isolation and crystallization of the enzyme urease preliminary paper. J. Biol. Chem. 1926, 69, 435–441.

Sun, X.; Miao, L.; Wu, L.; Wang, C. Study of magnesium precipitation based on biocementation. Mar. Georesources Geotechnol. 2019, 37, 1257–1266, doi:10.1080/1064119X.2018.1549626.

Tang CS, Cui YJ, Shi B et al (2011) Desiccation and cracking behaviour of clay layer from slurry state under wetting-drying cycles. Geod 166:111–118. https:// doi. org/ 10. 1016/j. geode rma. 2011. 07. 018

Tang CS, Wang DY, Shi B, Li J (2016) Effect of wetting-drying cycles on profile mechanical behavior of soils with different initial conditions. CATENA 139:105–116. https:// doi. org/ 10. 1016/j. catena.2015. 12. 015

Tang W, Mohseni E, Wang Z (2018) Development of vegetation concrete technology for slope protection and greening. Constr Build Mater 179:605–613. https:// doi. org/ 10. 1016/j. conbu ildmat. 2018. 05. 207

Tang, C.; Shi, B.; Gao, W.; Chen, F.; Cai, Y. Strength and mechanical behavior of short polypropylene fiber reinforced and cement stabilized clayey soil. *Geotext. Geomembranes* 2007.

Tang, C.-S.; Yin, L.; Jiang, N.; Zhu, C.; Zeng, H.; Li, H.; Shi, B. Factors affecting the performance of microbial-induced carbonate precipitation (MICP) treated soil: A review. Environ. Earth Sci. 2020, 79, 94, doi:10.1007/s12665-020-8840-9.

Teng, F.; Ouedraogo, C.; Sie, Y. Strength Improvement Of A Silty Clay With Microbiologically Induced Process And Coir Fiber. 2020, *15*, 79–88.

Teng, F.; Ouedraogo, C.; Sie, Y.C. Strength improvement of a silty clay with microbiologically induced process and coir fiber. *J. Geoengin.* 2020.

Tiano, P.; Biagiotti, L.; Mastromei, G. Bacterial bio-mediated calcite precipitation for monumental stones conservation: Methods of evaluation. J. Microbiol. Methods 1999, 36, 139–145.

Urrea-Ceferino, G.E.; Rempe, N.; dos Santos, V.; Savastano Junior, H. Definition of optimal parameters for supercritical carbonation treatment of vegetable fiber-cement composites at a very early age. *Constr. Build. Mater.* 2017, *152*, 424–433.

Van Paassen, L.A.; Ghose, R.; van der Linden, T.J.M.; van der Star, W.R.L. Quantifying Biomediated Ground Improvement by Ureolysis: Large-Scale

Biogrout Experiment. J. Geotech. Geoenviron. Eng. 2010, 136, 1721–1728.

Wang, Y.; Mao, X.; Xiao, W.; Wang, W. The Influence Mechanism of Magnesium Ions on the Morphology and Crystal Structure of Magnetized Anti-Scaling Products. Minerals 2020, 10, 997, doi:10.3390/min10110997.

Wani A.A., Sogi D.S., Singh P., Wani I.A. and Shivhare U.S., Characterisation and functional properties of watermelon (Citrullus lanatus) seed proteins. J. Sci. Food Agric., Vol. 91, Issue 1, 2011, pp. 113-121.

Wani, A.A.; Sogi, D.S.; Singh, P.; Wani, I.A.; Shivhare, U.S. Characterisation and functional properties of watermelon (Citrullus lanatus) seed proteins. J. Sci. of Food Agric. 2011, 91, 113–121, doi:10.1002/jsfa.4160.

Weber, M.; Jones, M.J.; Ulrich, J. Optimisation of isolation and purification of the jack bean enzyme urease by extraction and subsequent crystallization. Food Bioprod. Process. 2008, 86, 43–52, doi:10.1016/j.fbp.2007.10.005.

Wei, S.; Cui, H.; Jiang, Z.; Liu, H.; He, H.; Fang, N. Biomineralization processes of calcite induced by bacteria isolated from marine sediments. Braz. J. Microbiol. 2015, 46, 455–464.

Wen, K.; Bu, C.; Liu, S.; Li, Y.; Li, L. Experimental investigation of flexure resistance performance of bio-beams reinforced with discrete randomly distributed fiber and bamboo. *Constr. Build. Mater.* 2018, *176*, 241–249.

Whiffin, V.S.; van Paassen, L.A.; Harkes, M.P. Microbial carbonate precipitation as a soil improvement technique. Geomicrobiol. J. 2007, 24, 417–423.

Xia, H.; Zhou, M.; Wei, X.; Zhang, X.; Wu, Z. Slow and Sustained Release of Carbonate Ions from Amino Acids for Controlled Hydrothermal Growth of Alkaline-Earth Carbonate Single Crystals. ACS Omega 2020, 5, 14123–14132, doi:10.1021/acsomega.0c01719.

Xu, X.; Guo, H.; Cheng, X.; Li, M. The promotion of magnesium ions on aragonite precipitation in MICP process. Constr. Build. Mater. 2020, 263, 120057

Zhang ZB, Peng X, Wang LL et al (2013) Temporal changes in shrinkage behavior of two paddy soils under alternative flooding and drying cycles and its consequence on percolation. Geod 192:12–20. https:// doi. org/ 10. 1016/j. geode rma. 2012. 08. 009

Zhao, G.Z.; Li, J.; Qin, S.; Zhang, Y.Q.; Zhu, W.Y.; Jiang, C.L.; Xu, L.H.; Li, W.J. Micrococcus yunnanensis sp. nov., a novel actinobacterium isolated from surface-sterilized Polyspora axillaris roots. *Int. J. Syst. Evol. Microbiol.* 2009, *59*, 2383–2387.

Zhao, Y.; Xiao, Z.; Fan, C.; Shen, W.; Wang, Q.; Liu, P. Comparative mechanical behaviors of four fiber-reinforced sand cemented by microbially induced carbonate precipitation. *Bull. Eng. Geol. Environ.* 2020.

Zhu, T.; Dittrich, M.; Zhang, W.; Bhubalan, K.; Dittrich, M.; Zhu, T. Carbonate Precipitation through Microbial Activities in Natural Environment, and Their Potential in Biotechnology: A Review. Front. Bioeng. Biotechnol. 2016, 4, 4.